Disclaimer

This course material may contain copyrighted material the use of which has not been specifically authorized or licensed by the copyright owner. This material is used here for teaching purposes constituting a fair use as provided by Swiss copyright law (URG Art. 19 Abs. 1 lit. B).

The content of this presentation is meant for use as part of the course «Thin Films and Small Scale Mechanics» offered at Empa Thun. It is intended solely for the use of the registered course participants. Distribution to individuals who are not registered course participants is prohibited. If you are not a registered course participant, you are hereby notified that any review, dissemination, distribution, duplication or other use is strictly forbidden.

Ch. 5: Size effects

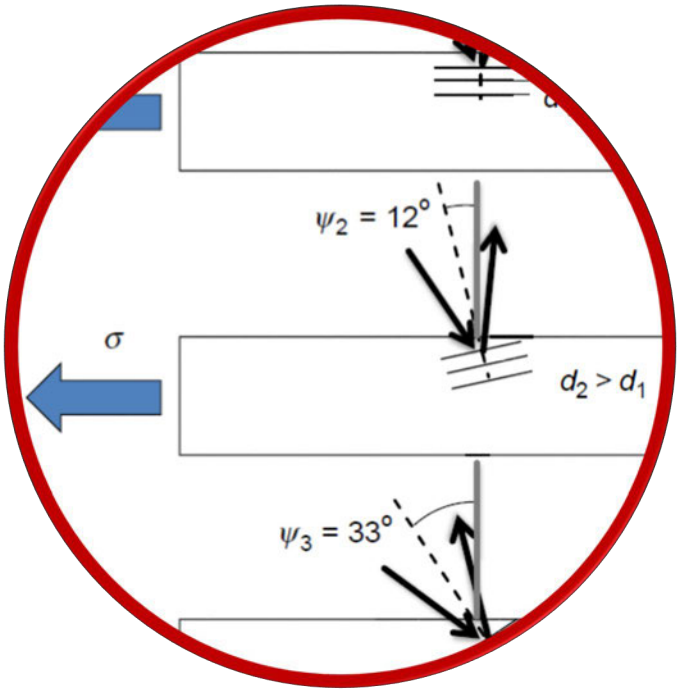

Length scale effects in metal plasticity

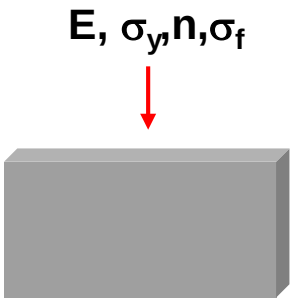

„You don't have to be small to be strong – just thin"

seminal work in small scale mechanics

Empa
Materials Science and Technology

BULK
MINIATURE SAMPLE
NANO TESTING

Hall 1951, Petch 1953 

Pharr, J. Mater. Res. 1992 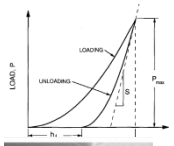

Rabe, Thin Solid Films, 2003 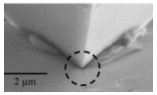

Maio, J. Mater. Res, 2005 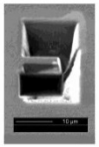

Oestlund, Adv. Func,. Mater, 2006 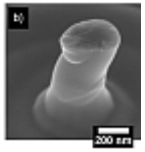

Kiener, Acta Mat, 2008 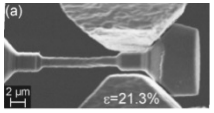

Pharr, Acta Mat 2008 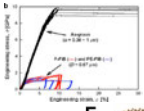

Schaedler, Science, 2011 

Meza, Science, 2014 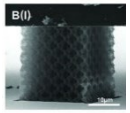

Gangaraj. Nature Com, 2018 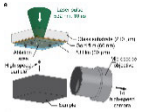

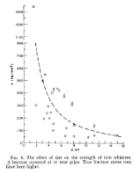

Brenner, J. Appl. Phys. 1956

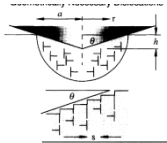

Nix, Met Trans A, 1989

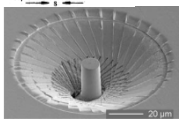

Uchic, Science 2004

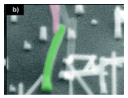

Hoffmann, Nanoletters, 2005

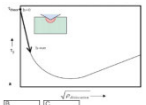

Lilleoden , Acta Mat, 2006

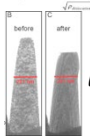

Minor, Nature Materials, 2008

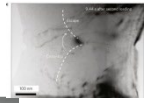

Oh, Nature Materials, 2009

Schwiedrzik, Nature Materials 2014

Tertuliano, Nature Materials, 2015

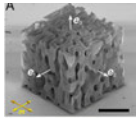

Portela, PNAS, 2020

seminal work in small scale mechanics

Empa
Materials Science and Technology

BULK
MINIATURE SAMPLE
NANO TESTING

Hall 1951, Petch 1953 

Pharr, J. Mater. Res. 1992

Rabe, Thin Solid Films, 2003 

Maio, J. Mater. Res, 2005 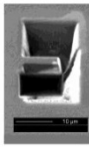

Oestlund, Adv. Func,. Mater, 2006

Kiener, Acta Mat, 2008 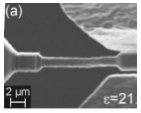

Pharr, Acta Mat 2008 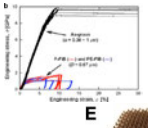

Schaedler, Science, 2011 

Meza, Science, 2014 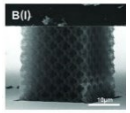

Gangaraj. Nature Com, 2018 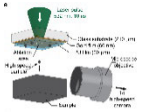

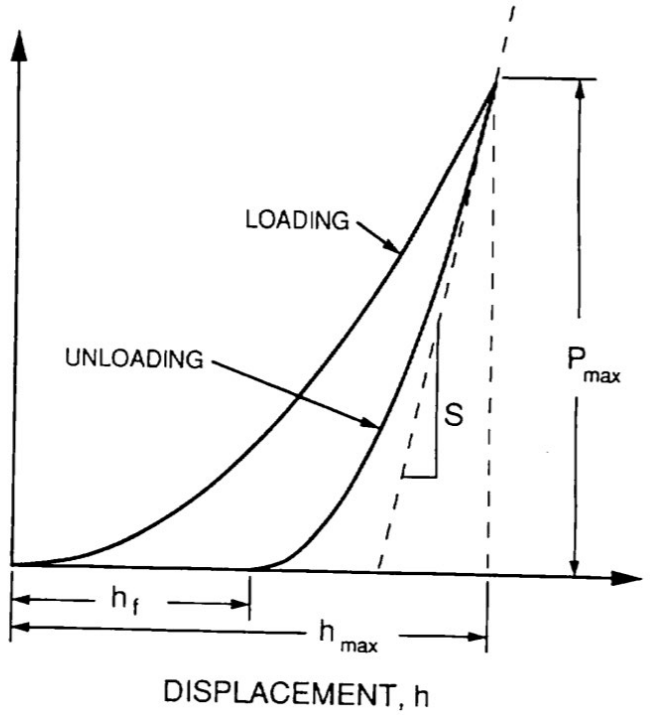

pl. Phys. 1956

Trans A, 1989

Science 2004

letters, 2005

cta Mat, 2006

aterials, 2008

Oh, Nature Materials, 2009 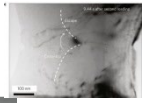

Schwiedrzik, Nature Materials 2014 

Tertuliano, Nature Materials, 2015 

Portela, PNAS, 2020 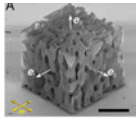

seminal work in small scale mechanics

Empa
Materials Science and Technology

Hall 1951, Petch 1953

Pharr, J. Mater. Res. 1992

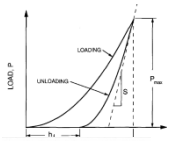

Rabe, Thin Solid Films, 2003

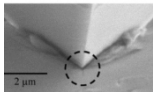

Maio, J. Mater. Res

Oestlund, Adv. Func

Kiener, Acta Mat, 2

Pharr, Acta Mat 20

Schaedler, Science,

Meza, Science, 2014

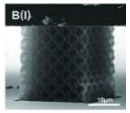

Gangaraj. Nature Com, 2018

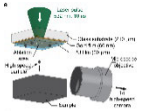

Brenner, J. Appl. Phys. 1956

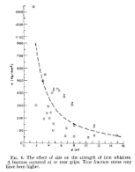

Nix, Met Trans A, 1989

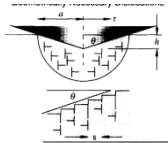

Uchic, Science 2004

n, Nanoletters, 2005

den , Acta Mat, 2006

ture Materials, 2008

ture Materials, 2009

Schwiedrzik, Nature Materials 2014

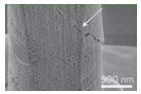

Tertuliano, Nature Materials, 2015

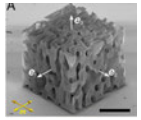

Portela, PNAS, 2020

BULK
MINIATURE SAMPLE
NANO TESTING
IN-SITU
MICRO- SAMPLE

seminal work in small scale mechanics

Empa
Materials Science and Technology

Hall 1951, Petch 1953

Pharr, J. Mater. Res. 1992

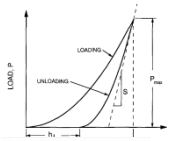

Rabe, Thin Solid Films, 2003

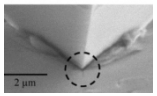

Maio, J. Mater. Res, 2005

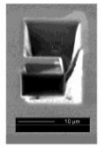

Oestlund, Adv. Func,. Mater, 2006

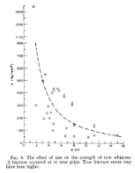

Brenner, J. Appl. Phys. 1956

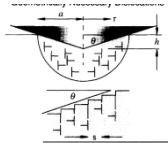

Nix, Met Trans A, 1989

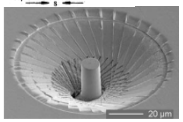

Uchic, Science 2004

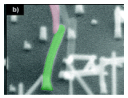

Hoffmann, Nanoletters, 2005

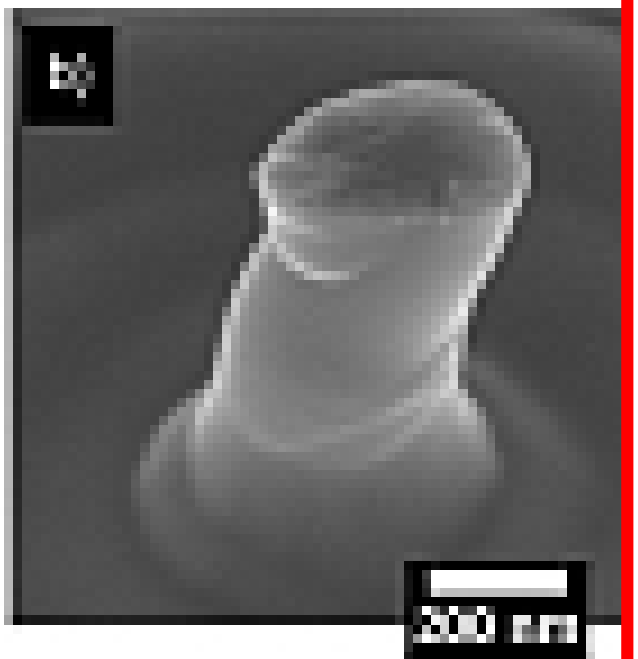

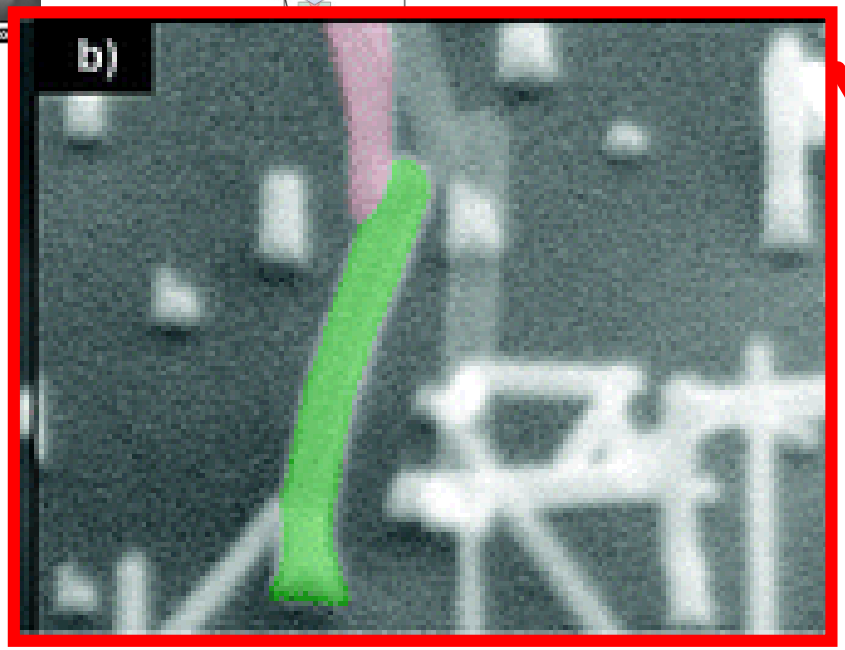

BULK

MINIATURE SAMPLE

NANO TESTING

IN-SITU

MICRO- SAMPLE

THEORETHICAL STRENGTH & BRITTLE IS DUCTILE

seminal work in small scale mechanics

Empa
Materials Science and Technology

Hall 1951, Petch 1953

Pharr, J. Mater. Res. 1992

Brenner, J. Appl. Phys. 1956

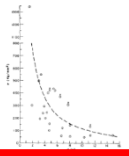

Rabe, Thin Solid

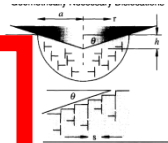

Nix, Met Trans A, 1989

Maio, J. Mater. R

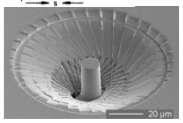

Uchic, Science 2004

Oestlund, Adv. F

Hoffmann, Nanoletters, 2005

Kiener, Acta Mat

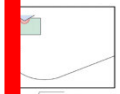

Lilleoden , Acta Mat, 2006

Pharr, Acta Mat

Minor, Nature Materials, 2008

Schaedler, Scien

Oh, Nature Materials, 2009

nwiedrzik, Nature Materials 2014

Meza, Science, 2

ertuliano, Nature Materials, 2015

Gangaraj. Nature

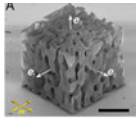

Portela, PNAS, 2020

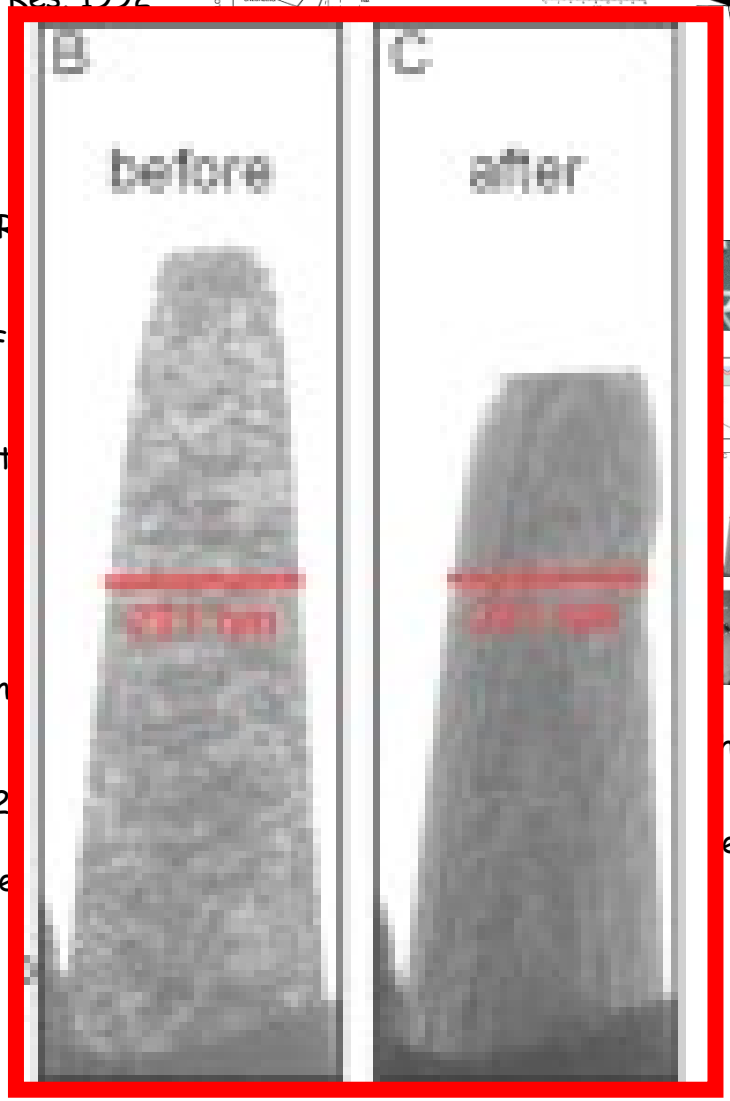

BULK

MINIATURE SAMPLE

NANO TESTING

IN-SITU

MICRO- SAMPLE

THEORETHICAL STRENGTH & BRITTLE IS DUCTILE

NUCLEATION VS STARVATION

seminal work in small scale mechanics

Empa
Materials Science and Technology

Hall 1951, Petch 1953

Pharr, J. Mater. Res. 1992

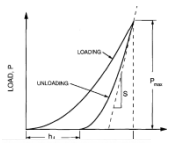

Rabe, Thin Solid Films, 2003

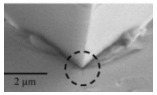

Maio, J. Mater. Res, 2005

Oestlund, Adv. Func,. /

Kiener, Acta Mat, 200

Pharr, Acta Mat 2008

Schaedler, Science, 20

Meza, Science, 2014

Gangaraj. Nature Com

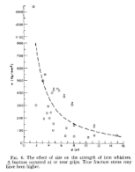

Brenner, J. Appl. Phys. 1956

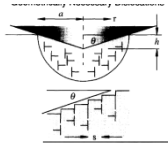

Nix, Met Trans A, 1989

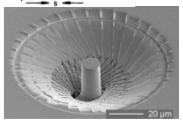

Uchic, Science 2004

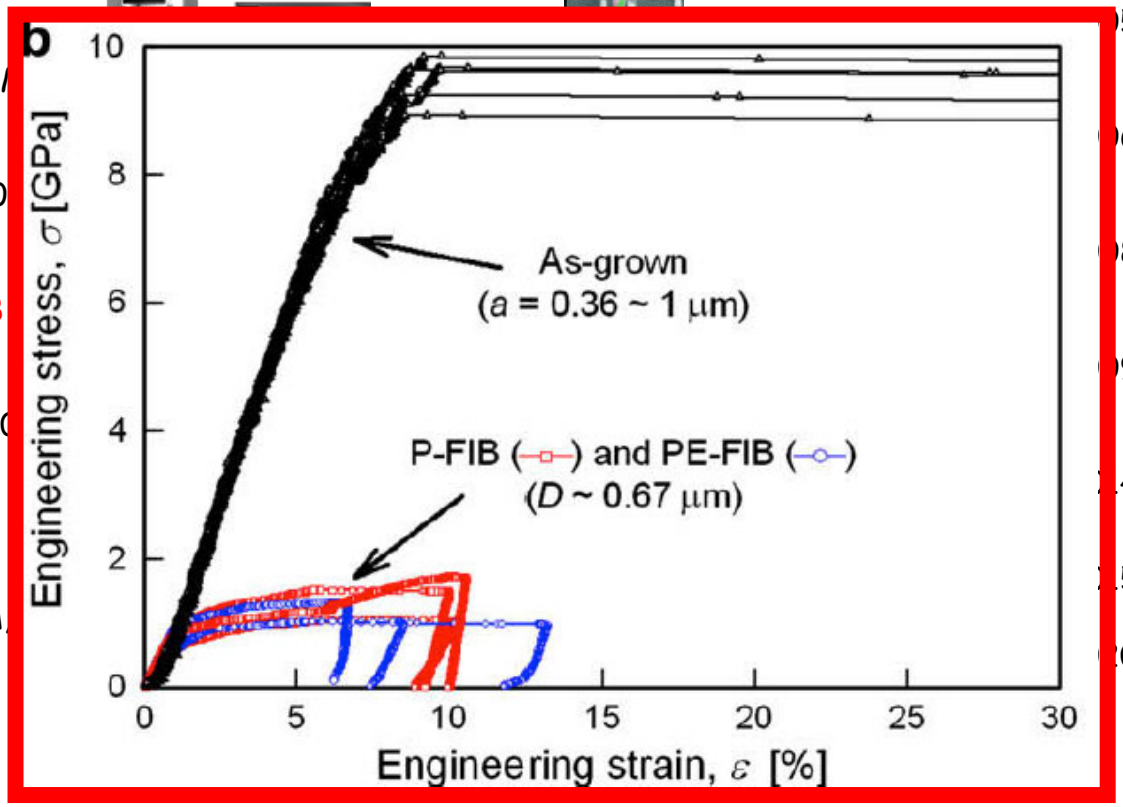

BULK

MINIATURE SAMPLE

NANO TESTING

IN-SITU

MICRO- SAMPLE

THEORETHICAL STRENGTH & BRITTLE IS DUCTILE

NUCLEATION VS STARVATION

FIB DAMAGE

seminal work in small scale mechanics

Empa
Materials Science and Technology

Hall 1951, Petch 1953

Pharr, J. Mater. Res. 1992

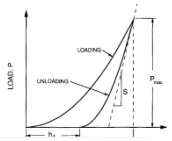

Rabe, Thin Solid Films, 2003

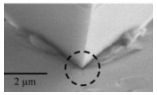

Maio, J. Mater. Res, 2005

Oestlund, Adv. Func,. Mater, 2

Kiener, Acta Mat, 2008

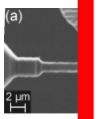

Pharr, Acta Mat 2008

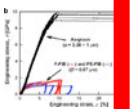

Schaedler, Science, 2011

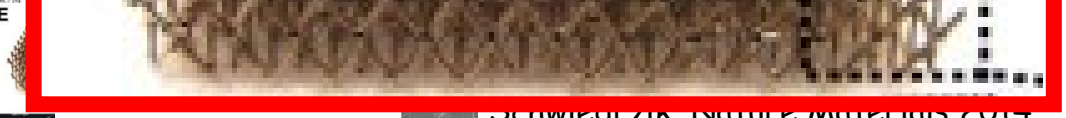

Meza, Science, 2014

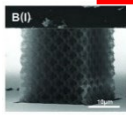

Gangaraj. Nature Com, 2018

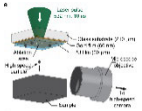

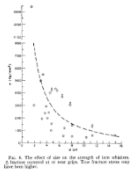

Brenner, J. Appl. Phys. 1956

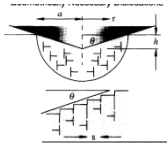

Nix, Met Trans A, 1989

Uchic, Science 2004

Schmidt, Nature Materials 2014

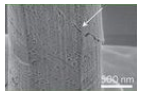

Tertuliano, Nature Materials, 2015

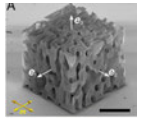

Portela, PNAS, 2020

BULK

MINIATURE SAMPLE

NANO TESTING

IN-SITU

MICRO- SAMPLE

THEORETHICAL STRENGTH & BRITTLE IS DUCTILE

NUCLEATION VS STARVATION

FIB DAMAGE

3D ARCHITECTURE

seminal work in small scale mechanics

Empa
Materials Science and Technology

Hall 1951, Petch 1953

Pharr, J.

Rabe, Thi

Maio, J. M

Oestlund,

Kiener, Ac

Pharr, Ac

Schaedler

Meza, Sci

Gangaraj.

Brenner, J. Appl. Phys. 1956

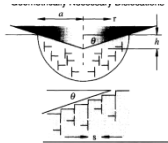

Nix, Met Trans A, 1989

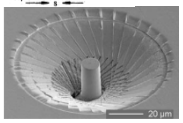

Uchic, Science 2004

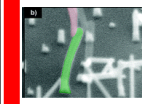

Hoffmann, Nanoletters, 2005

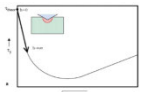

Lilleoden , Acta Mat, 2006

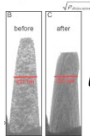

Minor, Nature Materials, 2008

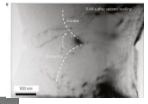

Oh, Nature Materials, 2009

Schwiedrzik, Nature Materials 2014

Tertuliano, Nature Materials, 2015

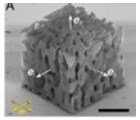

Portela, PNAS, 2020

BULK

MINIATURE SAMPLE

NANO TESTING

IN-SITU

MICRO- SAMPLE

THEORETHICAL STRENGTH & BRITTLE IS DUCTILE

NUCLEATION VS STARVATION

FIB DAMAGE

3D ARCHITECTURE

NATURAL MATERIALS

seminal work in small scale mechanics

Empa
Materials Science and Technology

Hall 1951, Petch 1953

Pharr, J. Mater. Res. 1992

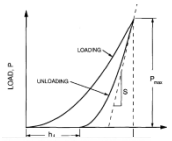

Rabe, Thin Solid Films, 2003

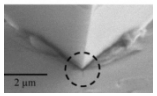

Maio, J. Mater. Res, 2005

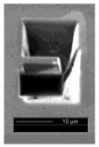

Oestlund, Adv. Func,. Mater, 2006

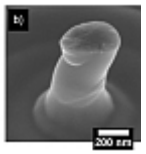

Kiener, Acta Mat, 2008

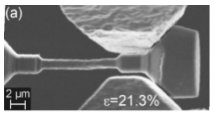

Pharr, Acta Mat 2008

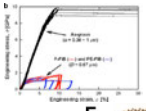

Schaedler, Science, 2011

Meza, Science, 2014

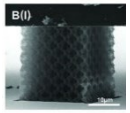

Gangaraj. Nature Com, 2018

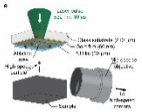

Brenner, J. Appl. Phys. 1956

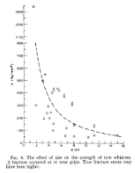

Nix, Met Trans A, 1989

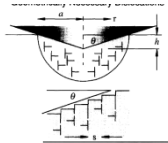

Uchic, Science 2004

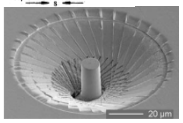

Hoffmann, Nanoletters, 2005

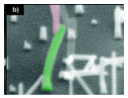

Lilleoden , Acta Mat, 2006

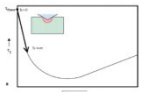

Minor, Nature Materials, 2008

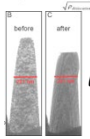

Oh, Nature Materials, 2009

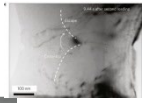

Schwiedrzik, Nature Materials 2014

Tertuliano, Nature Materials, 2015

Portela, PNAS, 2020

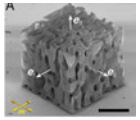

BULK

MINIATURE SAMPLE

NANO TESTING

IN-SITU

MICRO- SAMPLE

THEORETHICAL STRENGTH & BRITTLE IS DUCTILE

NUCLEATION VS STARVATION

FIB DAMAGE

3D ARCHITECTURE

NATURAL MATERIALS

@EXTREMES

DIFFRACTION

MODEL & METAMATERIALS

Size effects in materials

dimension of the physical phenomena involved => intrinsic length
micro-structural dimension => size parameter

Size Parameters:
Grain size D, Grain boundary width δ_b ,Obstacle spacing L, Obstacle radius R, Film thickness H

Characteristic lengths:
Equilibrium parameter of dislocation loop d, Spacing between partial dislocations w,
Width of magnetic domain wall d

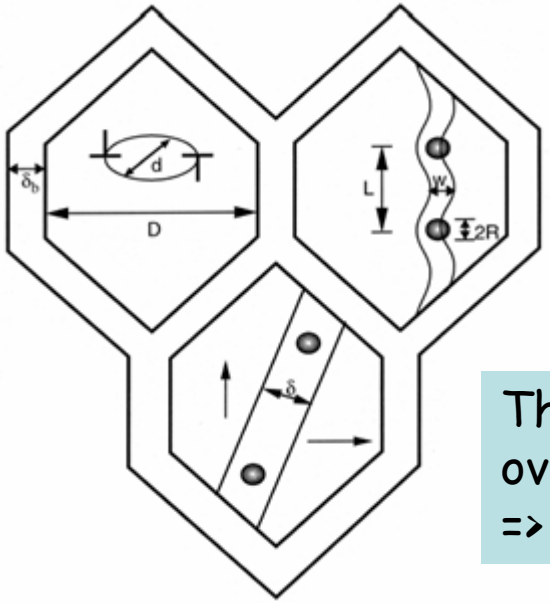

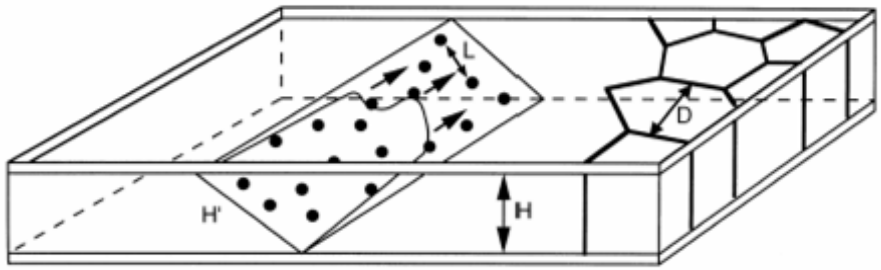

The range where charateristic lengths and size parameters overlap is of interest
=> conventional laws may break down

E. Arzt, Acta mater. 46(16), pp. 5611-5626, 1998

Material properties: static strength

Yield strength, elastic limit and ultimate strength

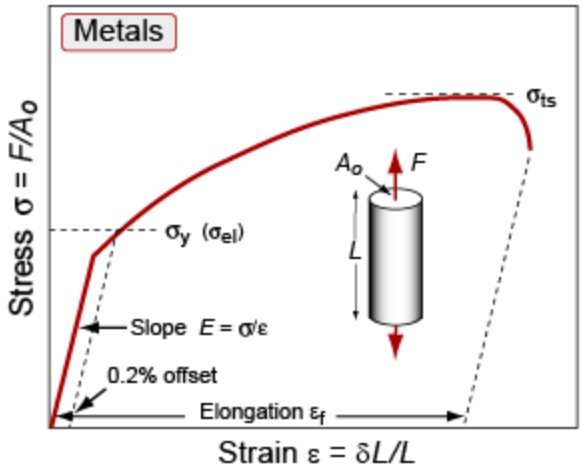

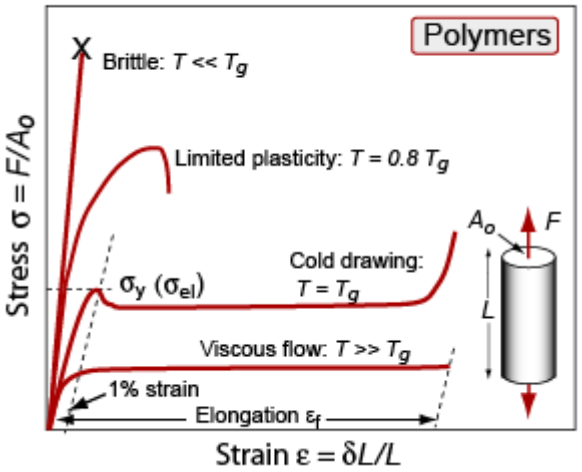

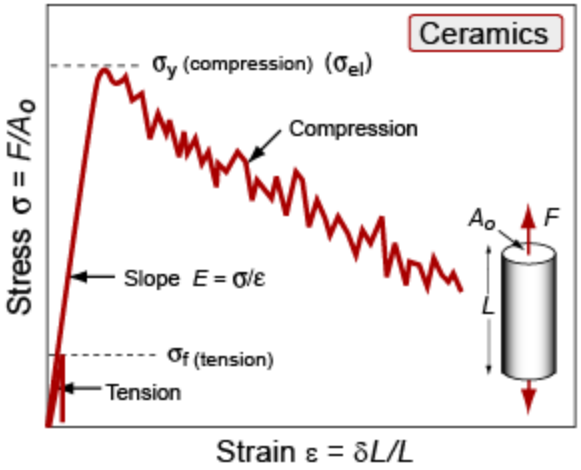

Definition of yield strength:

metals: 0.2% offset yield strength
polymers: 1% offset
polymer composites: 0.5% offset
ceramics and glasses: compressive strength

Origin of strength - yield strength limits

Range:
Theoretical strength: E/10
In applications: 0.01 MPa (foams) to 10GPa (diamond)

Mechanisms:
glide of dislocations in metals, slip of polymer chains, …
depends on temperature

Variability in strength:
Weibull statistics $P(V)=\exp(-\sigma/\sigma_0)^m)$

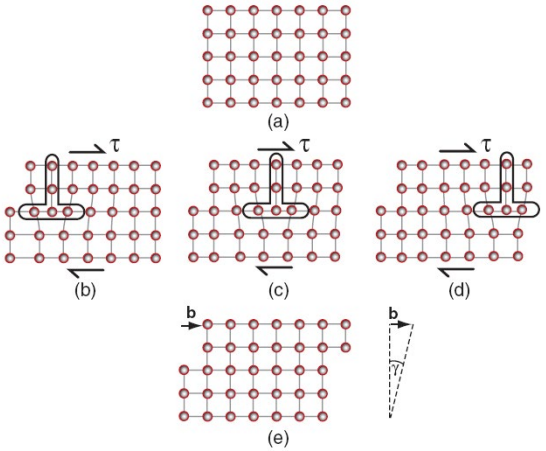

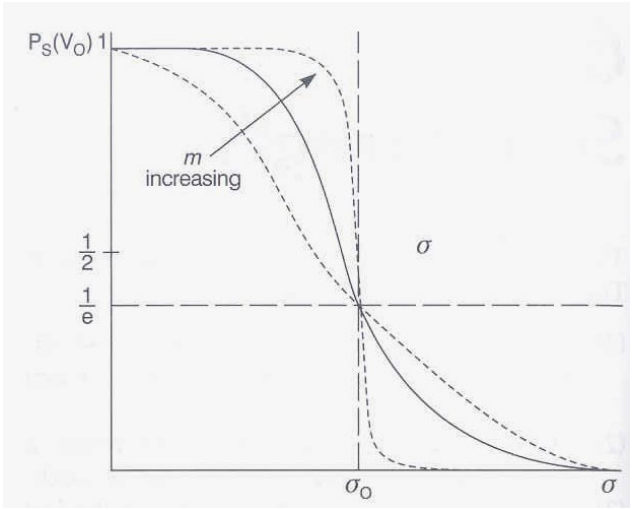

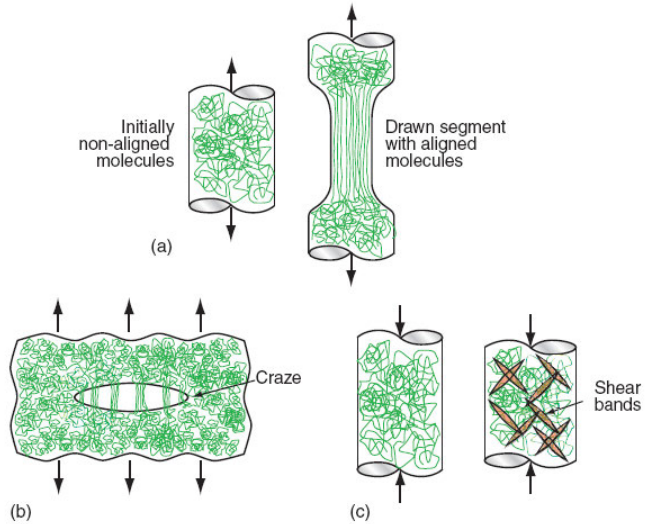

Strength: Mechanisms in crystals

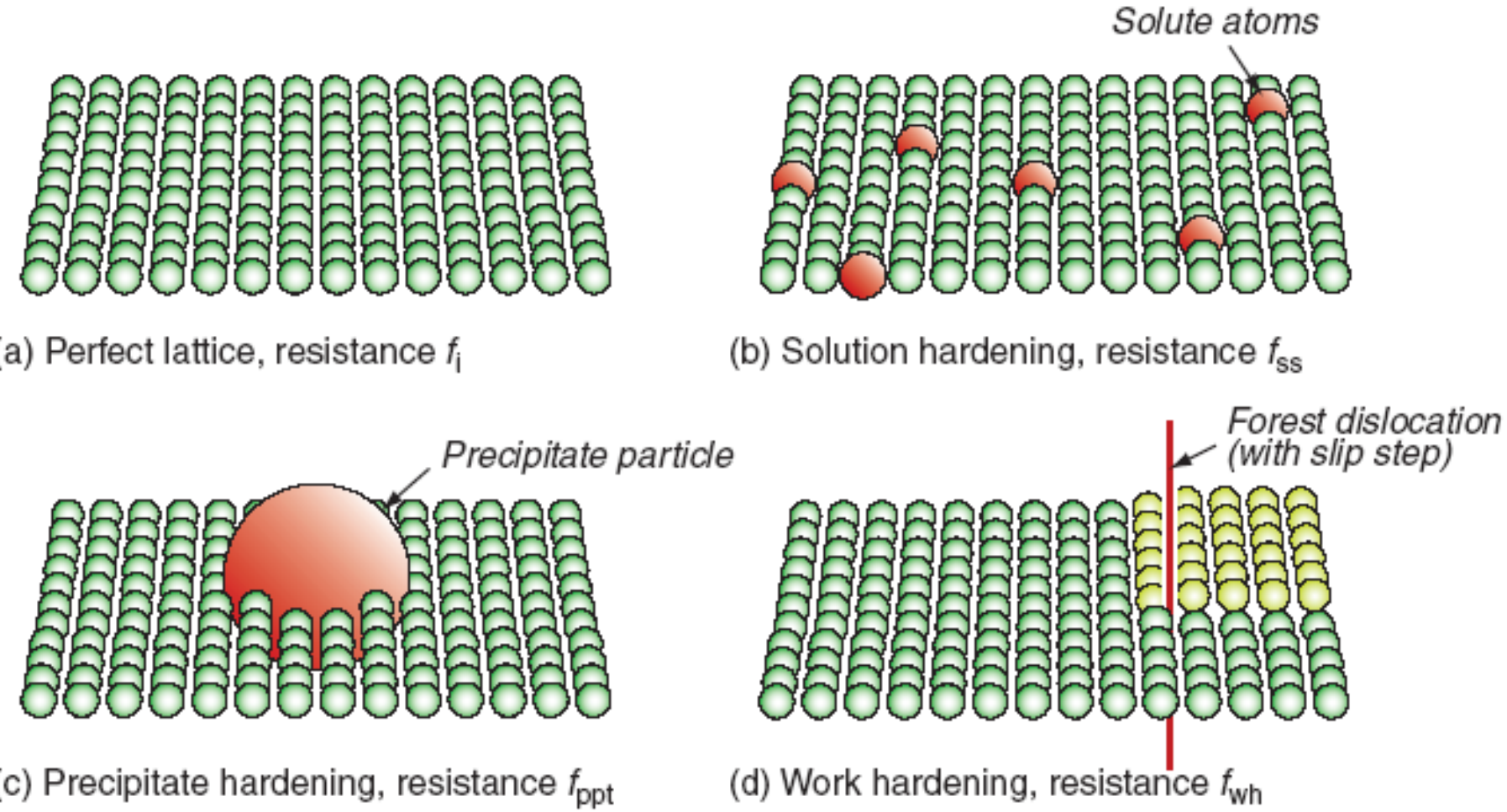

(a) Perfect lattice, resistance f_i

(b) Solution hardening, resistance f_{ss}

(c) Precipitate hardening, resistance f_{ppt}

(d) Work hardening, resistance f_{wh}

Strengthening by mechanisms

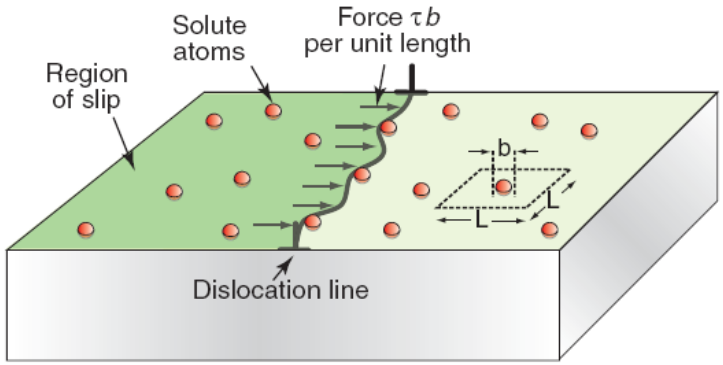

$$\tau_{ss} = \alpha E c^{1/2}$$

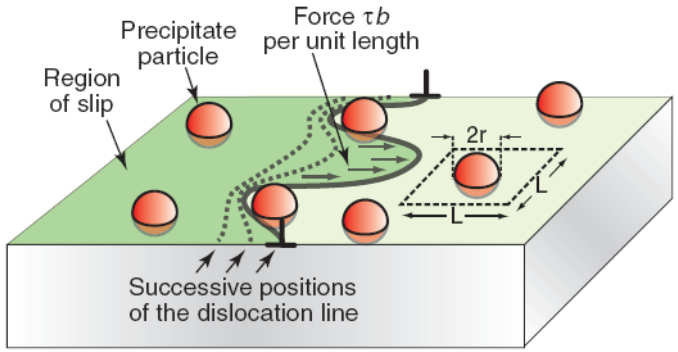

$$\tau_{ppt} = \frac{Eb}{L}$$

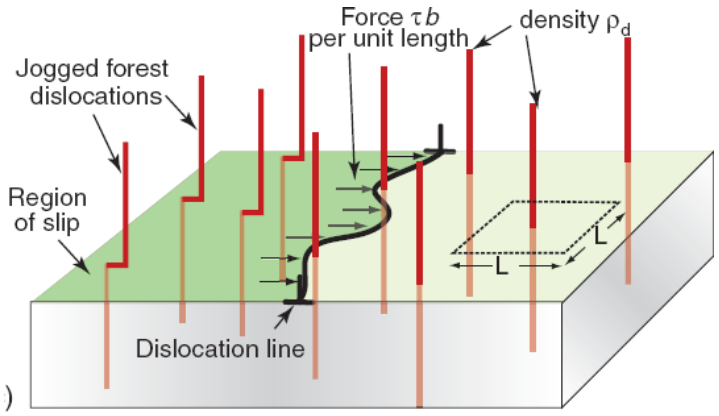

$$\tau_{wh} \approx \frac{Eb}{2}\sqrt{\rho_d}$$

Dislocations

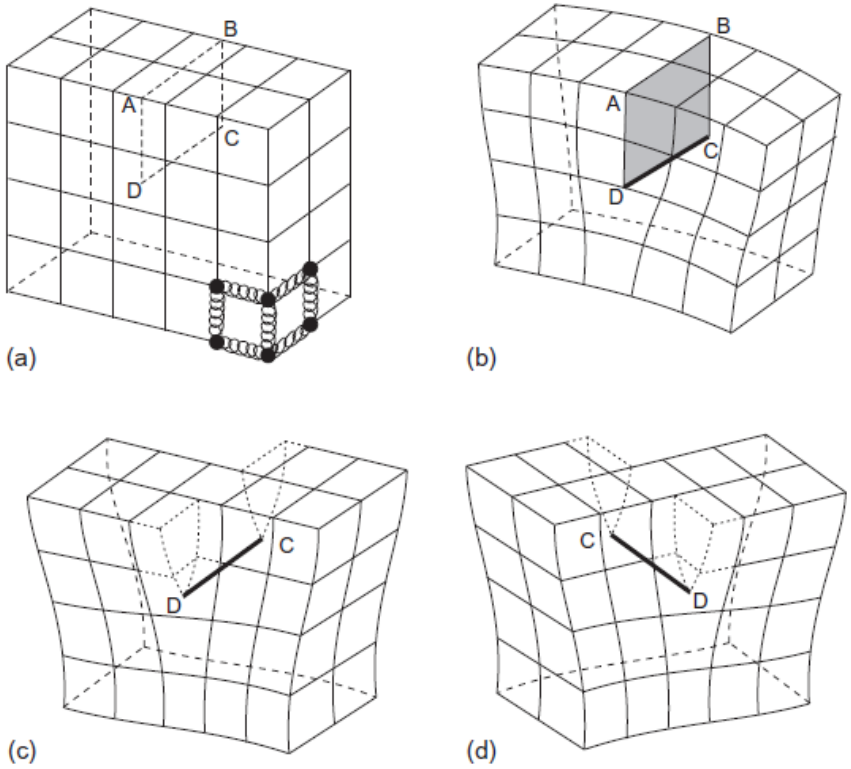

edge dislocation

screw dislocation

Hull and Bacon, Introduction to dislocations, 2010

Dislocation glide

- The effect of dislocation motion in a crystal: passage causes one half of the crystal to be displaced relative to the other. This is a *shear* displacement, giving rise to a *shear strain*.

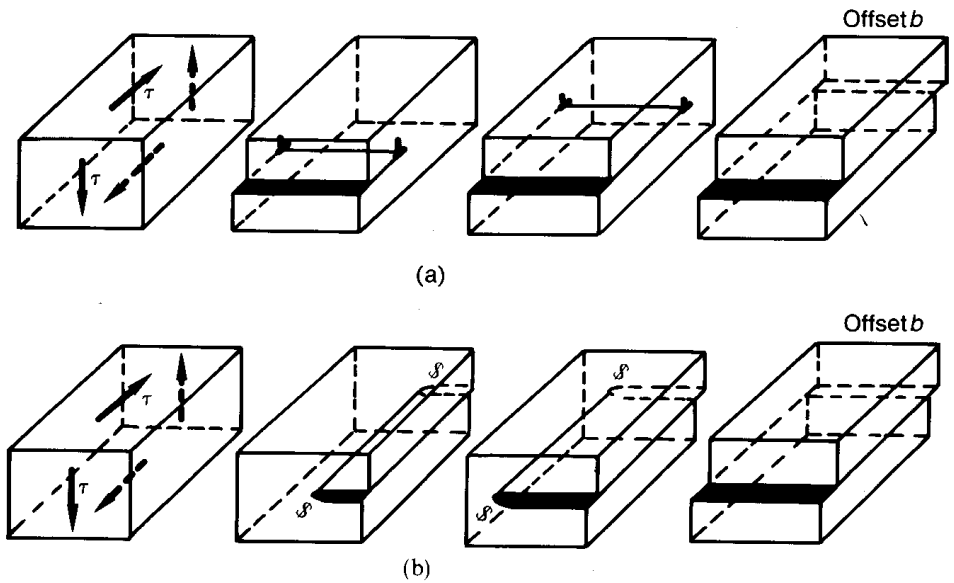

[Dieter]

Figure 5-4 (*a*) Macroscopic deformation of a cube produced by glide of an edge dislocation. (*b*) Macroscopic deformation of a cube produced by glide of a screw dislocation. Note that the end result is identical for both situations.

Resolved Shear Stress

- Geometry of slip: how big an applied stress is required for slip?
- Resolved shear stress: take the component of the tensile stress, P, along the slip direction which is given by $F\cos\lambda$,
  - divide by the area over which the shear force is applied, $A/\cos\phi$.

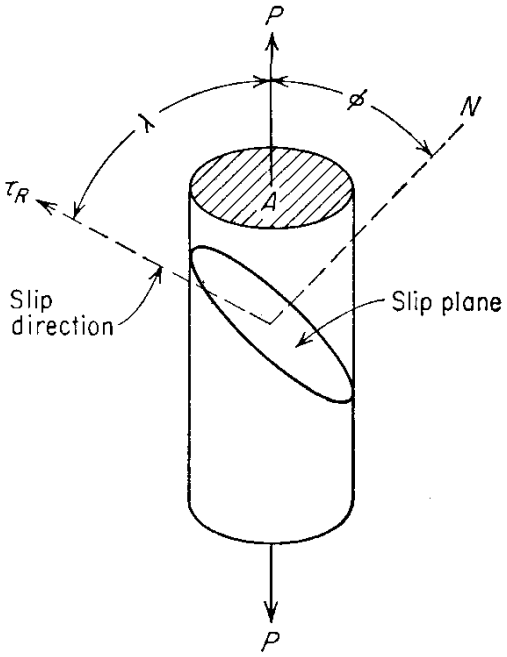

$$\tau_{CRSS} = (F/A)\cos\lambda\cos\phi = \sigma_y \underbrace{\cos\lambda\cos\phi}_{\text{Schmid factor} := m} = \sigma_y \times m$$

For FCC, random grains: m = 1/3.06

Peierls stress

- Lattice resistance, τ_{P}, at 0 K;
- Above, "lattice friction stress", $\tau_0 = \tau_{\mathrm{P}}\,(1\text{-}T/\,T_{\mathrm{m}})$

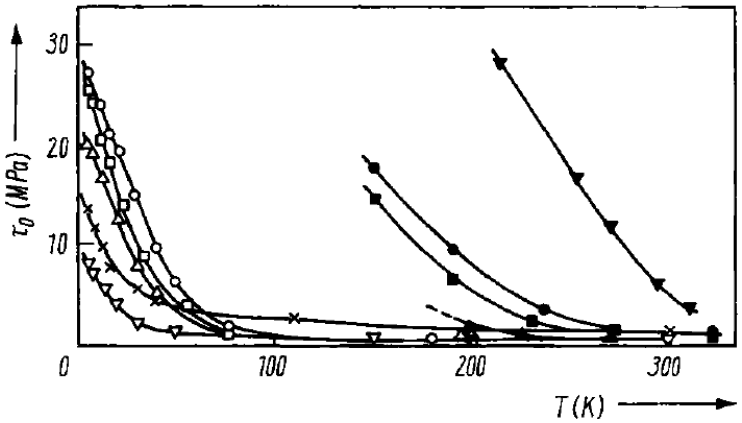

critical resolved shear stresses for slip on {110} and {100} planes. LiF: × {110}; NaCl: ▽ {110}, ▼ {100}; KCl: ○ {110}, ● {100}; KBr: □ {110}, ■ {100}; KI: △ {110}, ▲ {100}

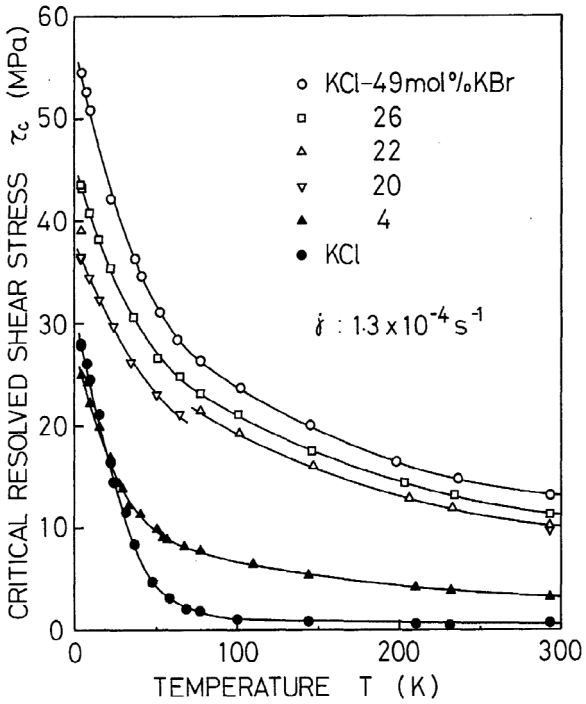

Kataoka, T. *et al.,* 1978 **Jpn. J. Appl. Phys. 17** 271
Skrotzki, W. et al., **Phys. Stat. Sol.**, 1981, 66, 2019

Peierls stress

- Calculations of Peierls stress:

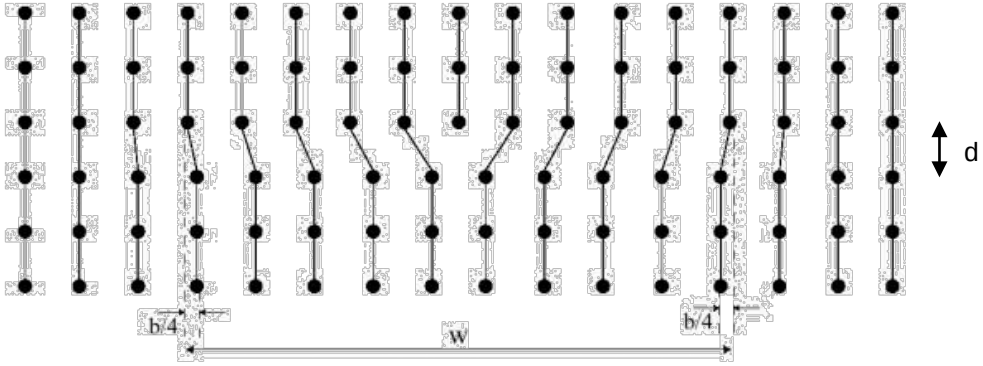

Isotropic elastic material

$$\tau_p = \frac{2G}{1-\nu}\exp\left(-\frac{2\pi d}{b(1-\nu)}\right)$$

- Shape of barrier is important:
  gradient = force

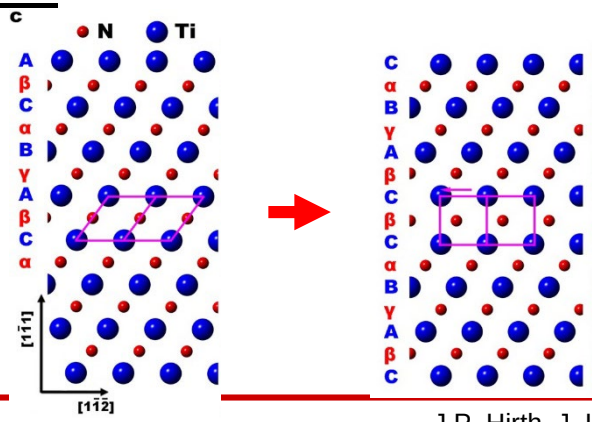

Dislocations in TiN: DFT @ 0 K !!!!

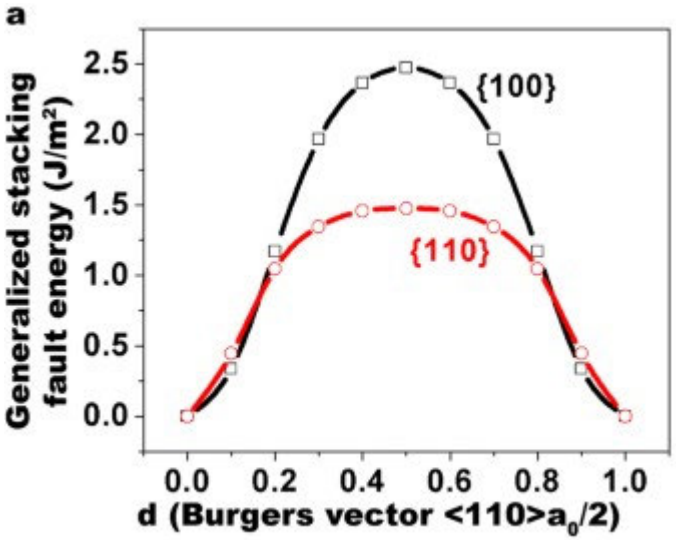

J.P. Hirth, J. Lothe, Theory of Dislocations
Li, N. et al., **Sci Rep**, 2015, 5, 15813

Peierls stress

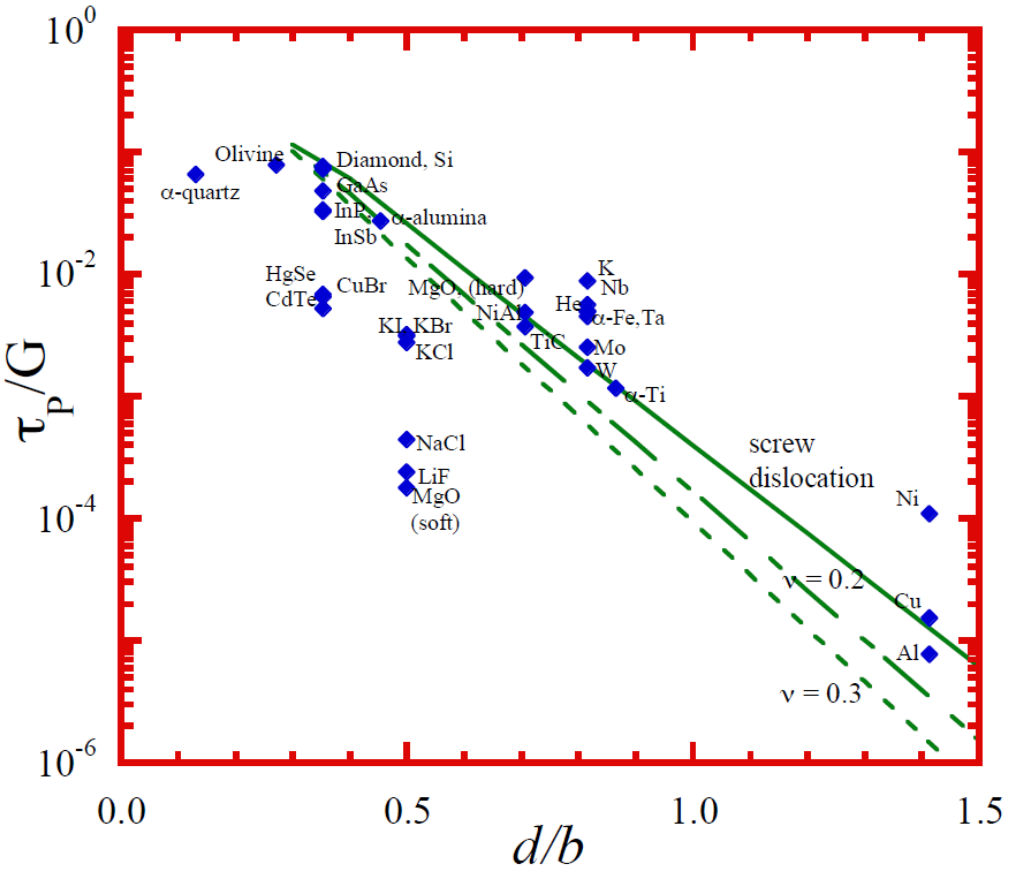

Isotropic elastic material

$$\tau_p = \frac{2G}{1-\nu}\exp\left(-\frac{2\pi d}{b(1-\nu)}\right)$$

Non-isotropic material

$$\tau_p = \frac{2G}{1-\nu}\exp\left(-\frac{4\pi w}{b}\right).$$

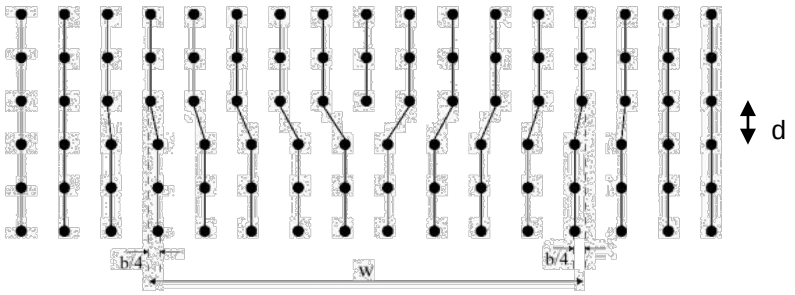

Dislocation interactions

- Kinks and jogs = sessile
- Forest of dislocations develops

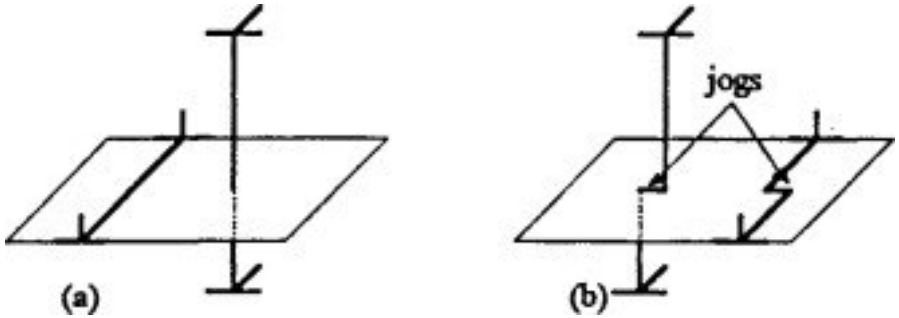

304 SS

α-Ti

Intrinsic size effect – dislocation spacing

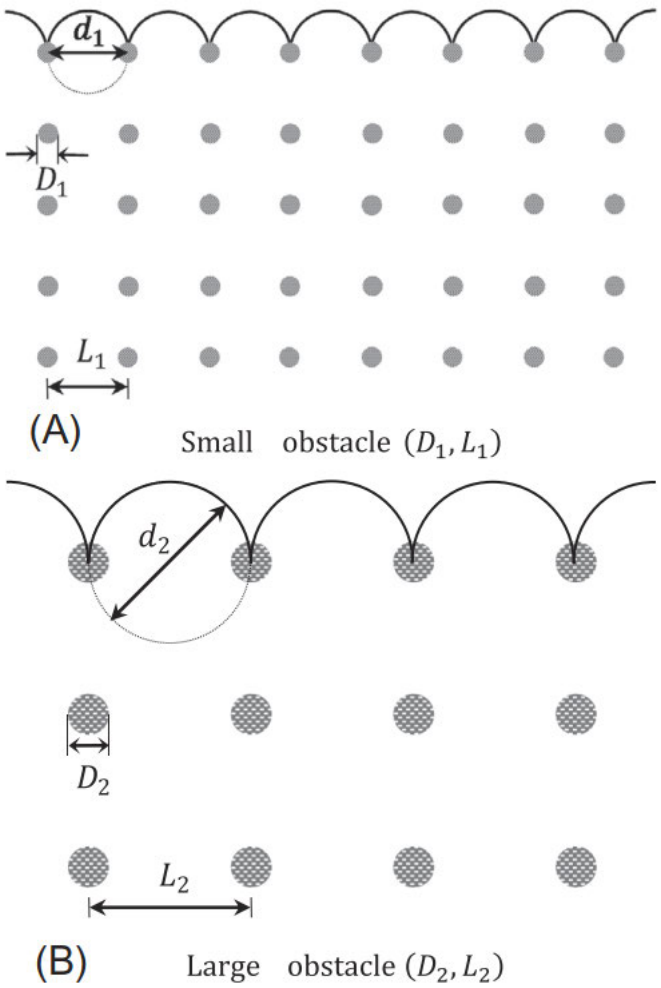

Some other microstructural equations can be reproduced using the Orowan mechanism. For example, the Taylor hardening model relates the shear strength to the dislocation density ρ as follows:

$$\tau = \alpha G b \sqrt{\rho}$$

where α is a material parameter. In this case, the obstacles are forest dislocations and the obstacle spacing can be approximated by average dislocation source length L_{ave}, which can be obtained as follows:

$$L_{\text{ave}} = \frac{1}{\sqrt{\rho}}$$

Therefore from above:

$$\tau = \frac{Gb}{L_{\text{ave}}} = Gb\sqrt{\rho}$$

However, one should notice that the forest dislocations as obstacles are penetrable. Accordingly we should use a reduction factor $\alpha < 1$ as follows:

$$\tau = \alpha G b \sqrt{\rho}$$ **Work hardening!**

G.Z. Voyiadjis and M. Yaghoobi. (2018)

Dislocation multiplication – Frank-Read source

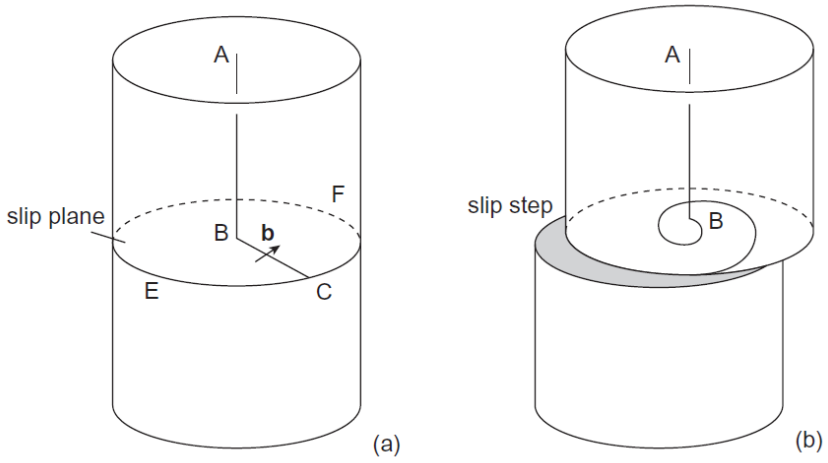

Single ended Frank-Read source.

(a) Dislocation lying partly in slip plane CEF.

(b) Formation of a slip step and spiral dislocation by rotation of BC about B.

Each revolution around B produces a displacement b of the crystal above the slip plane relative to that below.

The process is regenerative since it can repeat itself so that n revolutions will produce a displacement nb.

A large slip step will be produced at the surface of the crystal

Hull and Bacon, Introduction to dislocations, 2010

Dislocation multiplication – Frank-Read source

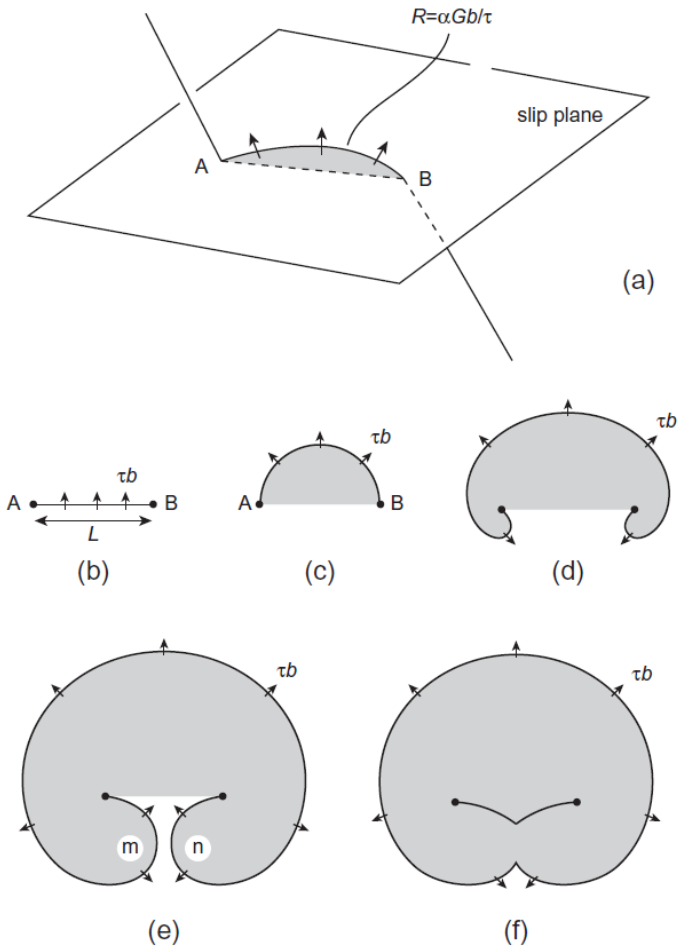

The dislocation segment is held at both ends by dislocation intersections, precipitates etc.

An applied resolved shear stress τ exerts a force τb per unit length of line and tends to make the dislocation bow

The radius of curvature R depends on the stress.

$$\tau_0 = \frac{\alpha G b}{R}$$

as τ increases, R decreases and the line bows out until the minimum value of R is reached at the position illustrated in Fig. c

Here, R equals L/2, where L is the length of AB, and the stress is

$$\tau_{max} = Gb/L$$

Hull and Bacon, Introduction to dislocations, 2010

Mechanical properties of nanocrystalline solids

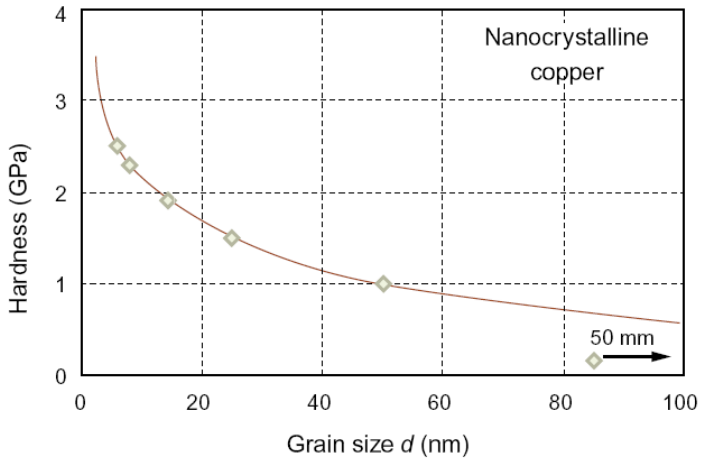

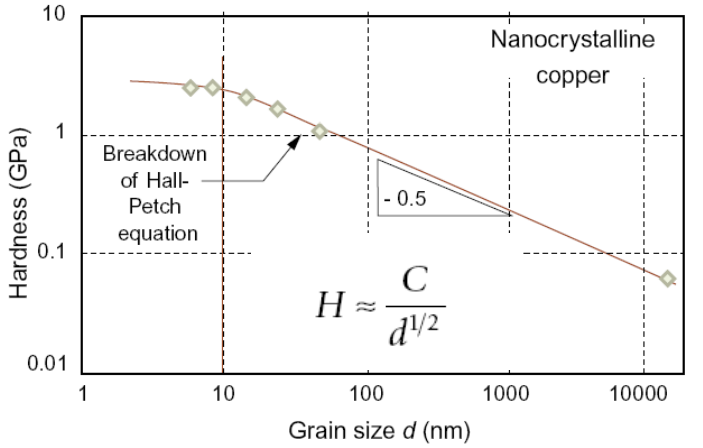

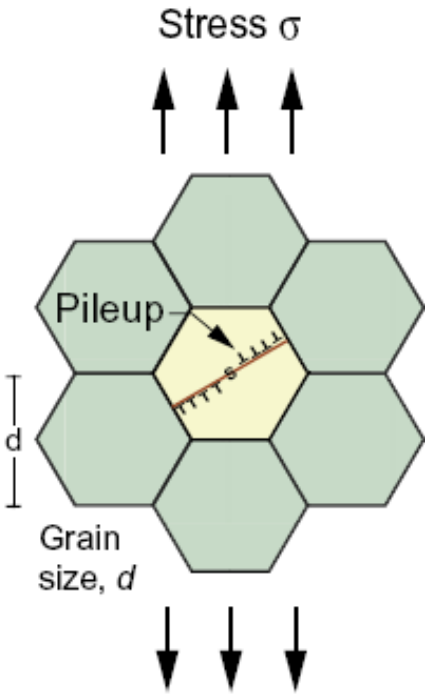

Intrinsic size effect – grain size

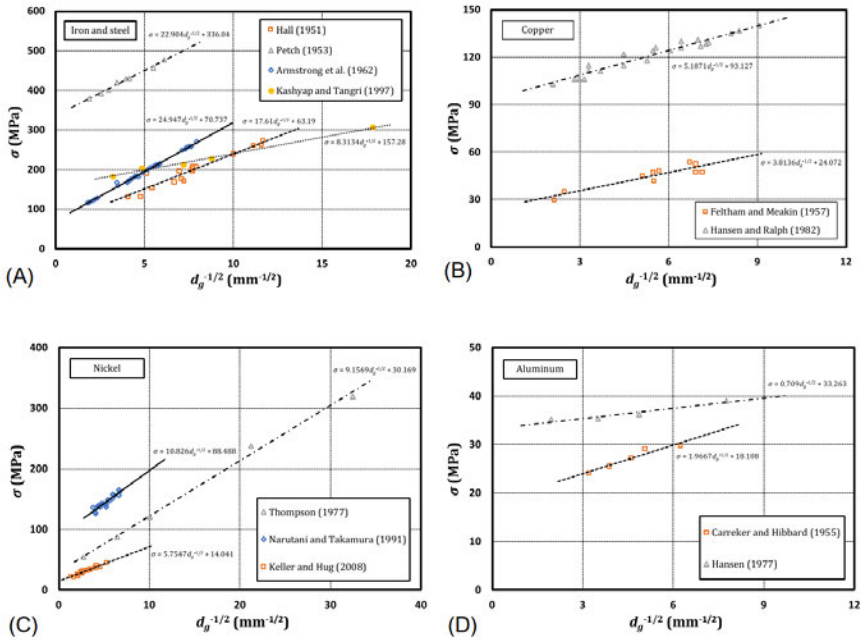

Following the studies of Hall (1951) and Petch (1953), the general equation for the dependency of the material strength on grain size can be described as follows:

$$\sigma = \sigma_0 + K_{HP} d_g^{-x}$$

here σ is the yield or flow stress, σ_0 is the corresponding stress for a very large grained bulk material or bulk single crystals, and K_{HP} is a material constant. The exponent x is a constant, where $0 < x < 1$.

Many different experimental and theoretical studies have been performed to obtain the appropriate values of σ_0, K_{HP}, and x.

G.Z. Voyiadjis and M. Yaghoobi. (2018)

Intrinsic size effect – grain size

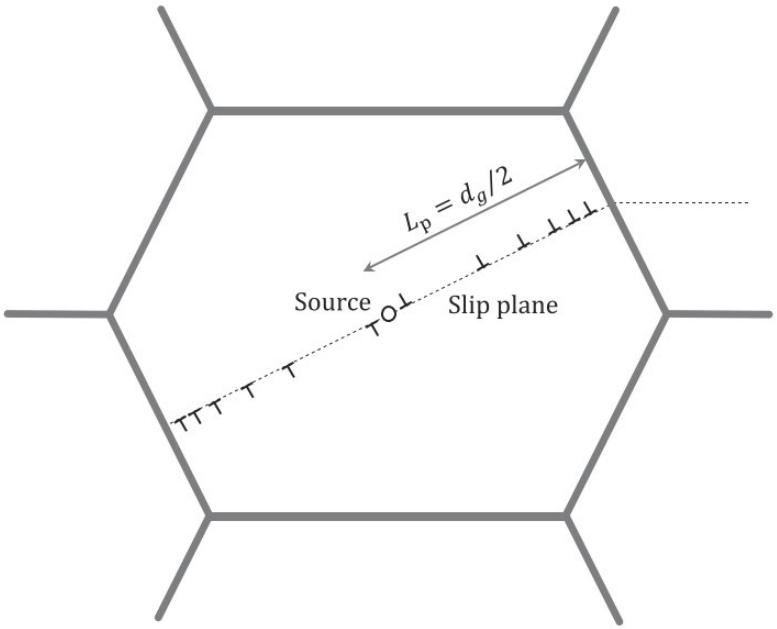

The **pile-up model** states that the dislocations are moving inside the grain until they reach the grain boundary that stops their movement.

Since the dislocations cannot pass the grain boundary because of the mismatch between grains, the grain boundary acts as an obstacle.

The dislocations form a pile- up behind the grain boundary with the length L_p ($L_p = d_g/2$). The pile-up process continues until the stress concentration induced by the array of dislocations τ_p reaches a critical value of τ_{cr}. At this moment, the dislocations will pass the grain boundary and material yield occurs.

Dislocation slip occurs as soon as the shear stress becomes larger than τ_0. The dislocations will be subjected to the slip stress τ_s which is

$$\tau_s = \tau - \tau_0$$

The pileup stress induced by blocked dislocation can be calculated as follows:

$$\tau_p = n\tau_s$$

Intrinsic size effect – grain size

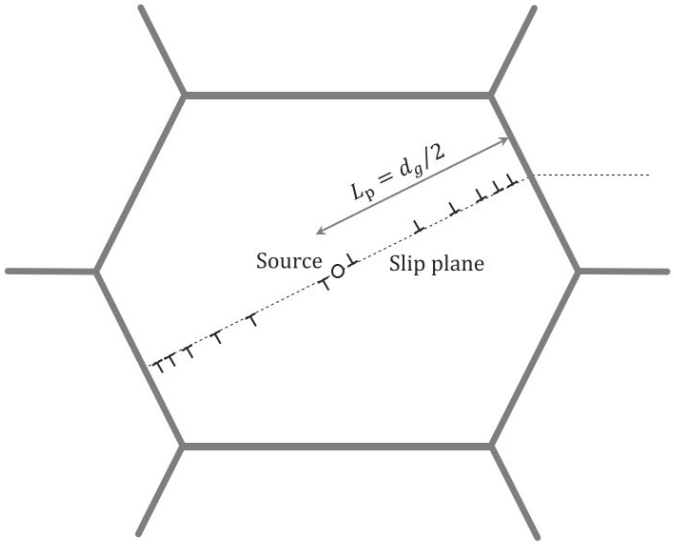

The number of dislocations n can be related to the pile-up length L_p as follows:

$$n = \frac{\tau_s L_p b}{T}$$

The material yields at $\tau_p = \tau_{cr}$. Accordingly, τ_s at yield can be calculated as follows:

$$\tau_s = \left(\frac{\tau_{cr} T}{L_p b}\right)^{1/2} \qquad \tau_p = n\tau_s$$

The shear stress at which the material yields τ_y can be obtained using

$$\tau_y = \tau_0 + \left(\frac{\tau_{cr} T}{L_p b}\right)^{1/2} \xrightarrow{L_p = d_g/2} \tau_y = \tau_0 + \left(\frac{2\tau_{cr} T}{d_g b}\right)^{1/2}$$

For crystalline metals, the relation between the flow stress σ_y and shear stress τ_y can be described as follows

$$\sigma_y = A\tau_y$$

where A is the Taylor factor (inverse of Schmid). Assuming $T = \alpha G b^2$, where α is a constant of the order of unity it follows

$$\sigma_y = \sigma_0 + \left(\frac{2\bar{\alpha} G \tau_{cr} b}{d_g}\right)^{1/2}$$

Comparing with the Hall-Petch relation yields, x = 1/2 and

$$K_{HP} = A(2\bar{\alpha} G \tau_{cr} b)^{1/2}.$$

$$\sigma = \sigma_0 + K_{HP} d_g^{-x}$$

Intrinsic size effect – grain size

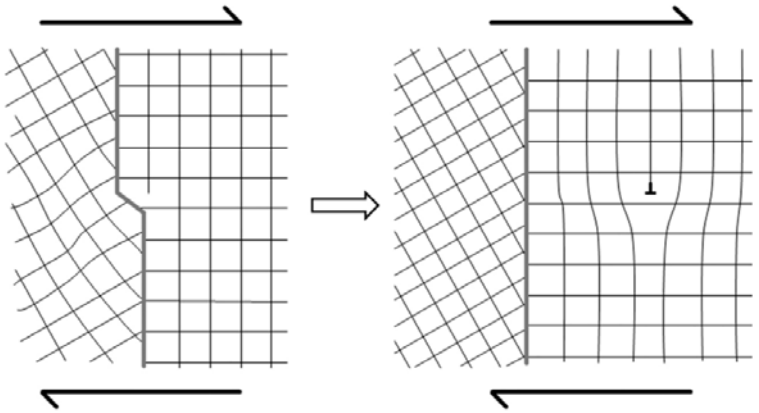

Other models that justify the Hall-Petch effect:

a) dislocation **nucleation from grain boundary ledges.** In this model, it is assumed that the yield stress is the one required to move the forest dislocations, which are nucleated from the grain boundary ledges, inside the grain.

b) **Dislocation density model.** In this model, it has been assumed that the dislocation mean free path has a linear relation with the grain size.

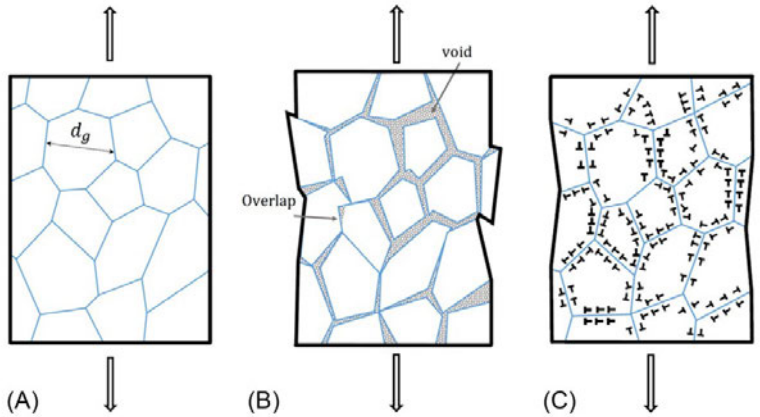

G.Z. Voyiadjis and M. Yaghoobi. (2018)

c) **The non-homogenous plastic deformation model** incorporated the concept of geometrically necessary dislocations (GNDs). The deformation in the sample is divided into two parts; a uniform deformation provided by the dislocation movement inside the grain, and a non- homogenous deformation which is the result of GNDs slip to produce the compatible deformation pattern between grains

d) **Confined layer slip model** (CLS, see later)

Intrinsic size effect – inverse Hall Petch

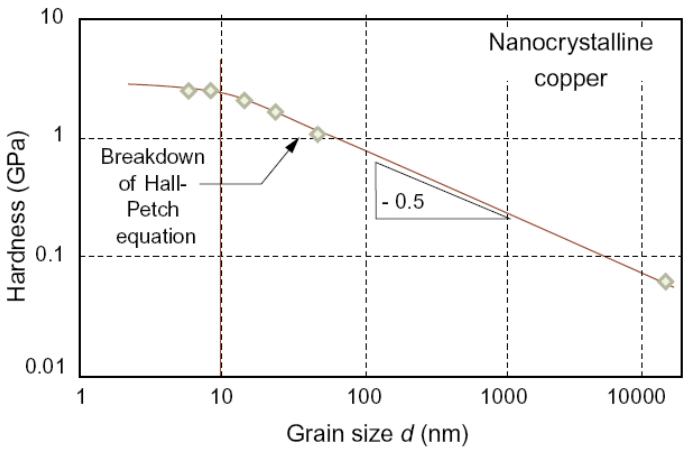

As the grain size decreases, two typical behaviors have been reported.

One trend states that the material yield or flow stress reaches a plateau for smaller grain sizes.

The other trend states that after some critical grain
size, the material yield or flow stress decreases as the grain size decreases, which
is commonly known as the inverse Hall-Petch effect.

Intrinsic size effect – inverse Hall Petch

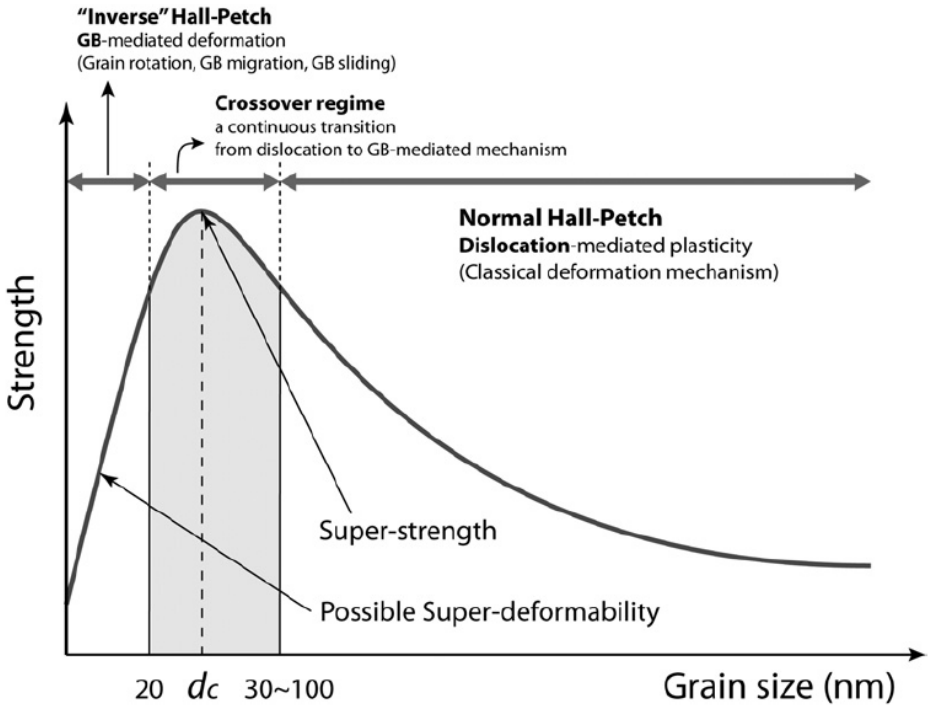

Plastic deformation of crystalline materials involves a wide range of interaction phenomena between dislocations and grain boundaries, which are still subject to extensive research.

When the grains are reduced to 40 nm they cannot accommodate multiple lattice dislocations, which engages alternative plastic deformation mechanisms like grain-boundary sliding, partial dislocation emission and absorption at grain boundaries.

At grain sizes below 20 nm, the Hall–Petch relation gives way to the so-called "inverse" Hall–Petch, due to the activation of grain boundary-assisted deformation.

J.R. Greer, J.Th.M. De Hosson / Progress in Materials Science 56 (2011) 654–724

Intrinsic size effect – inverse Hall Petch

Nanocrystalline materials are structurally characterized by a large volume fraction of grain boundaries.

As the grain size is decreased, an increasing fraction of atoms can be ascribed to the grain boundaries.

Different deformation mechanisms have been proposed to capture the deviation from the Hall-Petch relation including the

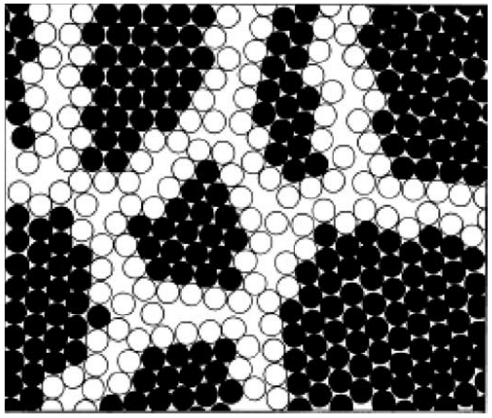

Diffusional creep
breakdown in pile-up model
grain boundary sliding
phase mixture model
grain coalescence
shear band formation

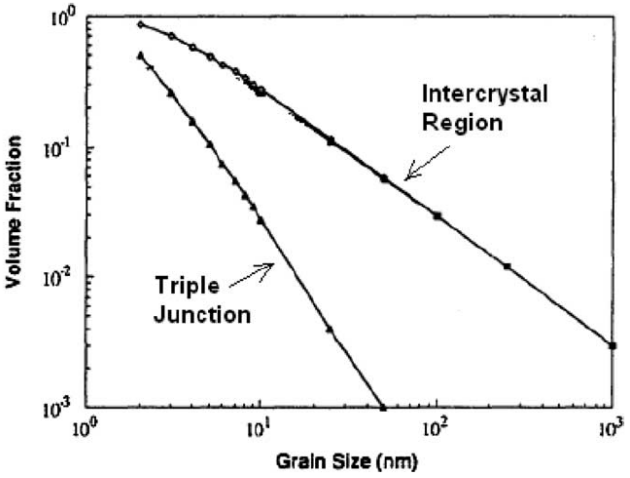

G.Z. Voyiadjis and M. Yaghoobi. (2018)
M.A. Meyers et al. / Progress in Materials Science 51 (2006) 427–556

Intrinsic size effect – inverse Hall Petch

The inverse Hall-Petch was firstly reported by Chokshi et al. (1989) in which they studied the effects of grain size on the Vickers microhardness for nanocrystalline copper and palladium. They attributed the inverse Hall-Petch effect to the **diffusional creep** occurring at room temperature for nanocrystalline materials.

They incorporated the Coble creep as the governing mechanism of deformation as follows

$$\dot{\varepsilon} = \frac{150\Omega\delta D_{gb}\sigma}{\pi k T d_g^3}$$

where ε̇ is the strain rate, Ω is the atomic volume, δ is the width of the grain boundary, D_{gb} is the diffusion coefficient of grain boundary, σ is the applied stress, k is the Boltzmann's constant, and T is the absolute temperature.

G.Z. Voyiadjis and M. Yaghoobi. (2018)

Intrinsic size effect – inverse Hall Petch

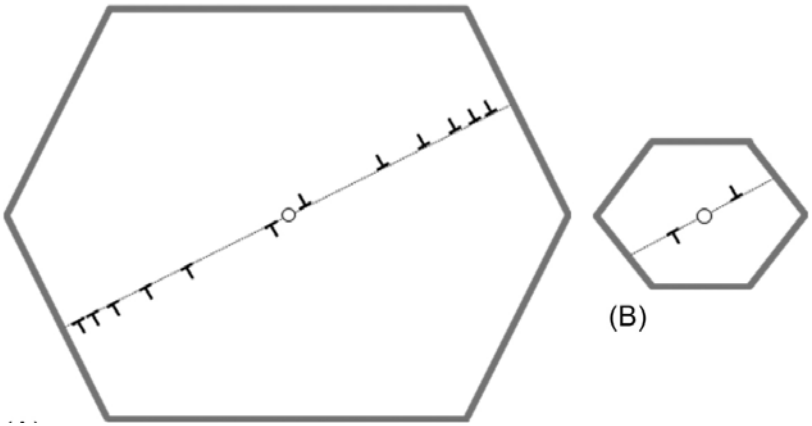

The stress concentration due to this pile-up against the grain boundary is the driving force of the pile-up model.

As the grain size decreases, the number of dislocations inside the grain also drops. Accordingly, there is a grain size at which the number of dislocations are so few that **the pile-up theory breaks down.**

G.Z. Voyiadjis and M. Yaghoobi. (2018)

Intrinsic size effect – inverse Hall Petch

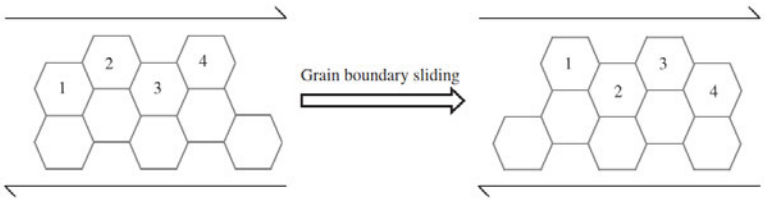

Grain boundary sliding has been introduced as one of the underlying mechanism of superplasticity and the combination of grain boundary sliding with diffusion creep, grain boundary migration, or dislocation slip and/or climb have been identified as superplasticity mechanisms.

As the grain size decreases, the number of dislocations fit in the grains decreases. Accordingly, the applied plastic flow cannot be sustained by the dislocations slip inside, and other mechanisms should govern the deformation process **such as diffusion or grain boundary shear**.

$$\tau_{\mathrm{GBS}} = \frac{1}{3}\left[L\frac{\rho_{\mathrm{m}}}{M_{\mathrm{Cu}}}\left(1-\frac{T}{T_{\mathrm{m}}}\right)f_{\mathrm{g}} + \left(\frac{\dot{\varepsilon}_{\mathrm{GBS}}}{\dot{\varepsilon}_{\mathrm{tot}}}-1\right)\frac{kT}{b^3}\right]$$

G.Z. Voyiadjis and M. Yaghoobi. (2018)

Twinning

- Cooperative shear
- In FCC: mediated by Shockley partial dislocations
  - 1/6<11$\bar{2}$>{111}
- In HCP: ask Nicoló

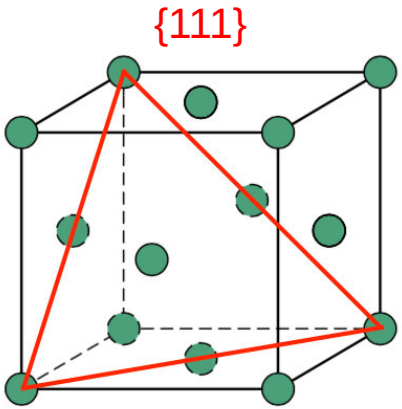

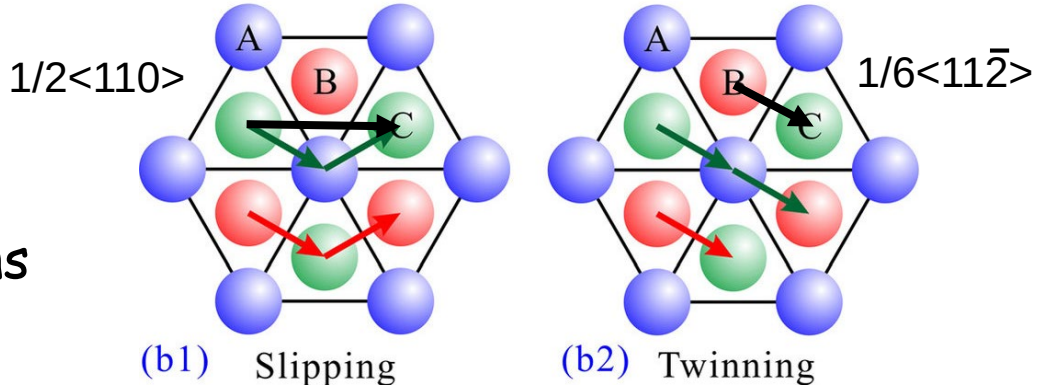

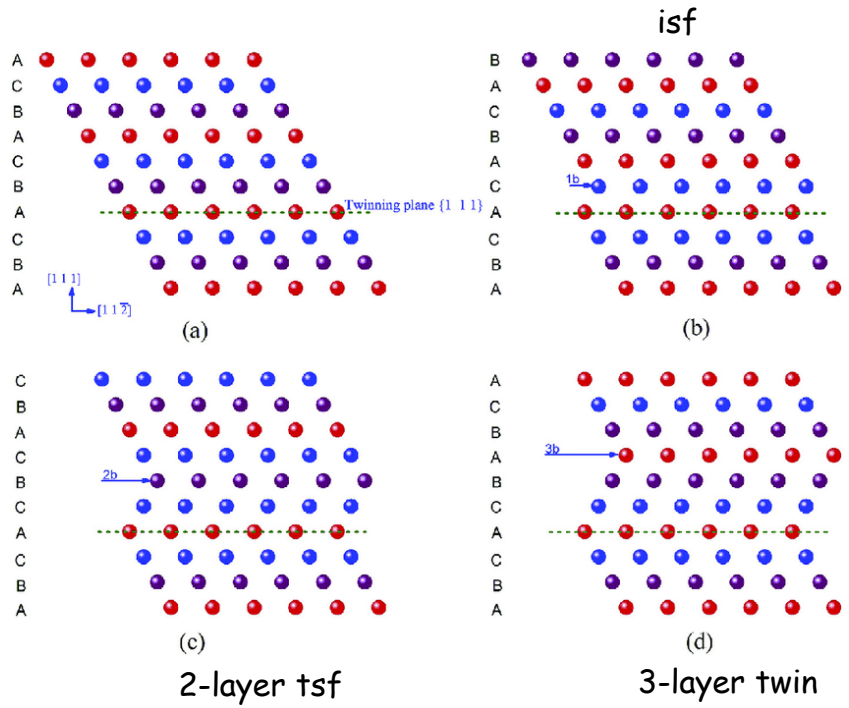

Kibey, S. et al., **Scripta Materialia**, 2007, 55, 6843-6851

Nanotwinned materials

- Stacking fault energy
- Make by
  - ECAP, torsion
  - Pulsed electroplating
  - Magnetron sputtering

	Materials	γ^{SF} (mJ/m^2)
Pure Metals	Pb	6-10
	Ag	16
	Au	32-46
	Cu	45
	Ni	125
	Al	166
	Pd	180
	Pt	322
Alloys	γ-TiAl	173
	CuNi	45-110
	FeCrNi	32-46
	Stainless steels	20-50
	FeNiCoCr	30
	FeNiCoCrMn	20-25
	CuZn	7-45
	CuAl	5-35
	$Fe_{30wt\%}Mn$	15
	$Cu_{12.1at\%}Al_{4.1at\%}Zn$	7

nt-Ag, sputtered

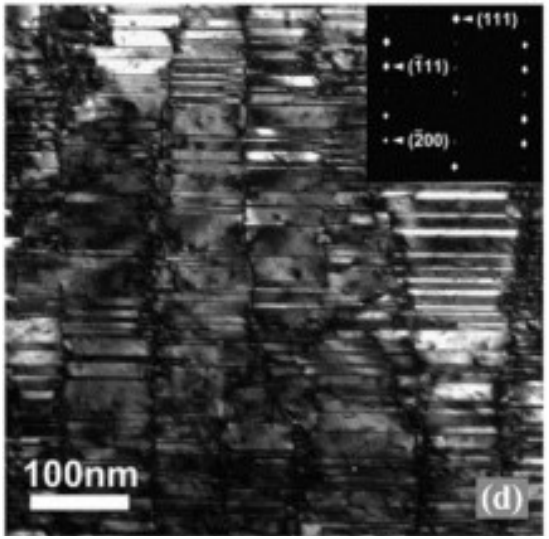

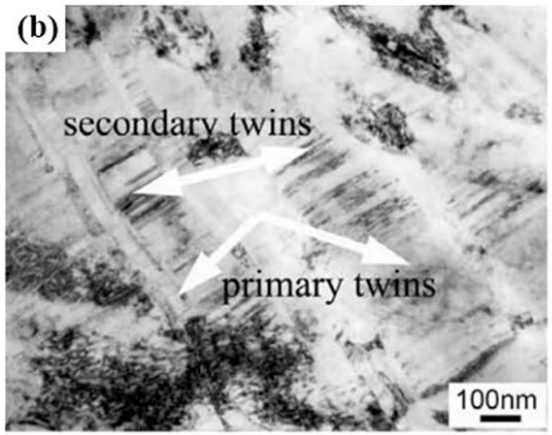

Cu-Al, ECAP

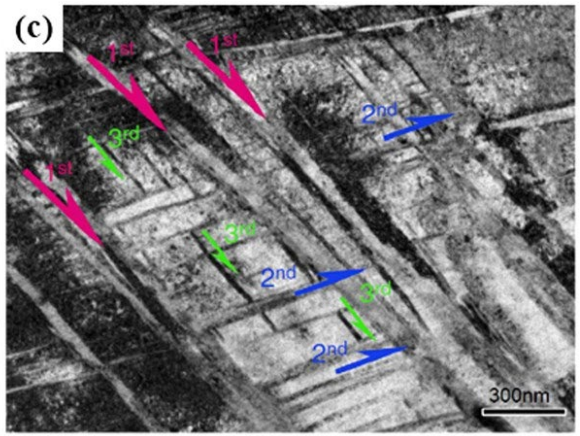

TWIP steel, torsion

Nanotwinned materials

- Stacking fault energy
- Make by
  - ECAP, torsion
  - Pulsed electroplating
  - Magnetron sputtering

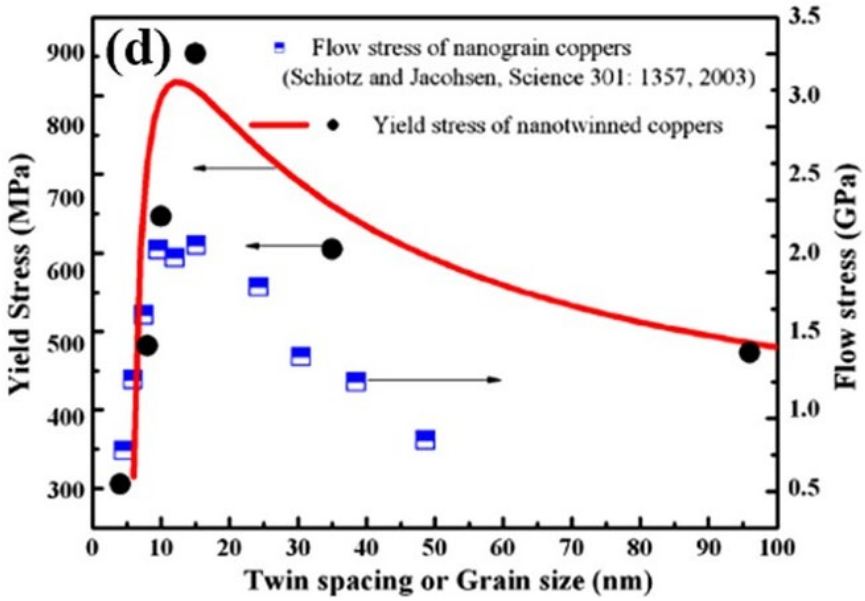

- Strength: competition between:
  - Pile-up type strengthening
  - Detwinning of the nanotwins
  - [or dislocation nucleation at the TB-GB junctions]

$$\sigma_{\mathrm{HP}} = \sigma_0 + k_{\mathrm{HP}}/\sqrt{\lambda}$$

$$\sigma_{\mathrm{detwinnning}} = M\left[\frac{2.28E_0\lambda}{\pi Rh} - \frac{\gamma_{\mathrm{isf}}}{h} + \left(\frac{\dot{\varepsilon}_{\mathrm{DT}}}{\dot{\varepsilon}_{\mathrm{tot}}} - 1\right)\frac{2kT}{\pi R^2 h}\right]$$

$$\sigma_{\mathrm{DN}} = M\left[\frac{\Delta U}{S^*V^*} - \frac{kT}{S^*V^*}ln\left(\frac{d\nu_{\mathrm{D}}}{\lambda\dot{\varepsilon}}\right)\right]$$

Solid solution strengthening

- Substitutional
- Interstitial

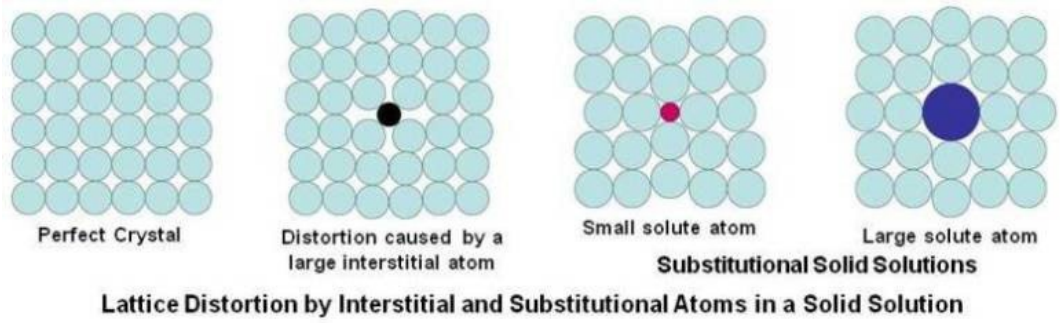

Lattice Distortion by Interstitial and Substitutional Atoms in a Solid Solution

- Key idea: local distortion of lattice

$$\Delta\tau_{SSS} = Gb\epsilon^{3/2}c^{1/2}$$

$$\epsilon = \left|\frac{\Delta G}{G\Delta c} - \beta\frac{\Delta a}{a\Delta c}\right|$$

i.e. the distortions in atomic positions and elastic moduli

Solid solution strengthening

- Arrangement of solutes along the dislocation line
- Interstitials
  - C in steel: Cottrell atmorpheres
  - Lüders bands, Portevin-Le Chatelier
  - Hinder formability

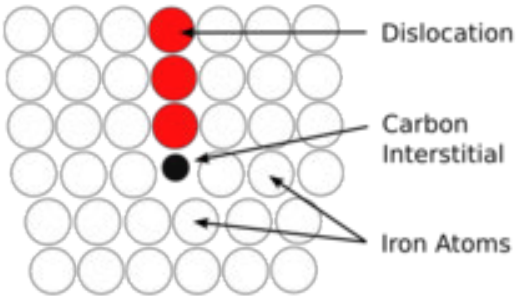

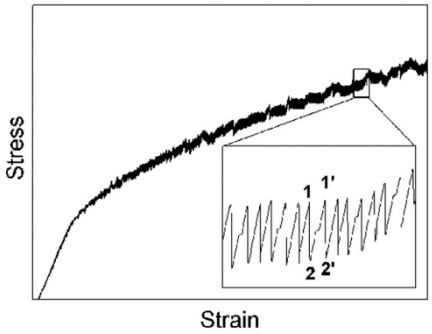

- But also substitutionals:
  - Ni superalloy:

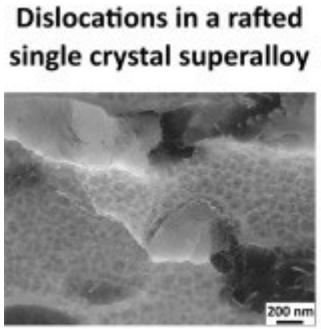

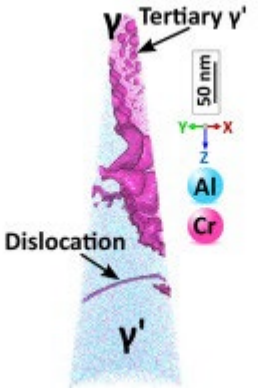

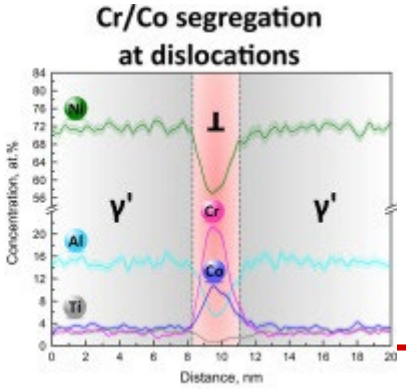

Solid solutions: Complexions

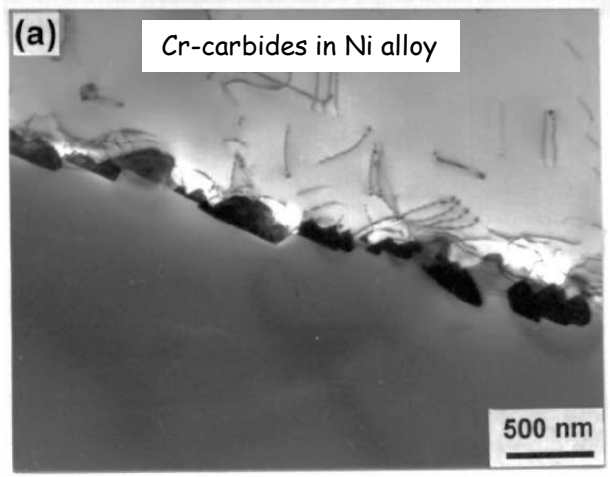

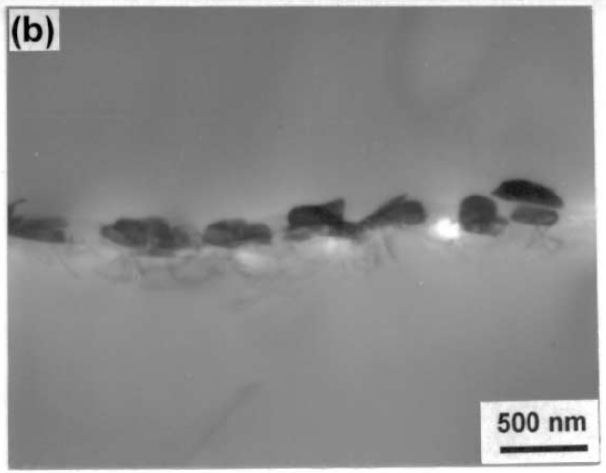

split-kite

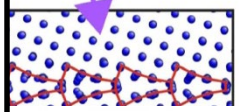

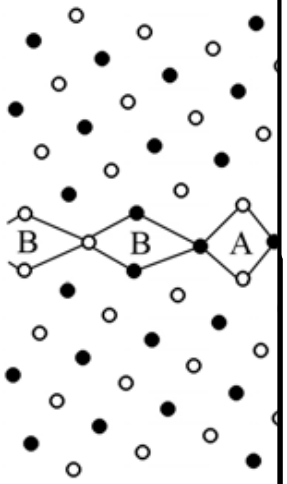

Σ17(410)θ=28.07
|B.BA|

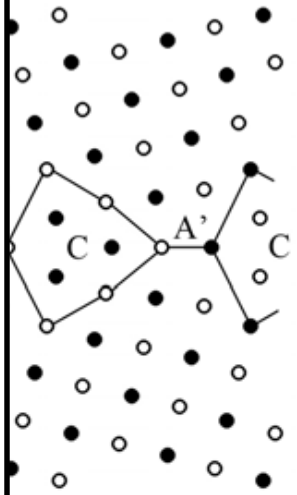

7(530)θ=61.93°
|CA'.CA'|

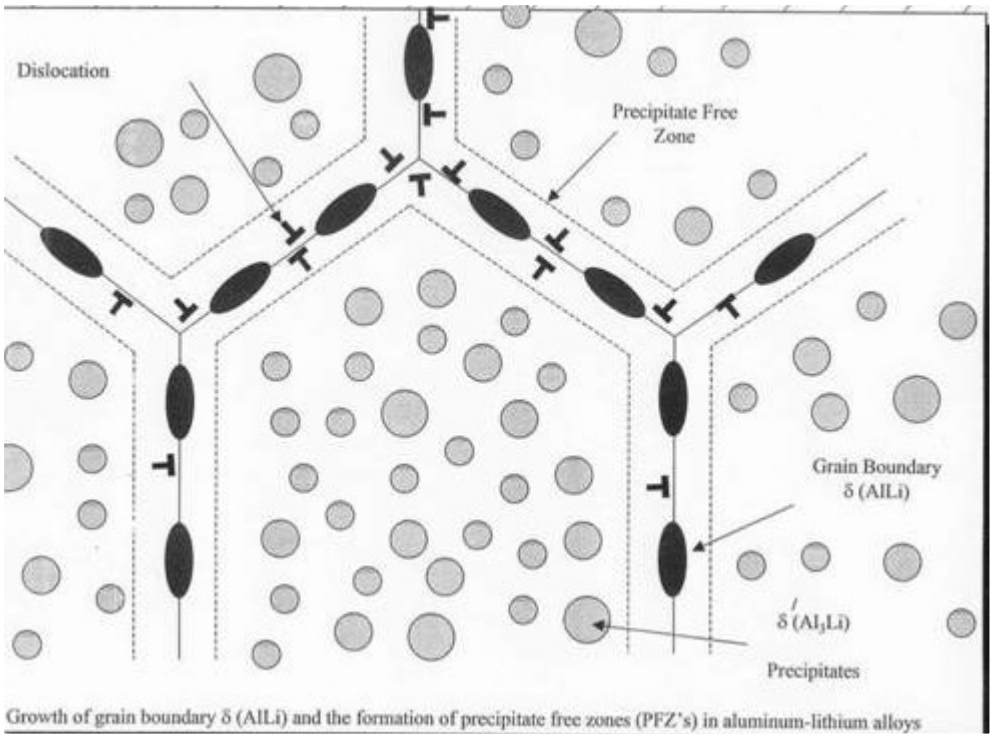

Growth of grain boundary δ (AlLi) and the formation of precipitate free zones (PFZ's) in aluminum-lithium alloys

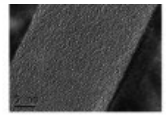

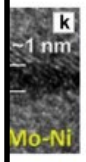

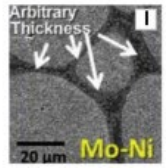

Complexion Transitions

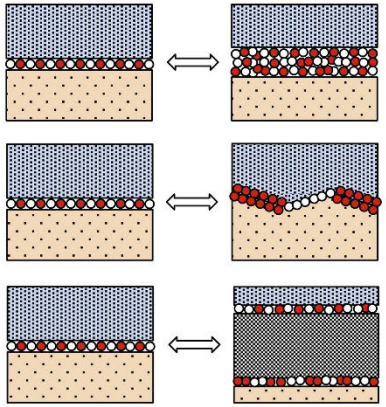

Grain boundary character $(\boldsymbol{R}, \hat{n})$ remains constant while atomic structure and/or chemistry of the grain boundary core changes. During a congruent transition, one complexion transforms into another.

Grain boundary facets into two new inclinations, $\hat{n}_1$ and $\hat{n}_2$, while the misorientation $\boldsymbol{R}$ remains constant. In general, the atomic structure and chemistry of the core will also change. During a faceting transition, one complexion decomposes into two.

A bulk phase completely wets the original grain boundary, creating two new grain boundaries with the same inclination $\hat{n}$ but different misorientations $\boldsymbol{R}_1$ and $\boldsymbol{R}_2$. During a dissociation transition, one complexion decomposes into two.

Complexion Categories

Dillon-Harmer Discrete Complexions

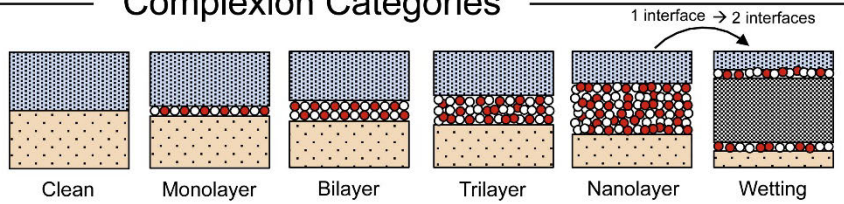

Dillon-Harmer discrete complexions are categorized based on the thickness of the grain boundary core converted to an integer number of atomic layers. The clean complexion has very little or no adsorbed solute (and hence may be extrinsic or intrinsic) while the thicker discrete complexions are extrinsic with one or more layers enriched in solute. Discrete complexions may have varying degrees of structural and chemical order. The transition from a single complexion (interface) to two complexions (interfaces) occurs between the nanolayer complexion and wetting.

Intrinsic vs. Extrinsic

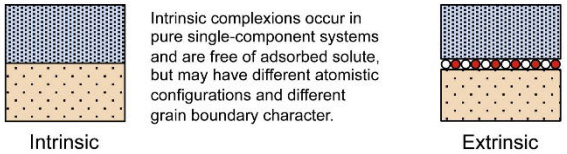

Intrinsic complexions occur in pure single-component systems and are free of adsorbed solute, but may have different atomistic configurations and different grain boundary character.

Extrinsic complexions contain adsorbed solute atoms that influence the atomistic structure, degree of crystalline order, and preferred grain boundary character.

Order vs. Disorder

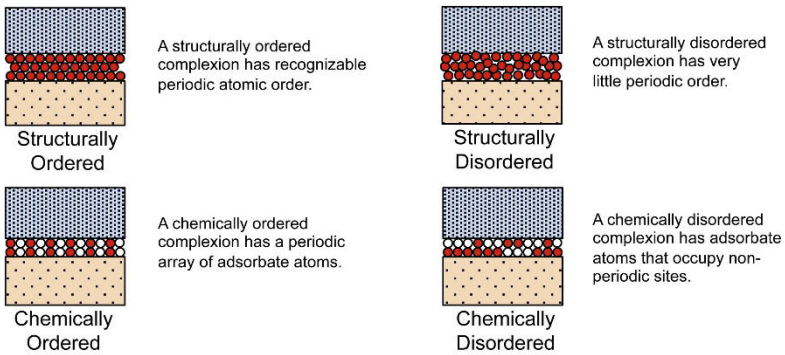

A structurally ordered complexion has recognizable periodic atomic order.

A structurally disordered complexion has very little periodic order.

A chemically ordered complexion has a periodic array of adsorbate atoms.

A chemically disordered complexion has adsorbate atoms that occupy non-periodic sites.

Solid solutions: Complexions

Phase diagrams

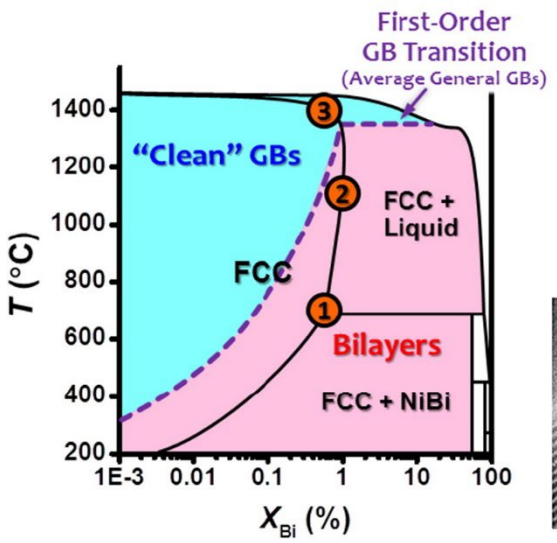

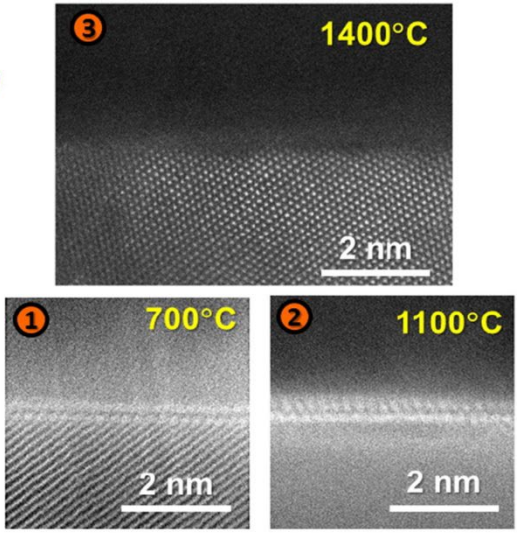

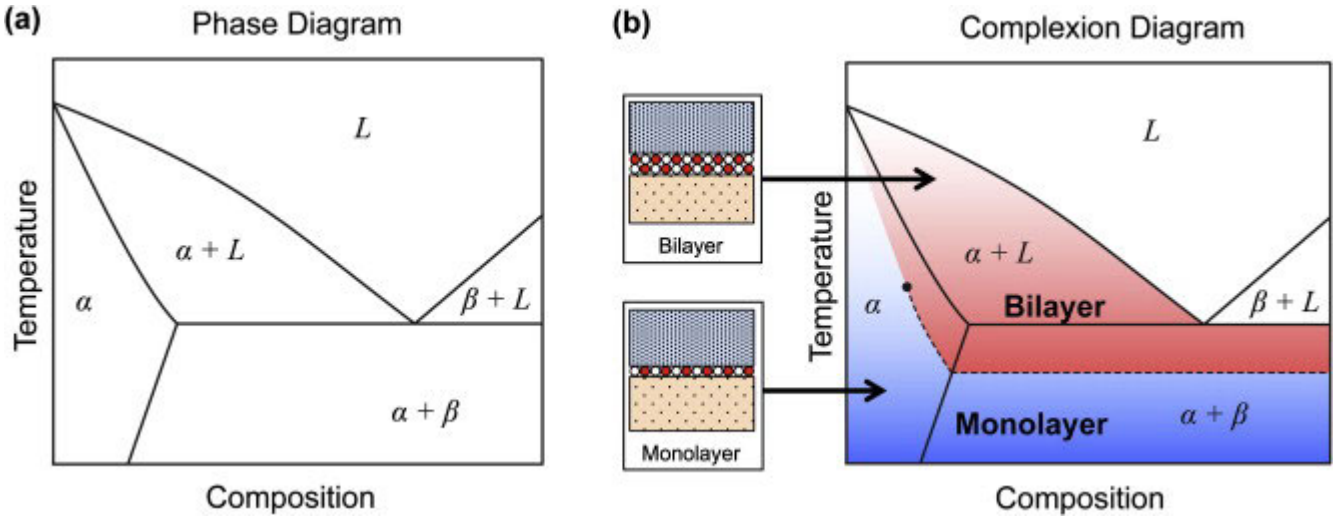

Complexions: Mechanical effects

Embrittlement…

- Ni-Bi

Ni-Bi alloy

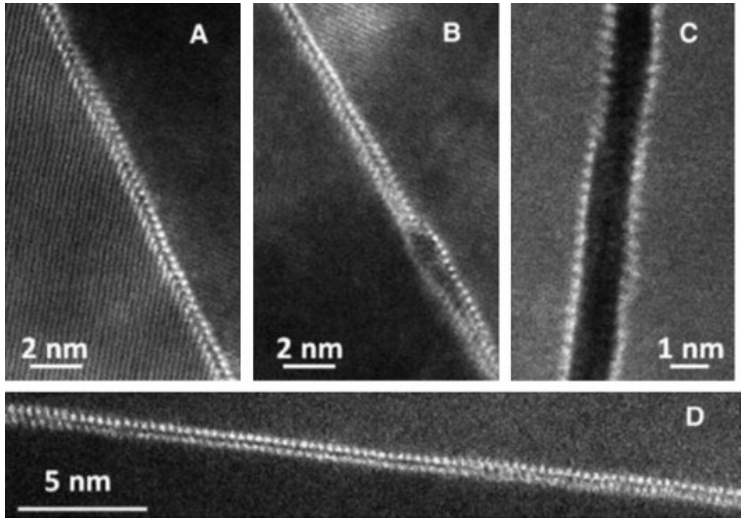

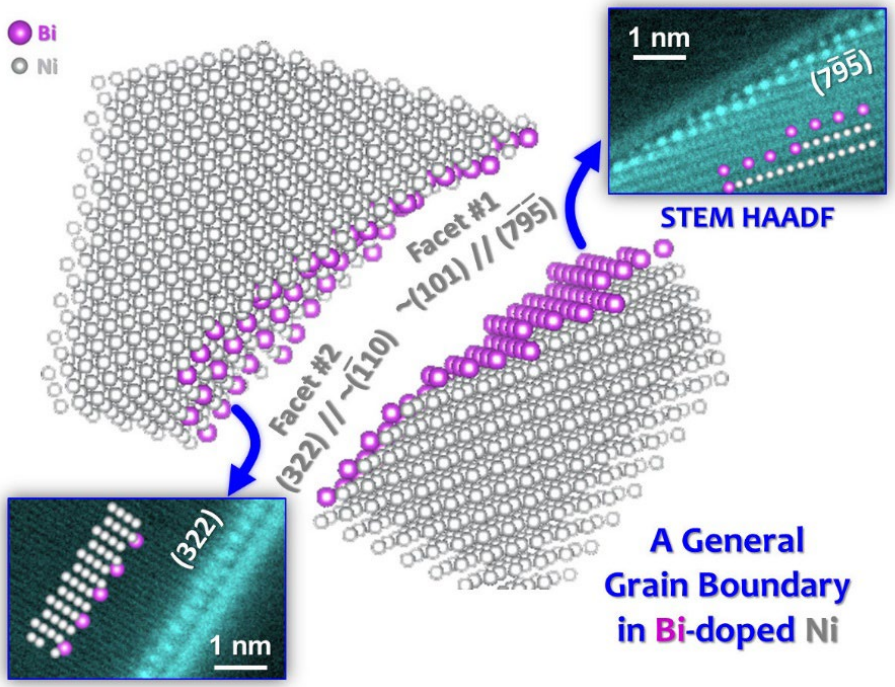

Complexions in Nano-materials

Strengthening:

- Grain refinement: nanocrystalline

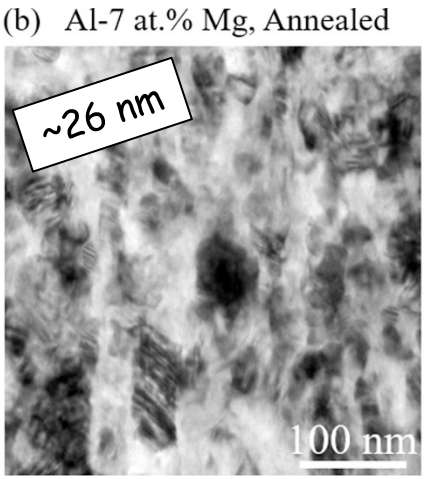

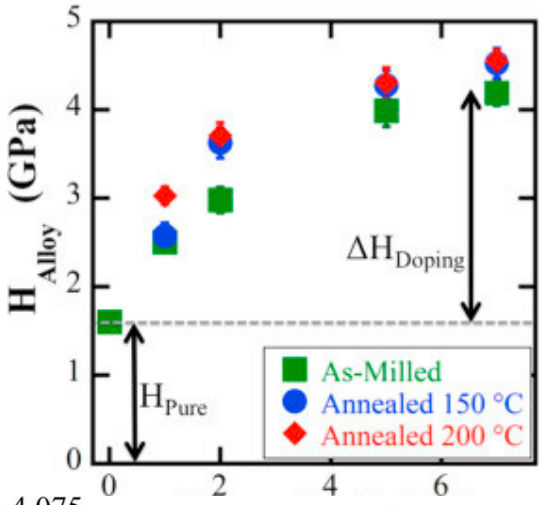

$$\tau_{ss} = \alpha E c^{1/2}$$

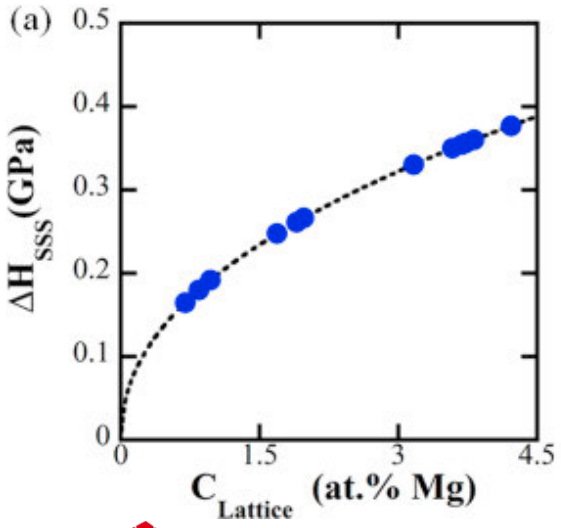

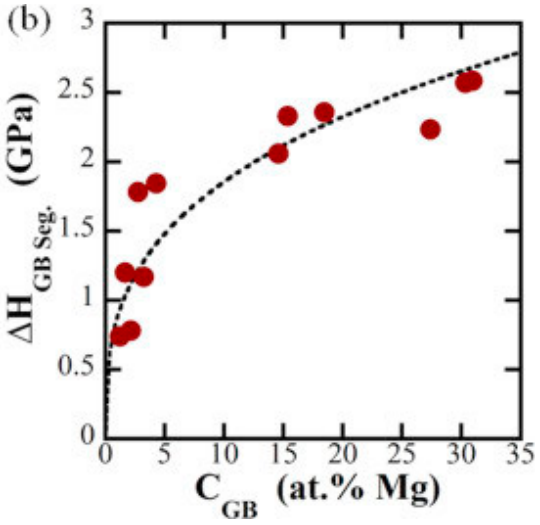

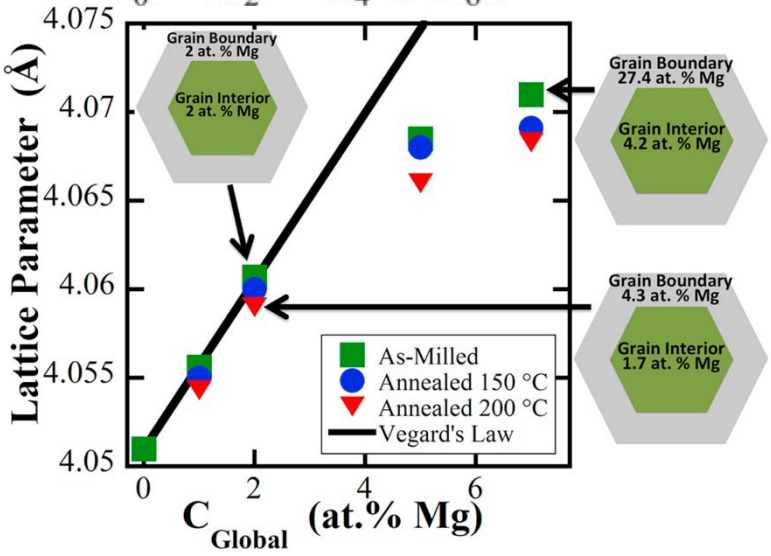

Pun, S.C., … Rupert, T.J., ***Mat Sci Eng A*** 2017, 696, 400–406

Complexions in Nano-materials

Strengthening:

- Grain refinement: nanocrystalline
- High temperature strength through microstructural stability

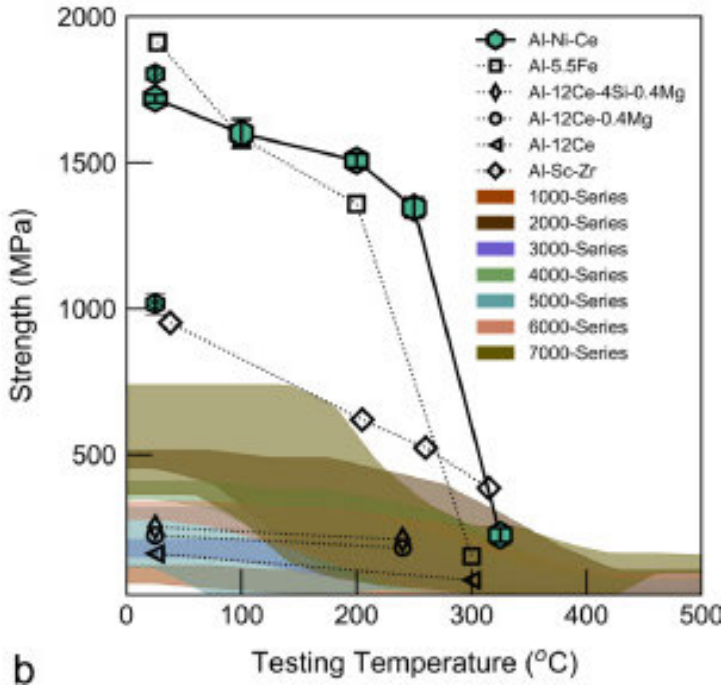

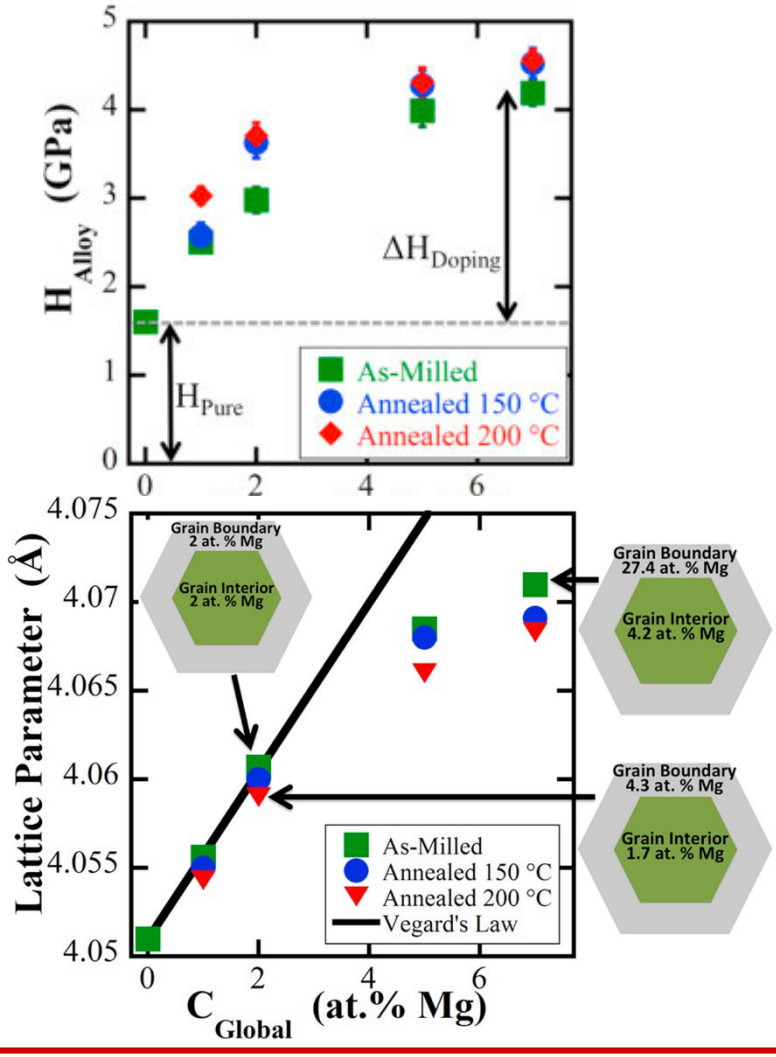

High entropy alloys

- 4 key effects:
  - Entropy stabilisation
  - **Severe lattice distortion**
  - **Sluggish diffusion**
  - Cocktail synergies

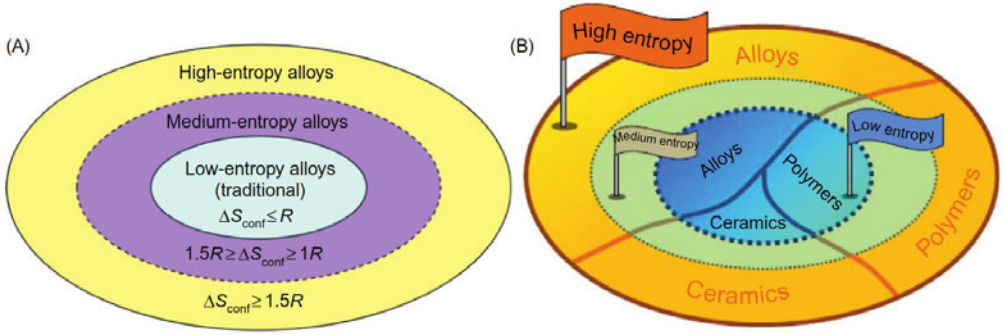

$$\Delta S_{mix} = -\mathrm{R} \sum_{i=1}^{n} \mathrm{c_i} \ln c_i$$

$$\Omega = \left| {}^{T_m \Delta S_{mix}} / {}_{\Delta H_{mix}} \right| \qquad \Omega \geq 1.1$$

fcc

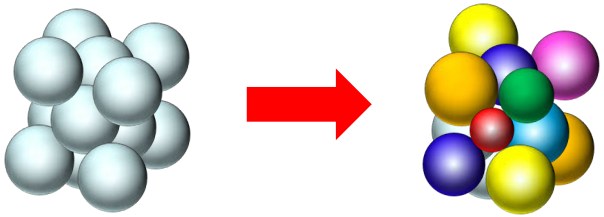

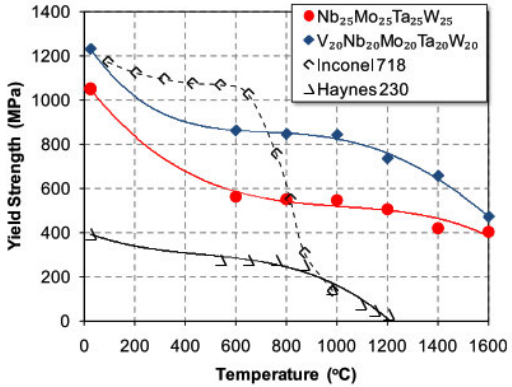

- magnitude of configurational entropy $\Delta Smix > 1{,}61R$
- more than 5 principal elements
- % of elements between 5% and 35%
- difference in atomic radii <6,6%
- ΔH_{mix} between $-10 \frac{kJ}{mol}$ a nd $5 \frac{kJ}{mol}$

High entropy nano-materials

- Mechanical alloying: milling powders + sinter
  - B.S. Murty & group: AlFeTiCrZnCu, CuNiCoZnAlTi, FeNiMnAlCrCo, and NiFeCrCoMnW
- High pressure torsion (HPT)
  - Cantor alloy: CrMnFeCoNi

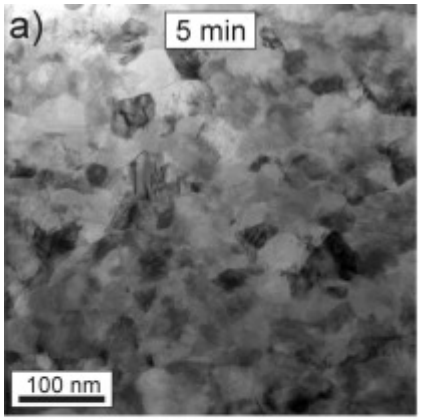

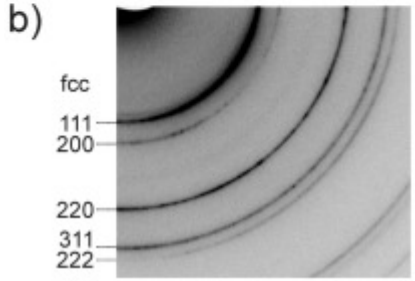

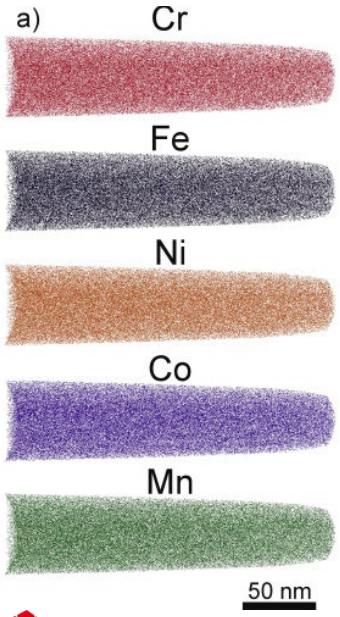

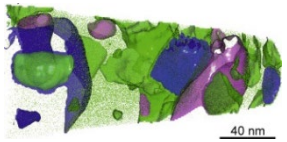

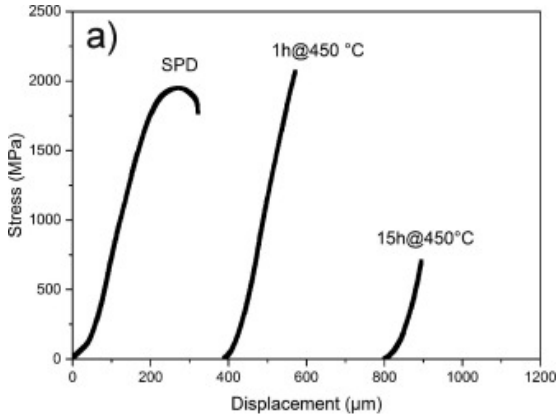

Yu Zou, ***Nano Letters*** 2017, 17, 1569−1574
Yu Zou, ***Nat Comms*** 2015, 6, 7748

High entropy nano-materials

- Nanocrystalline, e.g. $Nb_{25}Ta_{25}Mo_{25}W_{25}$

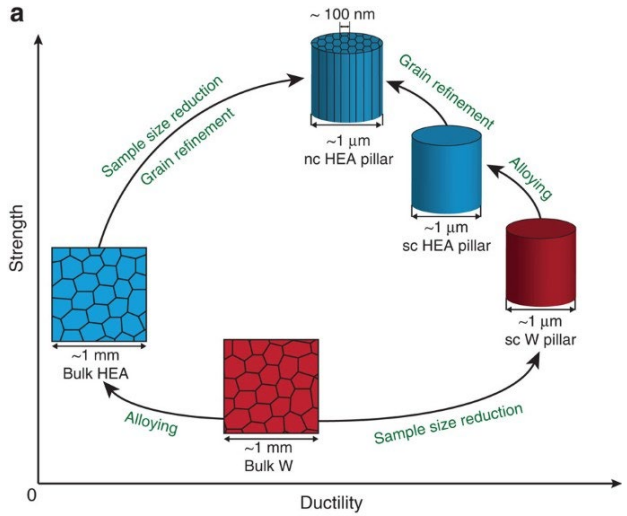

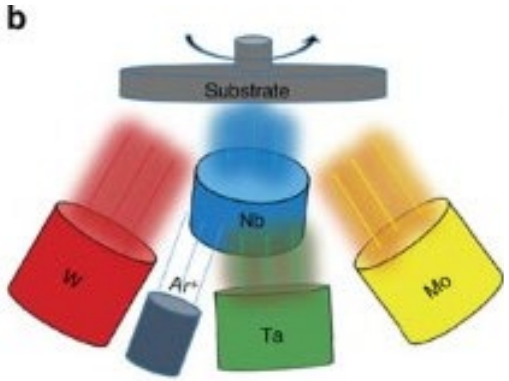

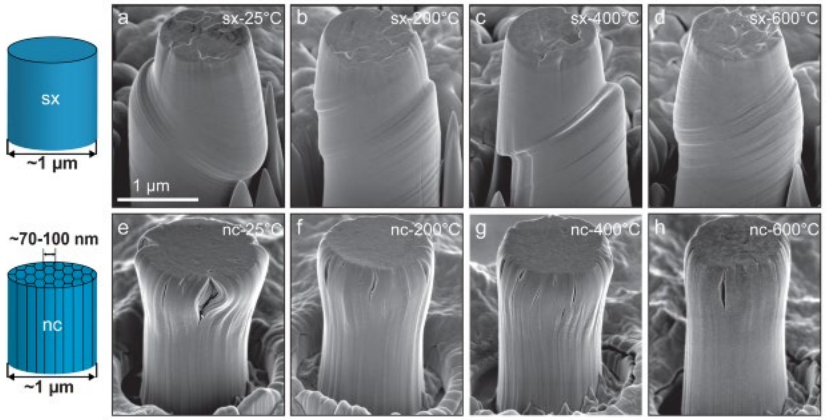

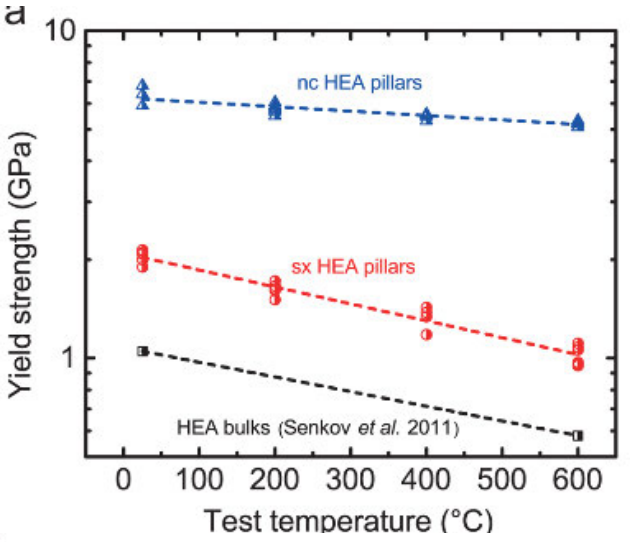

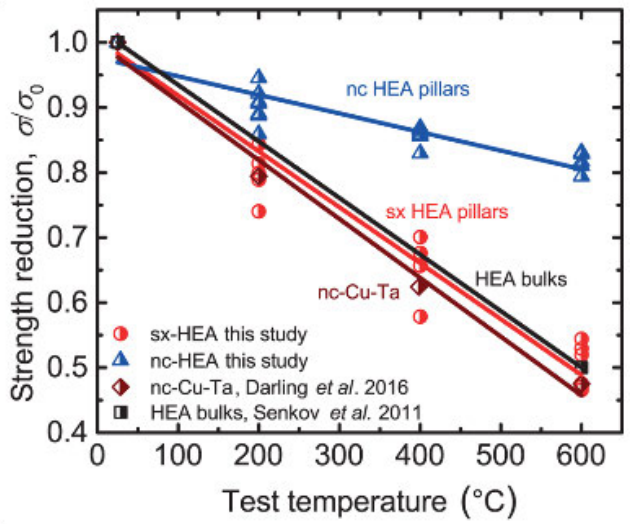

Yu Zou, ***Nano Letters*** 2017, 17, 1569−1574
Yu Zou, ***Nat Comms*** 2015, 6, 7748

Order strengthening

- Regular ordering in sub-lattices
- Relevant for:
  - Intermetallics: aluminides (FeAl, TiAl, Ni_3Al…), silicides (Mo_3Si…)
  - Salts
  - Ceramics (TiN: forbidden slip directions)
- Plasticity by super-dislocation motion

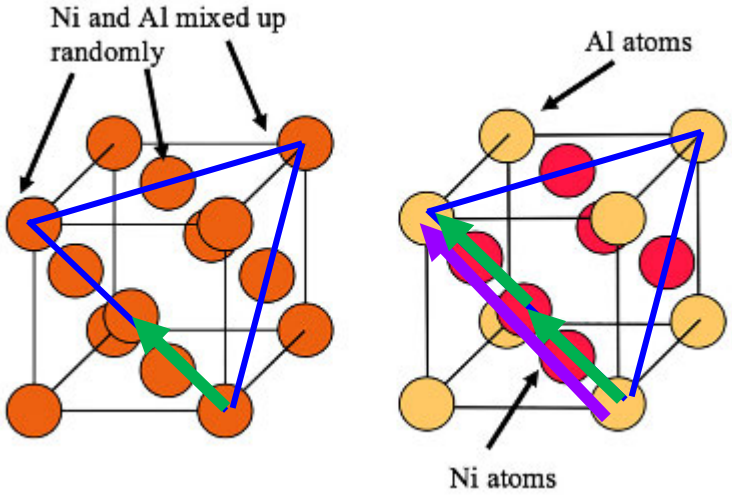

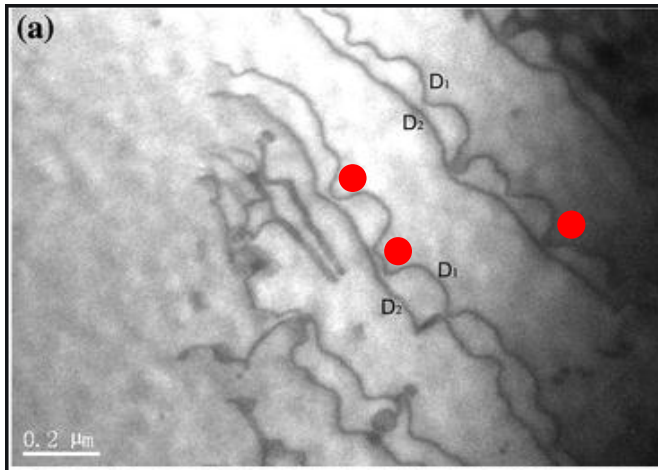

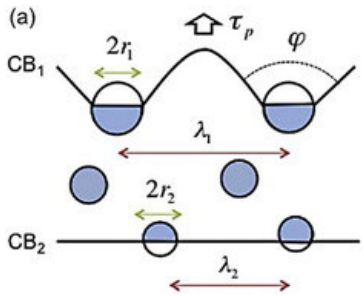

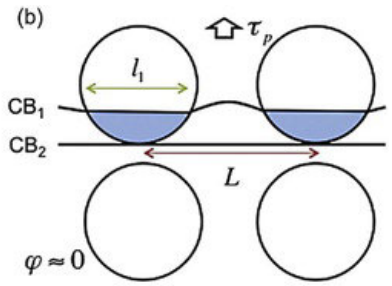

Particle dispersion strengthening

- "Particle":
  - Oxide: ODS; Al_2O_3 & Y_2O_3
  - Intermetallic
  - Metallic
- Sizes: few nm -> 100s nm
- Shapes: depend on formation
- Semi-coherent / incoherent
- Obtained by:
  - Segregation/internal reaction
  - Mechanical mixing
    - Alloy powders
    - Co-sputtering (Emese)

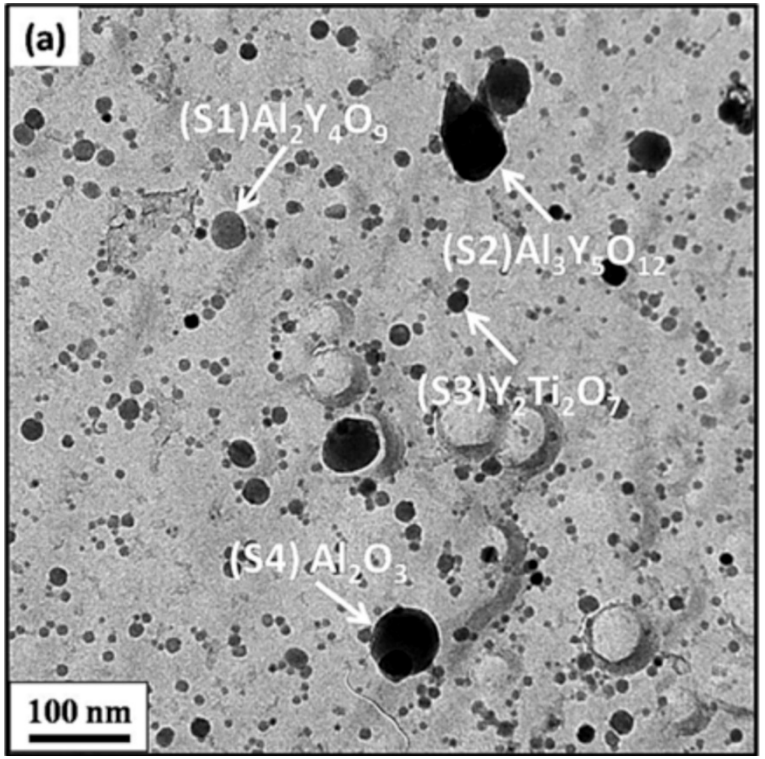

Mechanical properties of nanodispersion

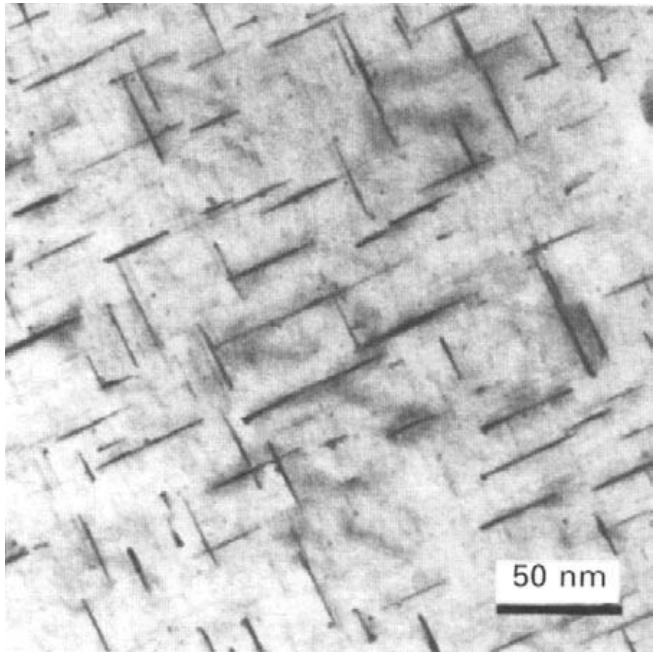

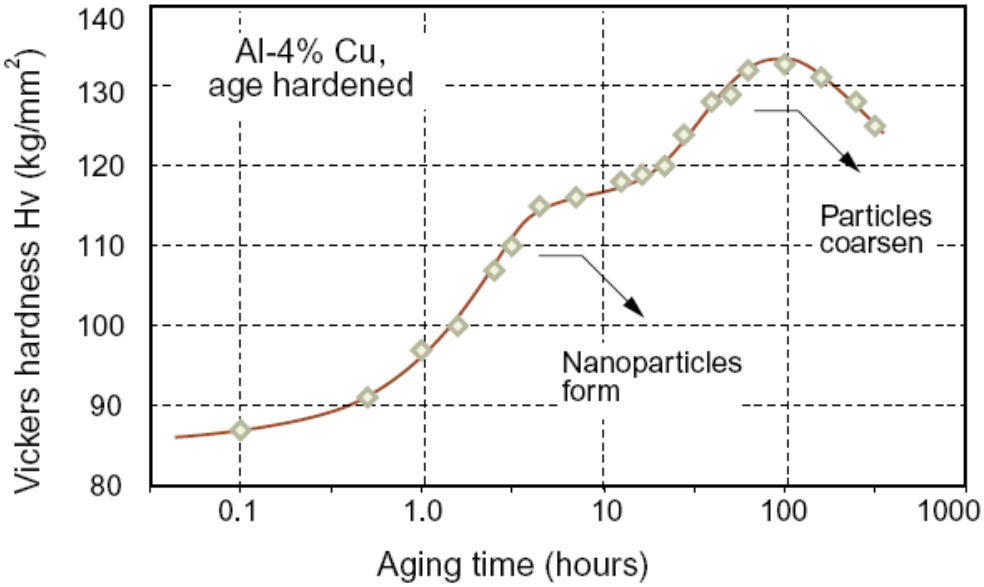

Intrinsic size effect – precipitate size

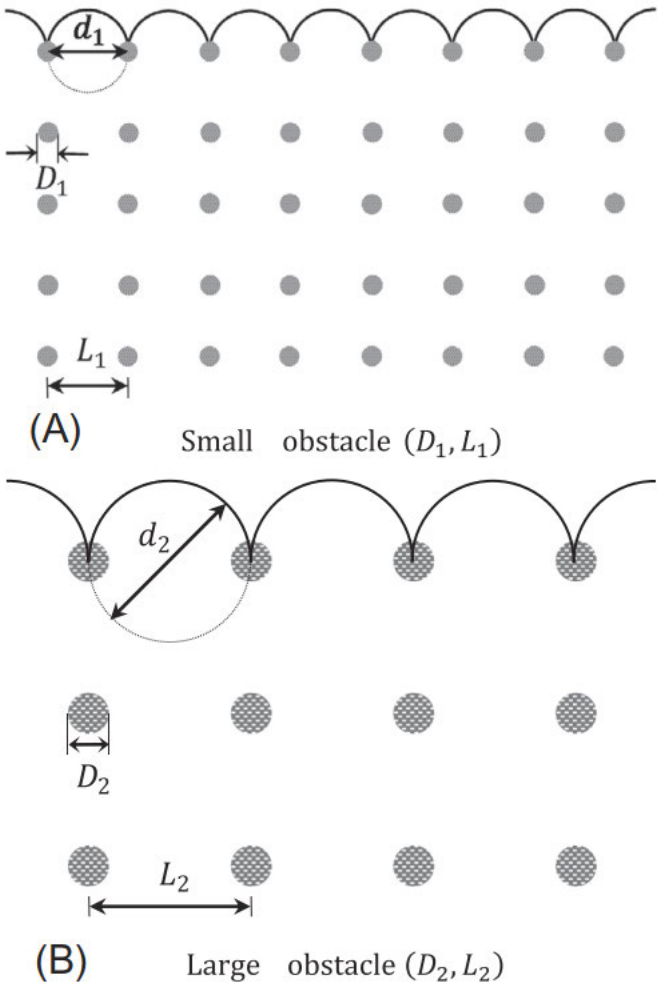

For an array of hard objects with different diameters of D_1 and D_2 for a given volume fraction: The smaller hard objects ($D_1 < D_2$) leads to the smaller obstacle spacing ($L_1 < L_2$).

The dislocation loop bypasses the hard obstacle if the equilibrium diameter of the curved dislocation d is smaller than the obstacle spacing L.

In other words, plastic deformation occurs through the elongation and multiplication of dislocation loops that can fit between two obstacles.

The equilibrium diameter of a dislocation for an elastic isotropic material can be described as follows:

$$d = \frac{2T}{b\tau} \approx \frac{Gb}{\tau}$$

where τ is the shear stress, G is the shear modulus, b is the magnitude of Burgers vector, and T is the dislocation line tension, which can be simplified as $T = Gb^2/2$.

G.Z. Voyiadjis and M. Yaghoobi. (2018)

Intrinsic size effect – precipitate size

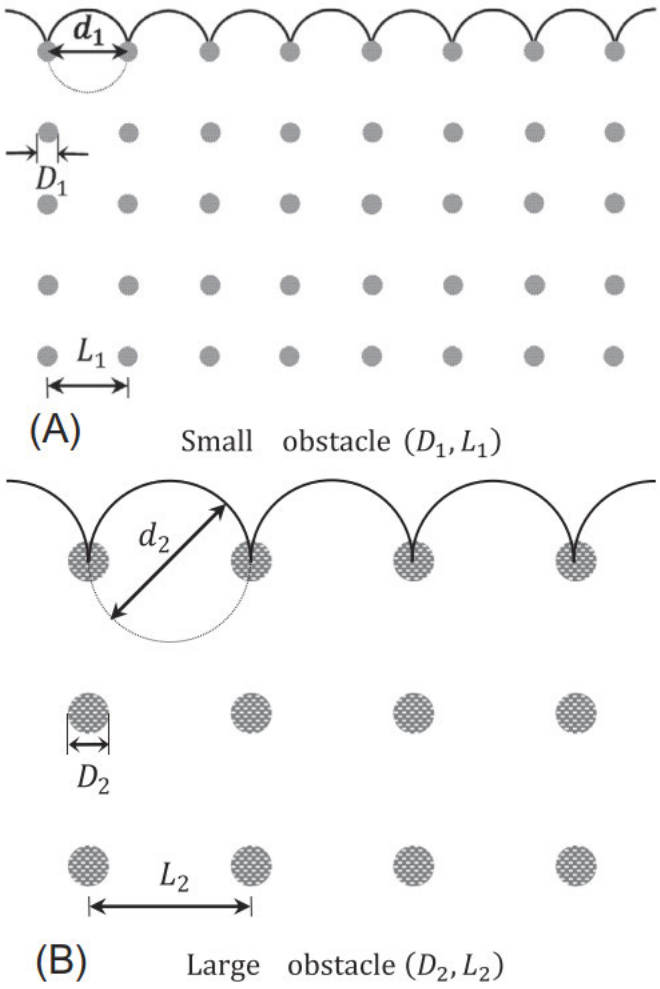

Now, the minimum shear stress to activate the dislocation source, i.e. d = L, can be calculated as follows:

$$\tau \approx \frac{Gb}{L}$$

accordingly, the sample with the smaller obstacle spacing L_1 shows more strength compared to the one with the larger obstacle spacing L_2

G.Z. Voyiadjis and M. Yaghoobi. (2018)

Particle concentration and spacing?

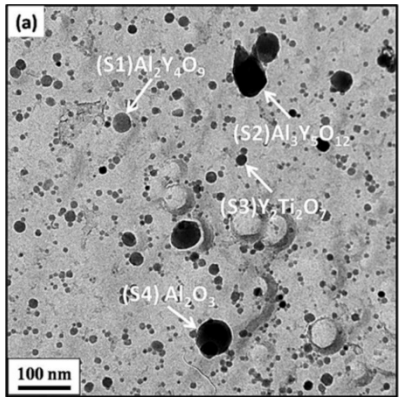

- Measure vol. fraction, *f*, and number density, *n*
  - By area: optical, SEM
  - By vol.: TEM: less straightforward
- Particle spacing, *χ* (or *L*)
  - Cubic

$$\chi_{cubic} = \left(\frac{1}{n}\right)^{1/3} - 2r$$

  - Average spacing nearest-neighbours 3D (ideal gas)

$$\chi_{3D} = 0.893\left(\frac{3}{4\pi n}\right)^{1/3} - 2r$$

  - Average spacing IN slip plane (2D)

$$\chi_{2D} = \left(\sqrt{\pi/f} - 2\right)r_s$$

$$r_s = \sqrt{2/3}\, r$$

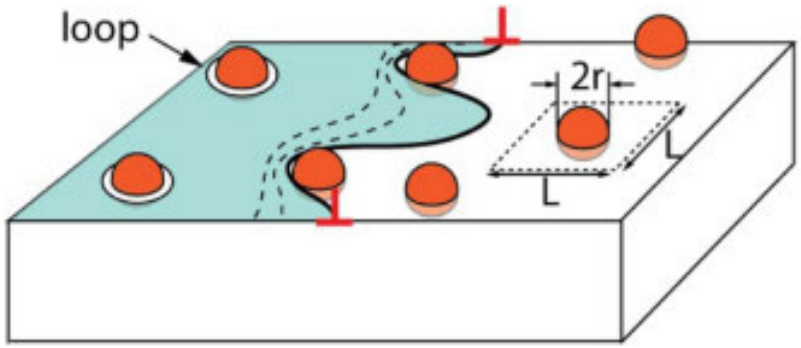

The full story – particle strengthening

$$\tau \approx \frac{Gb}{L}$$

- Orowan bowing:

$$\Delta\tau_{\mathrm{Oro}} = 0.4\,\frac{Gb_{\mathrm{p}}}{\pi\chi}\,ln\left(\frac{2r_{\mathrm{s}}}{b_{\mathrm{p}}}\right)(1-\nu)^{-0.5}$$

$$\chi = \left(\sqrt{\pi/f} - 2\right)r_{\mathrm{s}} \qquad r_{\mathrm{s}} = \sqrt{2/3}\,r$$

- Cutting (for semi-coherent particles):

$$\Delta\sigma_{\mathrm{Cut}} = \sqrt{\frac{Gb_{\mathrm{p}}G_{\mathrm{W}}}{2C\chi}}$$

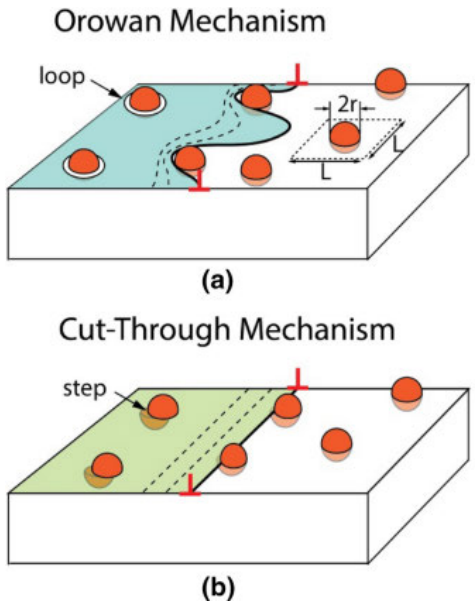

A. Kelly, R. Nicholson, *Strengthening methods in crystals*, 1972

Dispersion strengthening in Nano-materials

- Particle strengthening
- But mainly: microstructural stability
  - Zener pinning of boundaries
  - Nucleation sites for nanotwins?

Critical grain radius: $R_c = \frac{Kr}{f^m}$

K = 0.17 and m = 1 for f < 0.05

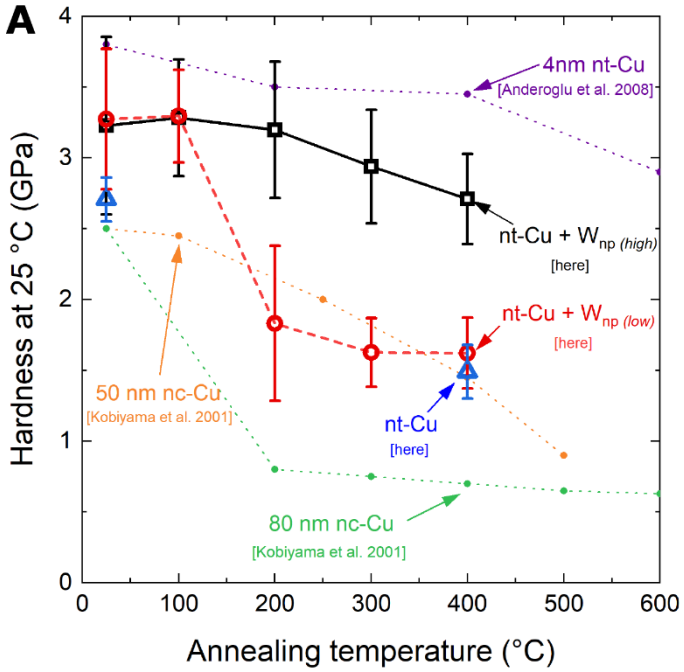

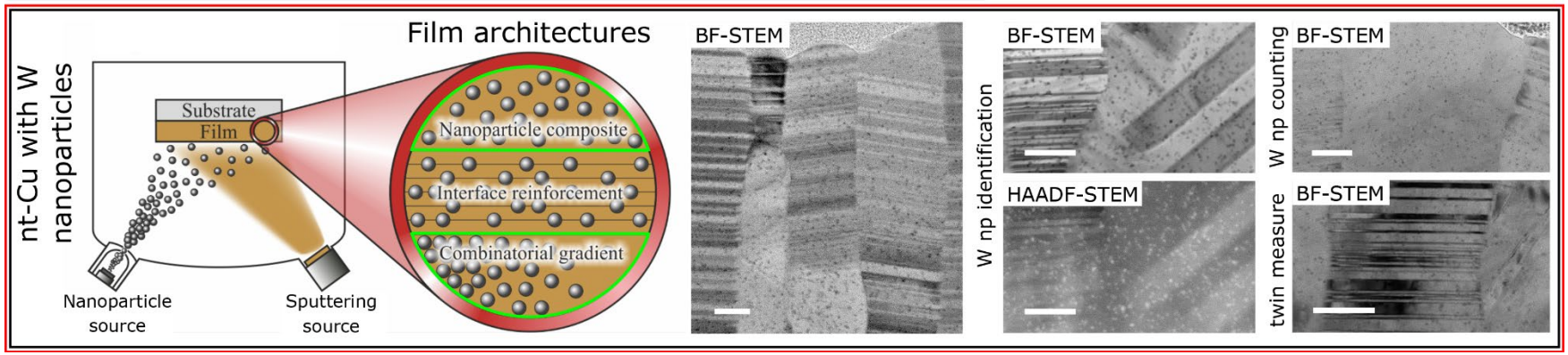

Combining strength contributions

$$\sigma_Y = \left[{\sigma_0}^i + {\sigma_{HP}}^i + {\sigma_{Tay}}^i + {\sigma_{SSS}}^i + {\sigma_{Oro}}^i + {\sigma_{twin}}^i + {\sigma_{coh}}^i + {\sigma_{ord}}^i\right]^{1/i}$$

(already converted from σ to τ using Schmid factor)

e.g. ODS copper:

$$\sigma_Y = \sigma_0 + \sigma_{HP} + \sigma_{SSS} + \sqrt{{\sigma_{Tay}}^2 + {\sigma_{Oro}}^2}$$

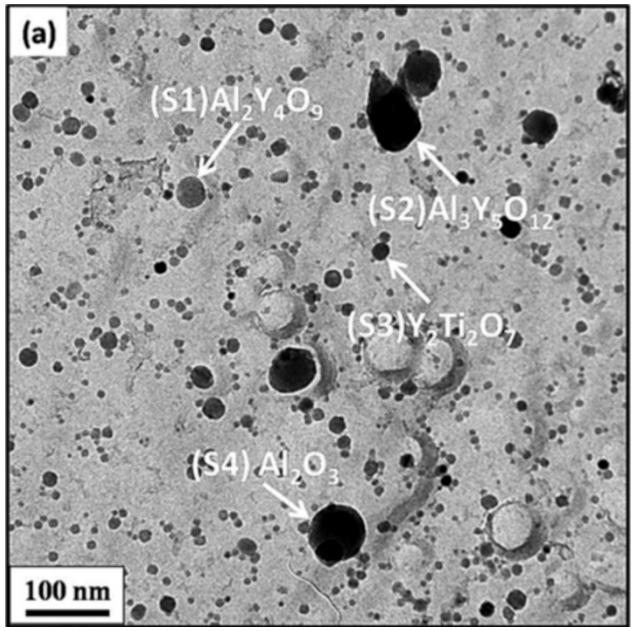

Size dependence of mechanical materials properties

physical size effects

Size effects ductile materials

size effects can be attributed to many different deformation and strengthening mechanisms.

They can be **originated** from

internal characteristic length scales, such as grain size

or

external length scales, such as the film thickness, pillar diameter, and indentation depth.

The size effects in crystalline metals are commonly categorized in two groups of

intrinsic, related to the internal characteristic length scales such as grain size and dislocations mean free path,

and

extrinsic, originated from an external length scale such as thin film thickness or pillar diameter.

G.Z. Voyiadjis and M. Yaghoobi. (2018) Size Effects in Plasticity: Fram Macro to Nano, Academic Press, Elsevier

Extrinsic size effects

Materialeigenschaften und Längenskalen

Plastizität Bruch

<= *Intrinsische Längen*

Elastizität Ermüdung

Nano-Devices

MEMS

engines etc.

microelectronics

conventional testing

Objekt Dimensionen < Intrinsische Längen => Neue mech. Eigenschaften

Size effects in materials: Swiss version

nanowires for solar cells / microelectronics

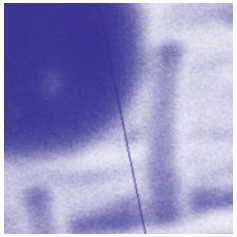

UV-LIGA watch part

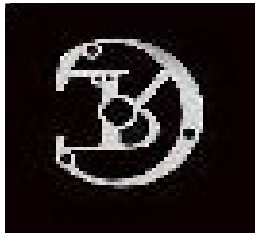

sawing of thin solar cells

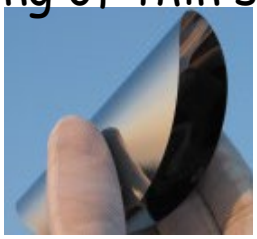

MEMS device

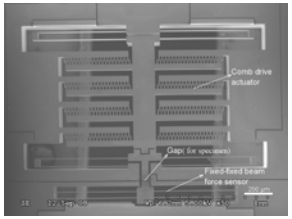

multilayer hard coatings

cleavage of laser bars

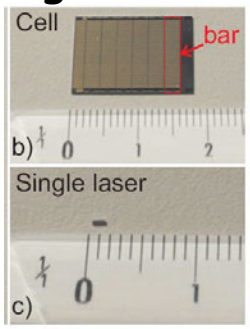

10^{-9} m — 10^{-6} m — 10^{-3} m — 1 m

plasticity

fracture

elasticity

fatigue

<= intrinsic length scale

Size effects in materials

dimension of the physical phenomena involved => intrinsic length
micro-structural dimension => size parameter

Size Parameters:
Grain size D, Grain boundary width δ_b ,Obstacle spacing L, Obstacle radius R, Film thickness H

Characteristic lengths:
Equilibrium parameter of dislocation loop d, Spacing between partial dislocations w,
Width of magnetic domain wall d

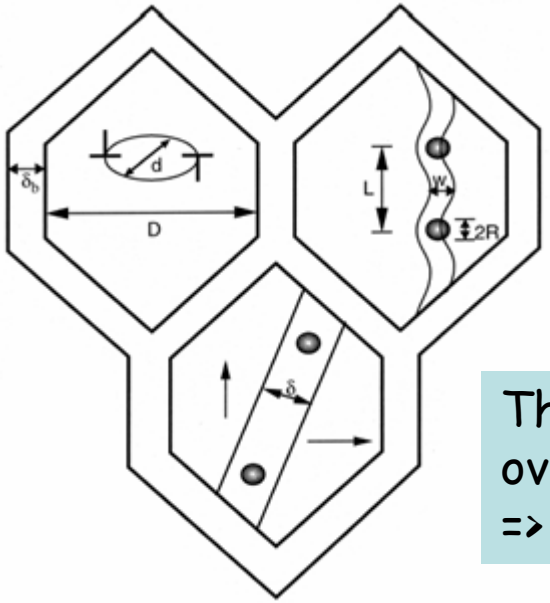

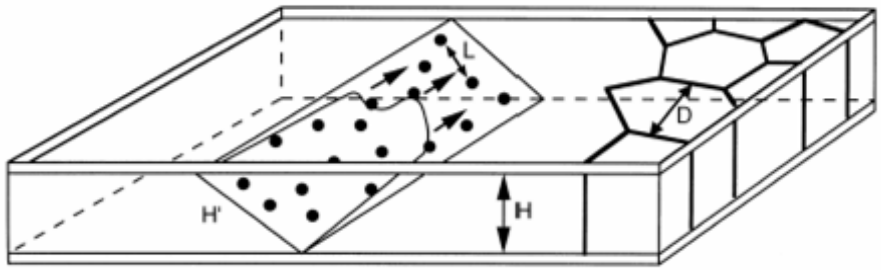

The range where charateristic lengths and size parameters overlap is of interest
=> conventional laws may break down

E. Arzt, Acta mater. 46(16), pp. 5611-5626, 1998

Early studies of size effects

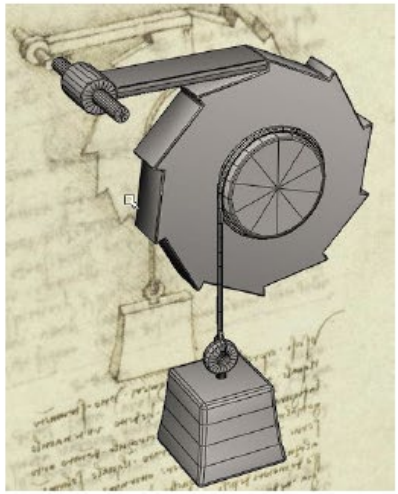

da Vinci found that the shorter the wire…

… the higher the fracture strength

Leonardo da Vinci, 1500s

Observe what the weight was that broke the wire, and in what part the wire broke . . . Then shorten this wire, at first by half, and see how much more weight it supports; and then make it one quarter of its original length, and so on, making various lengths and noting the weight that breaks each one and the place in which it breaks.

Early studies of size effects

A METHOD OF DRAWING METALLIC FILAMENTS AND A DISCUSSION OF THEIR PROPERTIES AND USES

By G. F. Taylor

Bureau of Plant Industry,
U. S. Department of Agriculture,
Washington, D. C.
December 10, 1923.

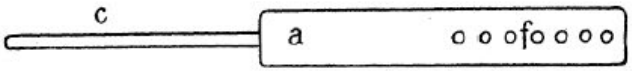

Fig. 1

The smaller sizes have greater tensile strength and the extremely small sizes, .002 cm and less, will stand indefinite bending.

-G.F. Taylor, Phys. Rev. 23, 655 - 660 (1924)

Early studies of size effects

JOURNAL OF APPLIED PHYSICS VOLUME 27, NUMBER 12 DECEMBER, 1956

Tensile Strength of Whiskers

S. S. BRENNER
General Electric Research Laboratory, Schenectady, New York
(Received June 2, 1956)

Tensile tests have been performed on whiskers of iron, copper, and silver 1.2 to 15 μ in diameter. The strongest whiskers which were less than 4 μ in diameter exhibited resolved elastic shear strengths of from two to six percent of their shear moduli. Stress-strain determinations on iron have shown that large deviations from Hooke's law occur beyond two percent strain. As the whiskers increase in size, their strengths decrease with considerable scatter.

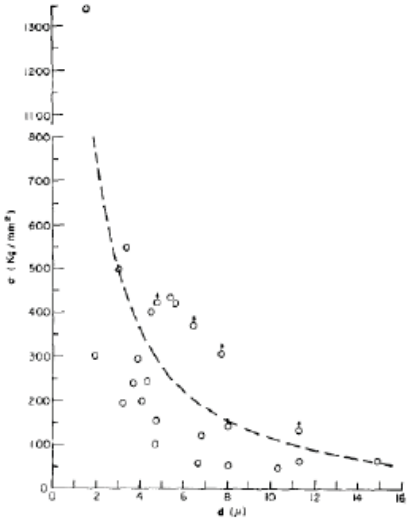

FIG. 6. The effect of size on the strength of iron whiskers. δ fracture occurred at or near grips. True fracture stress may have been higher.

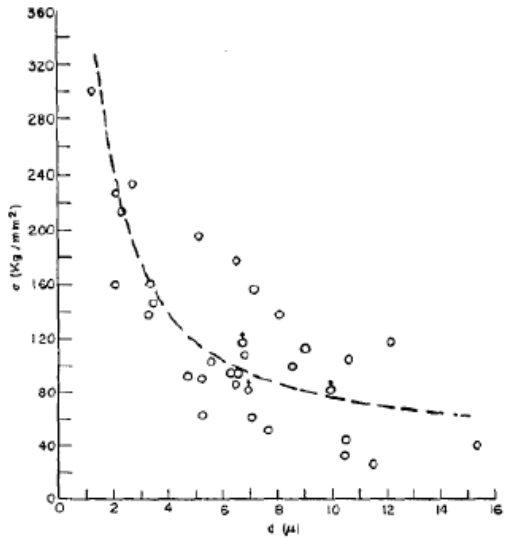

FIG. 7. The effect of size on the strength of copper whiskers.

Hardness testing: scale effects

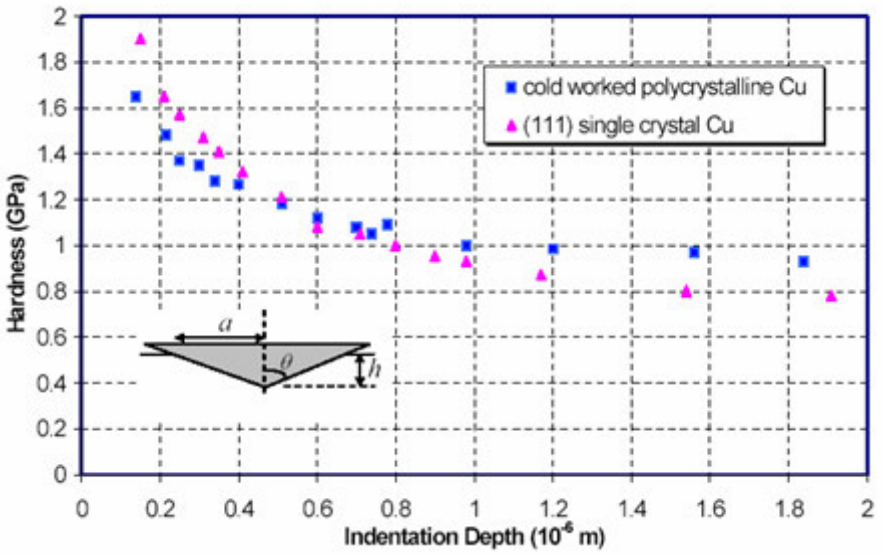

Explanation:

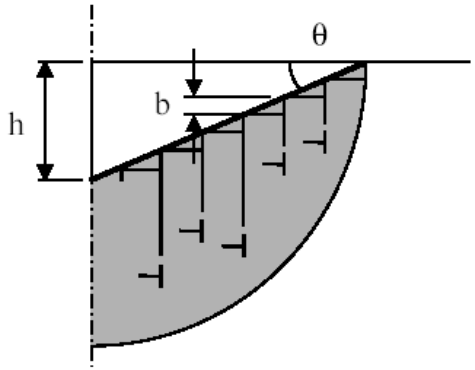

Stress concentration at tip leads to higher dislocation density, which leads at low penetration depth to higher hardness

strain bursts – gold dots in compression

E, σ_y, n, σ_f

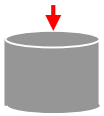

ordered arrays of gold dots

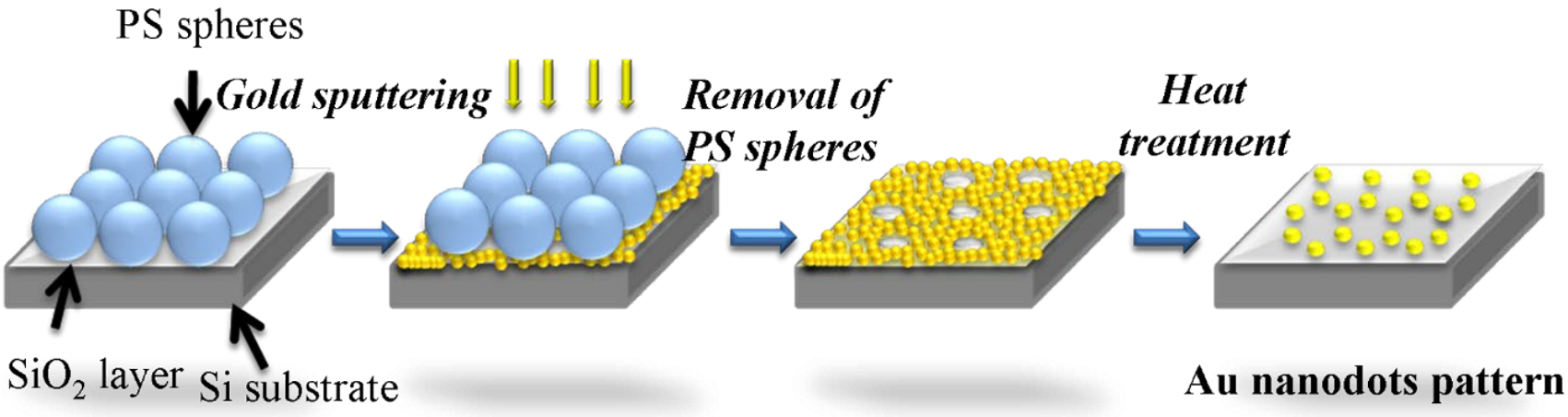

ordered arrays of gold dots

Fabrication steps:

- Colloidal templating
- Au PVD
- annealing at 1000°C/1h

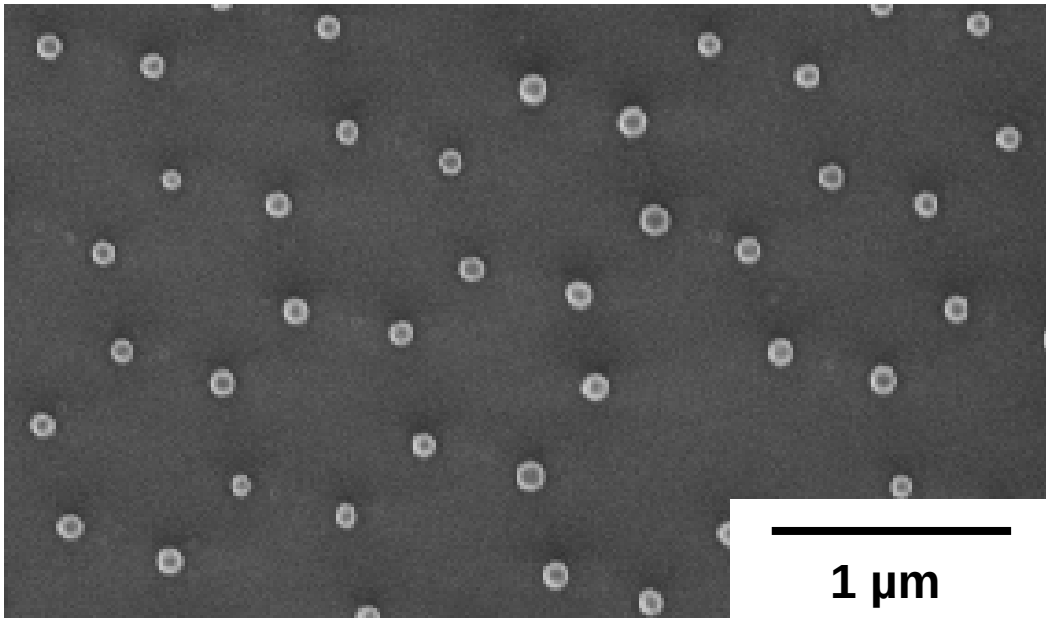

yield or flow stress of gold pillars and wires

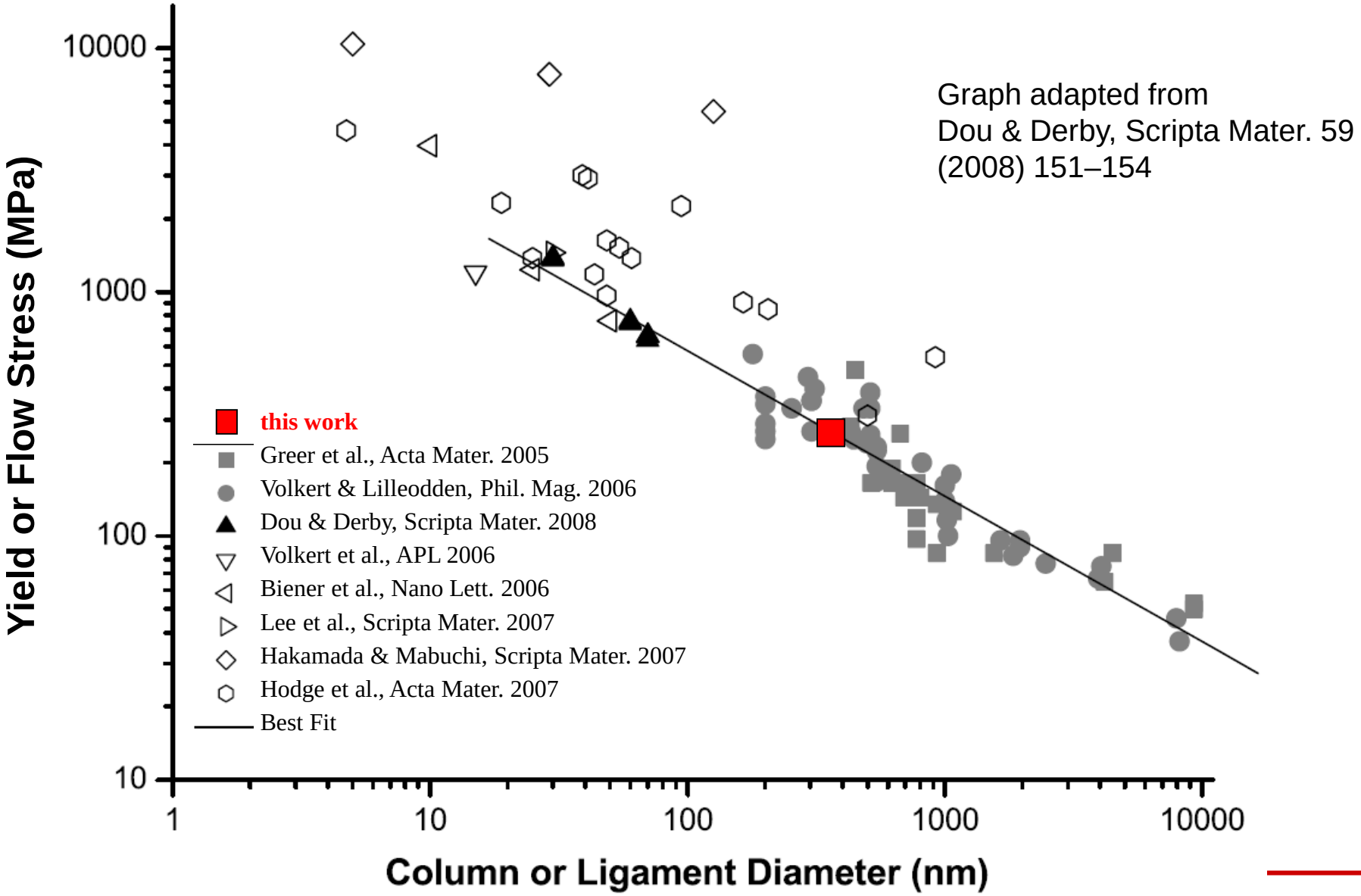

Graph adapted from
Dou & Derby, Scripta Mater. 59 (2008) 151–154

yield or flow stress of gold pillars and wires

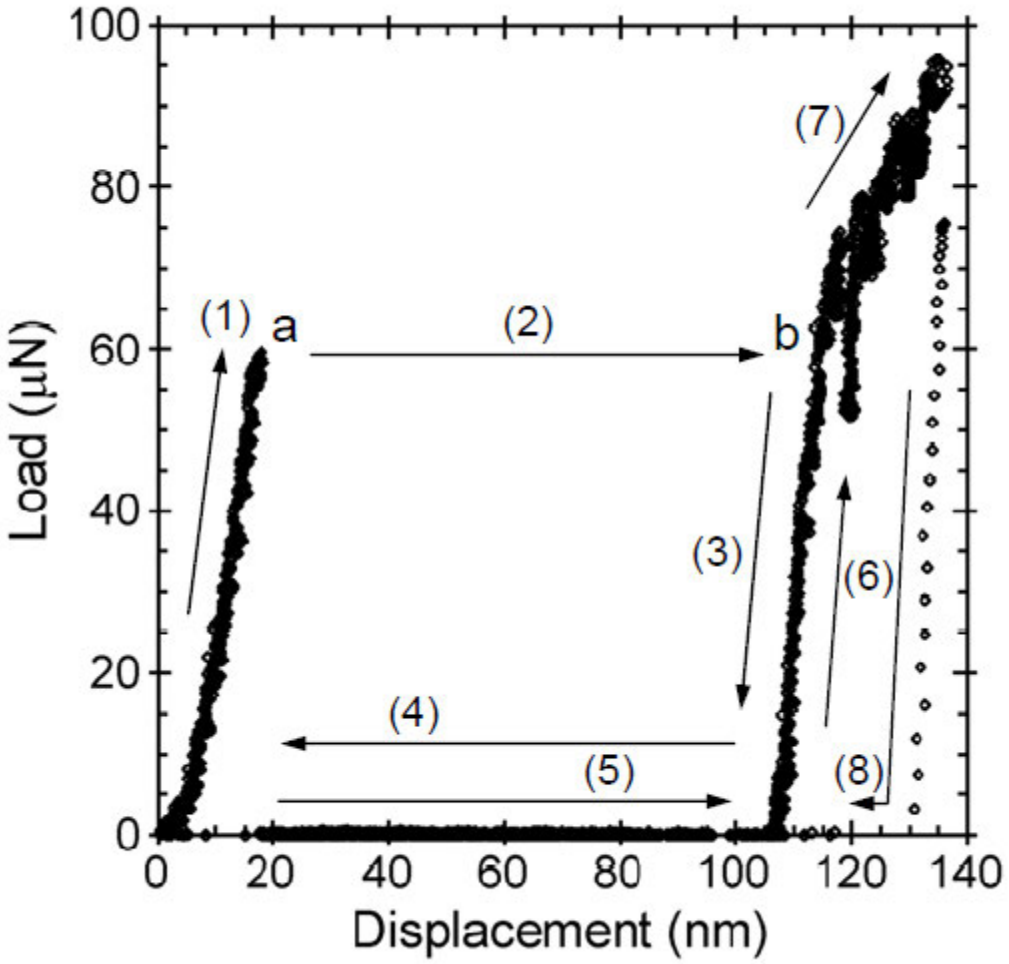

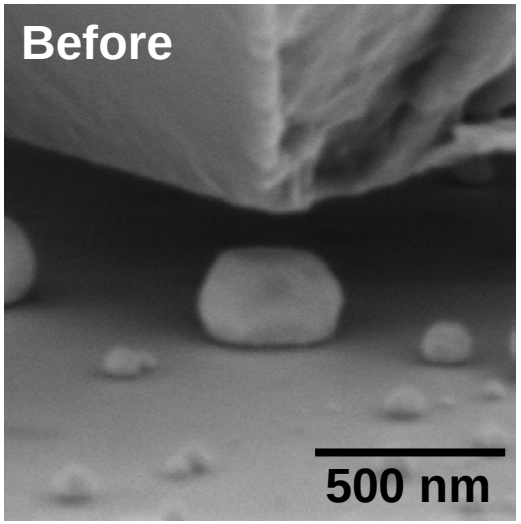

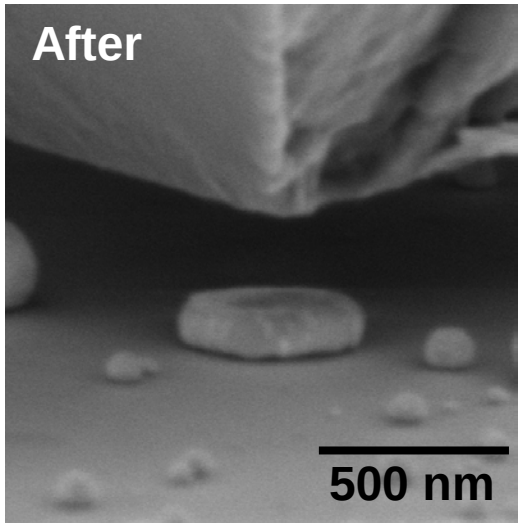

yield or flow stress of gold pillars and wires

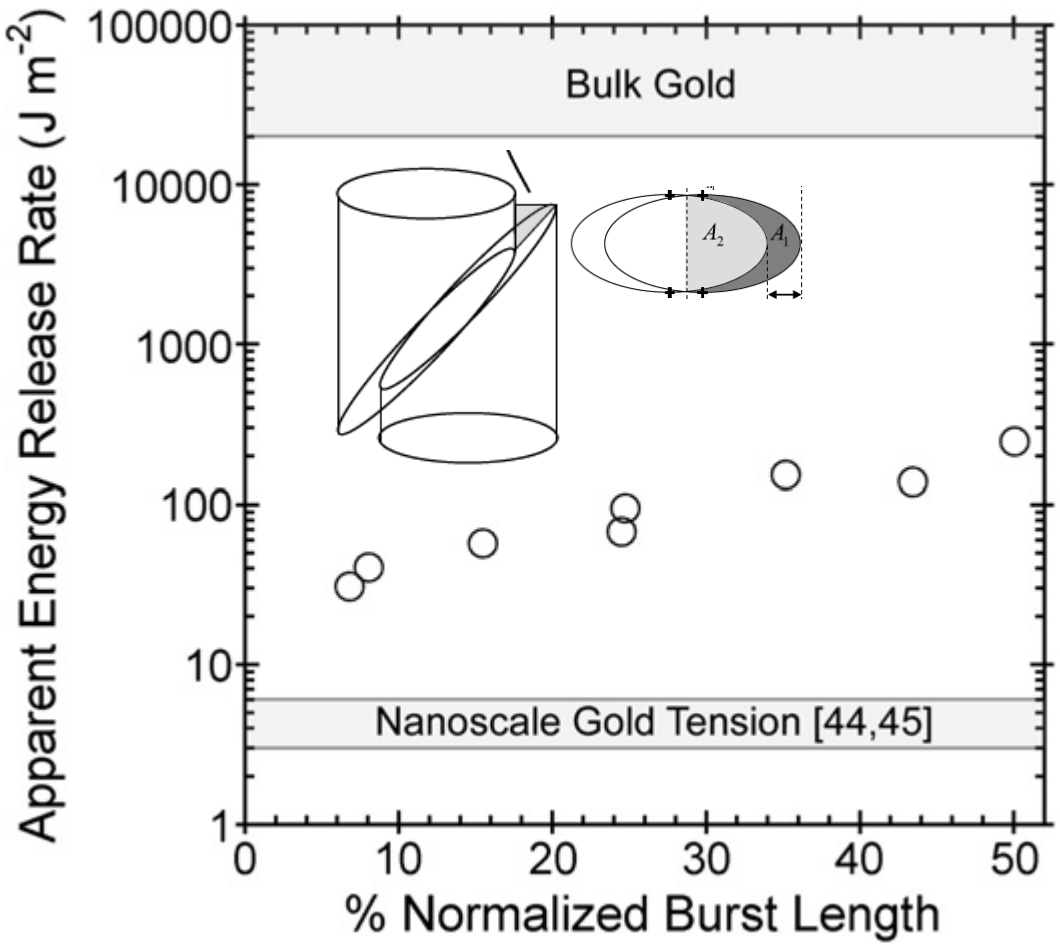

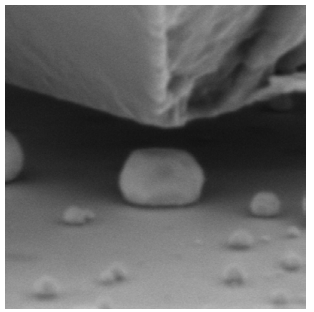

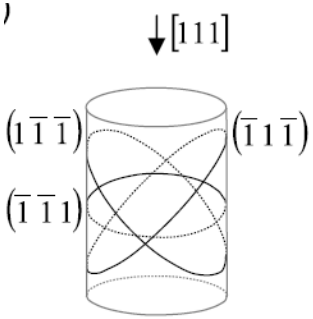

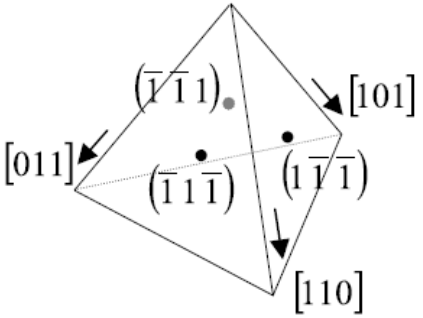

Extrinsic size effect – thin films

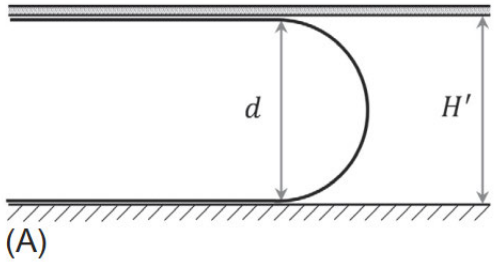

(A)

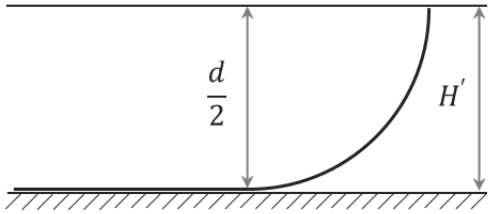

(B)

The thin film yield occurs by the motion of dislocations which are constrained to move inside the thin film.

For an inpenetrable film surface (A) the yield occurs when a dislocation loop can fit inside the thin film:

$$d(\tau) = H'$$

where d(τ) is the equilibrium diameter of a dislocation loop for an elastic isotropic material.

H′ = H/ sin (ϕ) is the size variable, where ϕ is the angle between thin film normal and that of the dislocation loop plane. Accordingly,
the yield stress can be described as follows:

$$\tau = \frac{G_f b}{H'}$$

where G_f is the thin film shear modulus.

In the case of free film surface (B), the surface induces image forces the yield stress occurs when half of the dislocation loop fits inside the thin film.

G.Z. Voyiadjis and M. Yaghoobi. (2018)

Composite mechanics

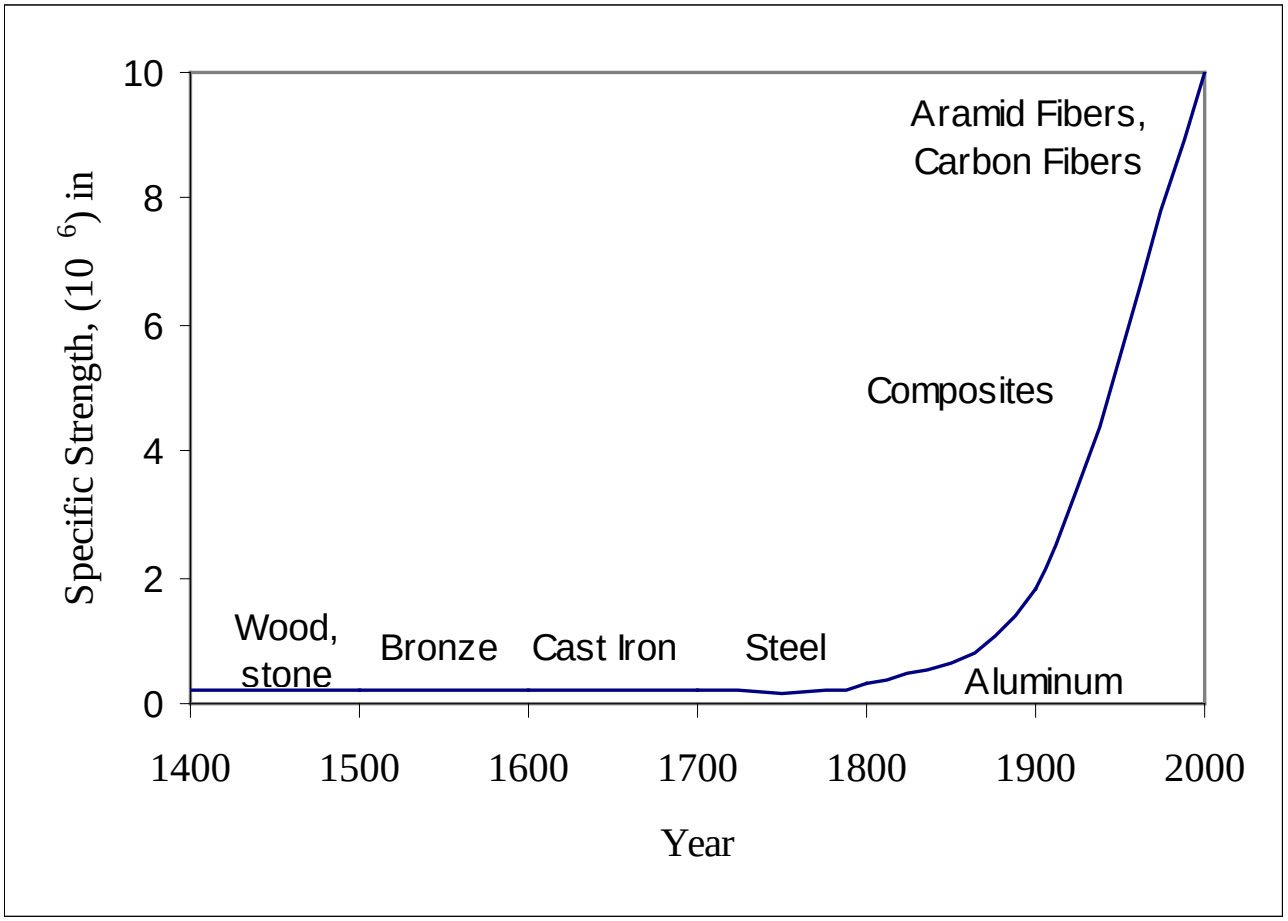

Composite mechanics

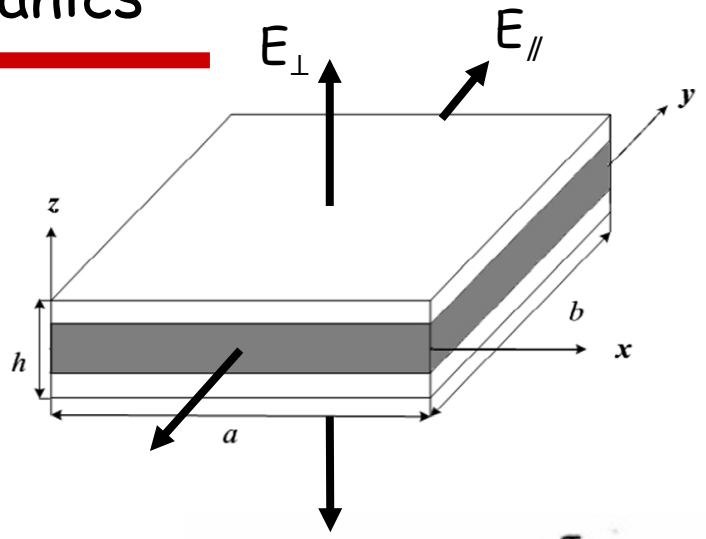

- Tailored stiffness

$$E_{//} = v_f E_f + v_m E_m$$

$$E_{\perp} = \frac{E_f E_m}{v_f E_m + v_m E_f}$$

- Tailored strength: Tsai Hill failure criterion

$$\left[\frac{\sigma_1}{(\sigma_1^T)_{ult}}\right]^2 - \left[\frac{\sigma_1\sigma_2}{(\sigma_1^T)^2_{ult}}\right] + \left[\frac{\sigma_2}{(\sigma_2^T)_{ult}}\right]^2 + \left[\frac{\tau_{12}}{(\tau_{12})_{ult}}\right]^2 < 1$$

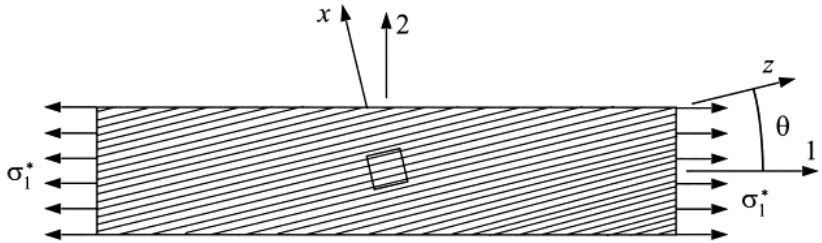

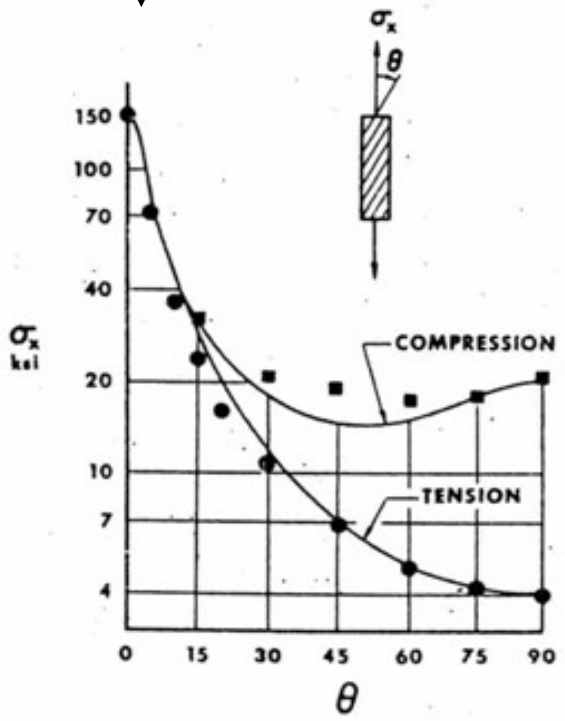

- Classically, brittle failure of strong phase:
  - Fibre pullout, …

Plasticity of multilayers - mechanisms

"Incoherent metallic multilayered composites"!

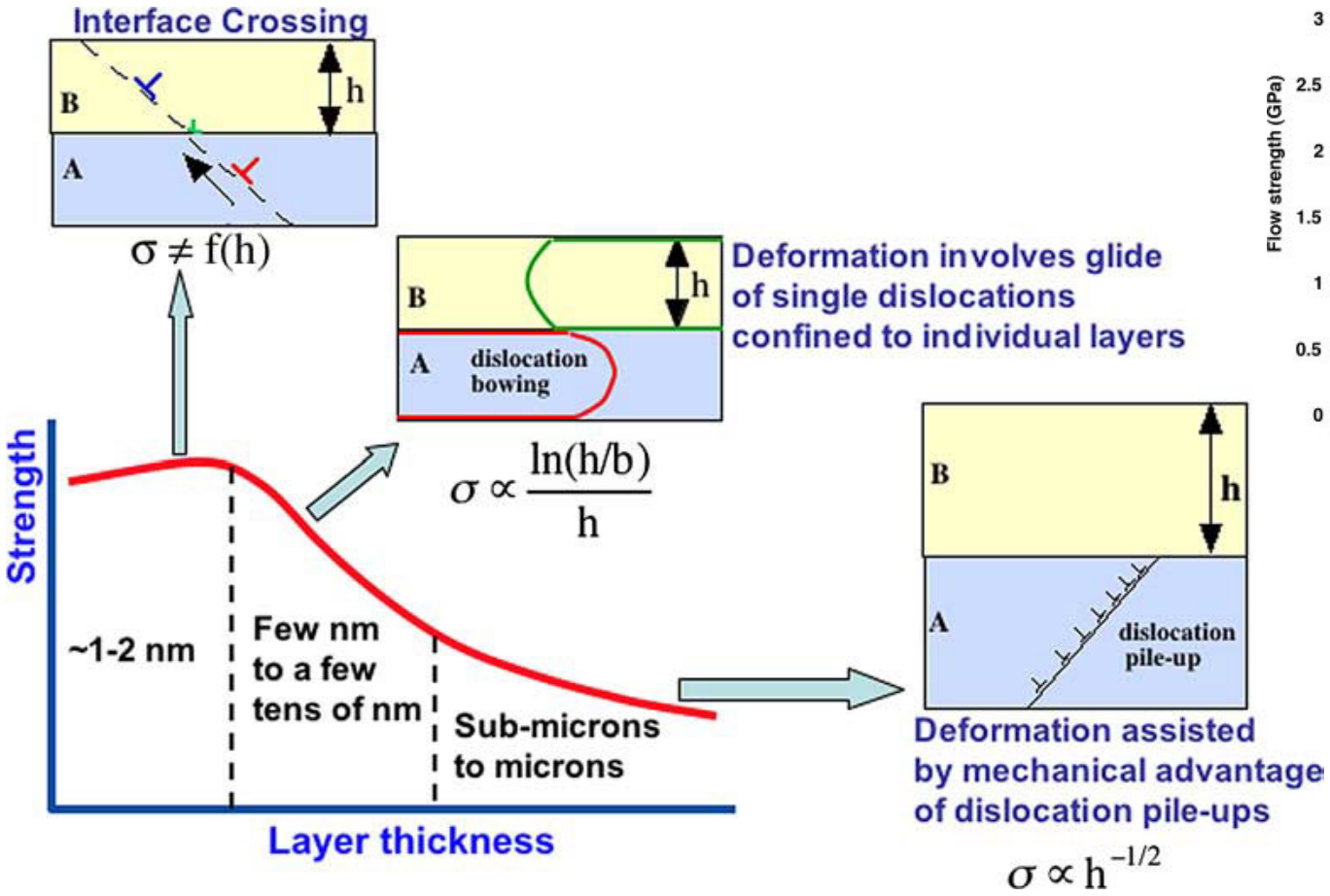

(A. Misra, R.G. Hoagland, J.P. Hirth, Acta Mater., (2005)

Cu-Nb multilayers

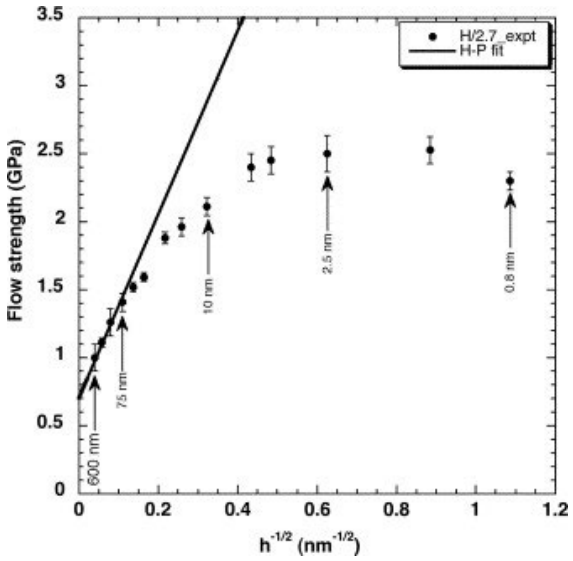

Cu-Ta multilayer

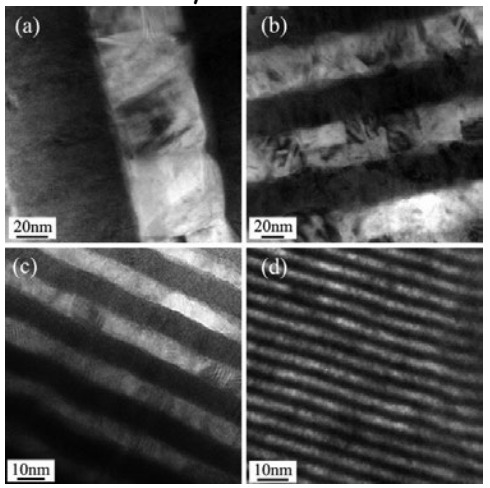

Plasticity of multilayers - mechanisms

- Bulging/extrusion of softer phase
- Shear banding: thinner layers
  - Shear by slip perpendicular to layers
  - Or interfacial sliding of incoherent boundaries?

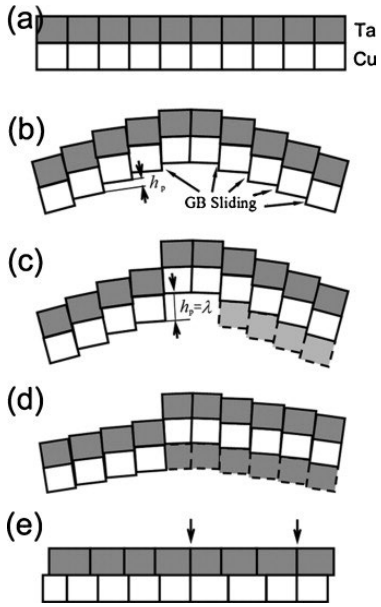

200 nm layers

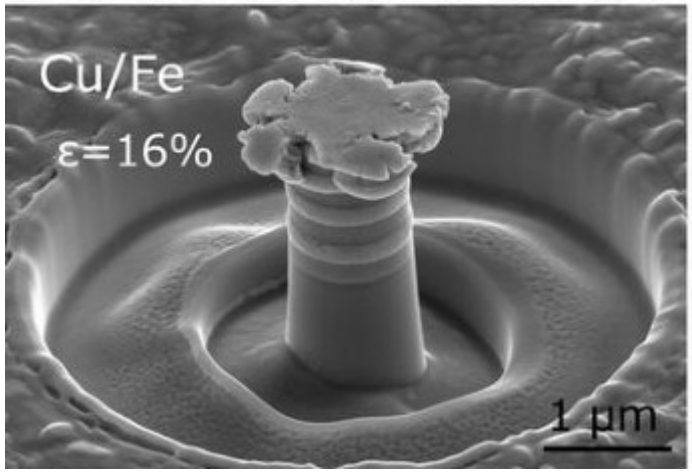

40 nm layers

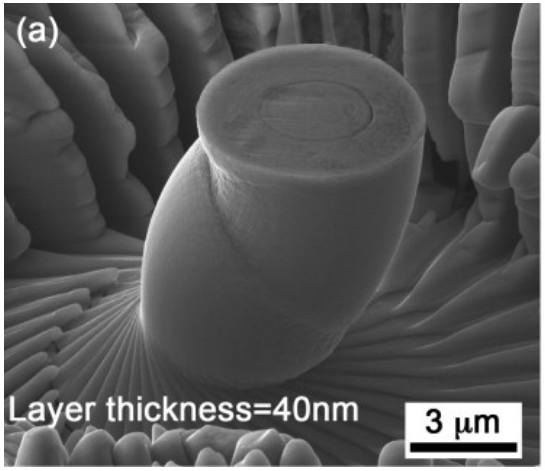

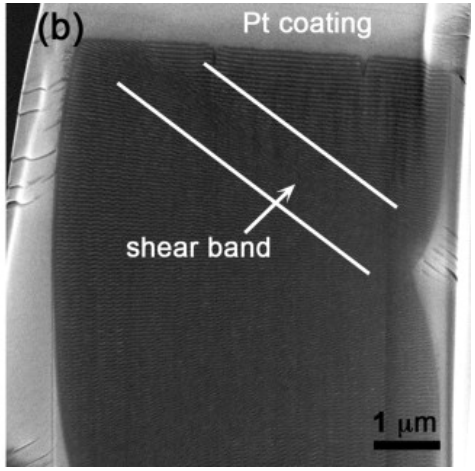

Mara, N, **APL**, 2010, 97, 021909
Wang, J et al., **Met Mat Trans A**, 2016, 46, 1405-1412

Micropillars, but… why?

- **Micro-compression**, -tensile, -cantilever

- Small volumes:
  achieve plasticity in brittle materials:
  - ceramics, intermetallics, glasses

  mechanical properties at the small scale
  - metals, multiphase alloys, nano-materials

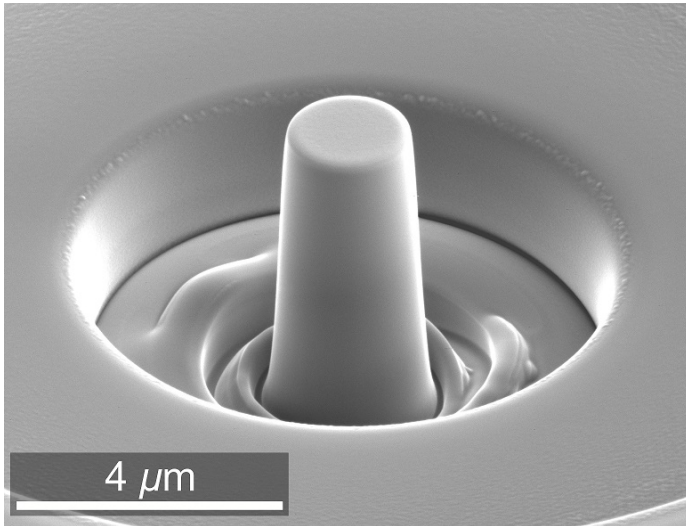

Cr_2AlC, Pürstl, J. (2018) Thesis, Cambridge

- Measure mechanical properties of individual grains or deformation mechanisms:
  - τ_c : slip, twinning, shear banding
  - E (elastic modulus): *not a good choice*
  - $\dot{\varepsilon}$ [jump tests]: activation volumes & energies

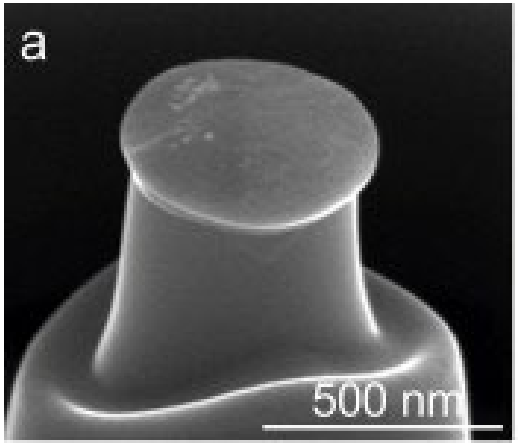

Si, 500nm, 25 °C; Korte, S. et al, Int J Plast, 2011, 27

Micro compression tests

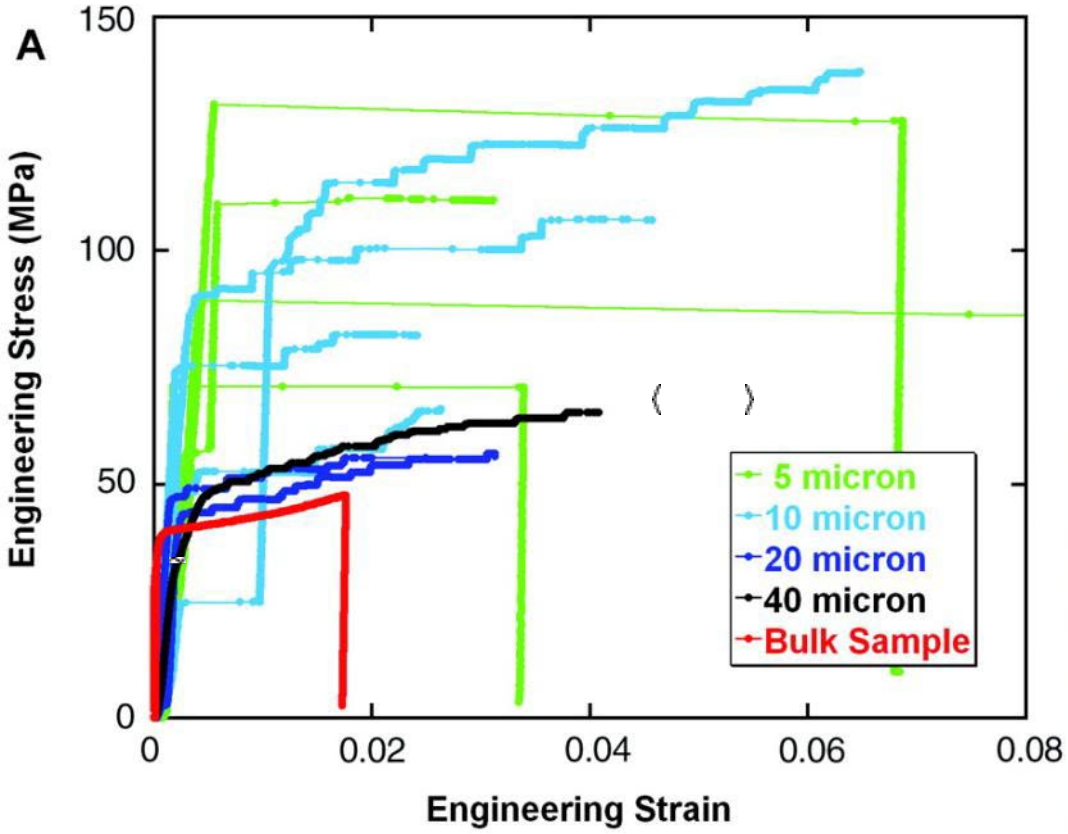

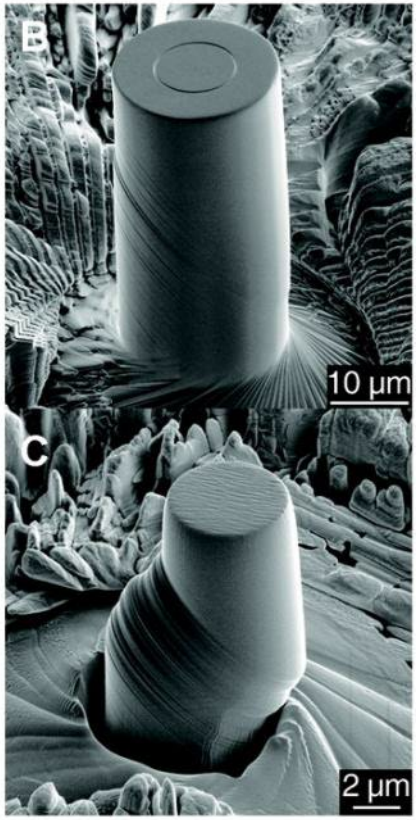

Note: true load-controlled device ! ≠ Alemnis

MD Uchic, DM Dimiduk, JN Florando, WD Nix (2004) Sample dimensions influence strength and crystal plasticity, SCIENCE 305, 986-989

Smaller is stronger

Smaller is stronger

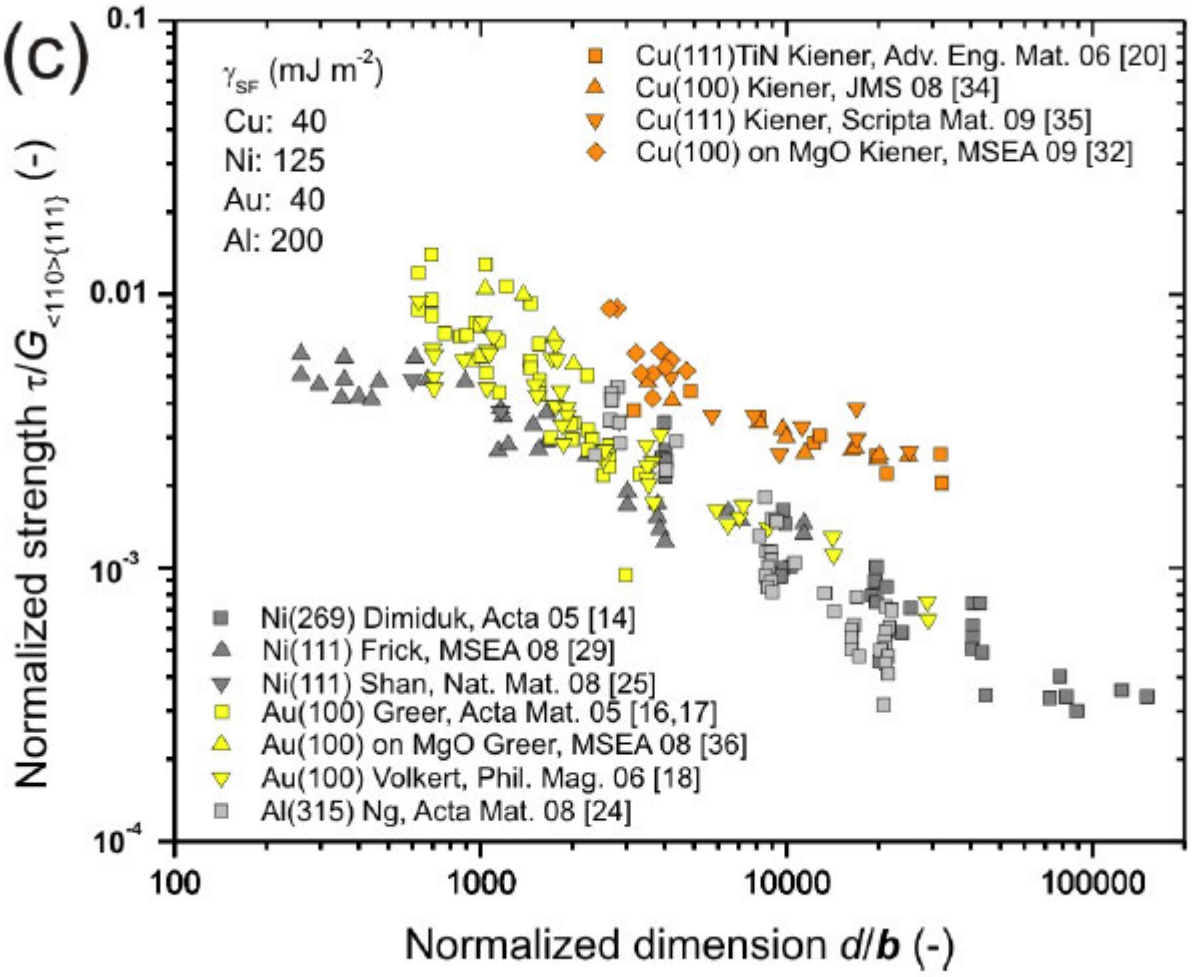

Kiener D, Motz C, Dehm G, Pippan R. Int. J. Mat. Res. 2009;100.

Extrinsic size effect – pillars

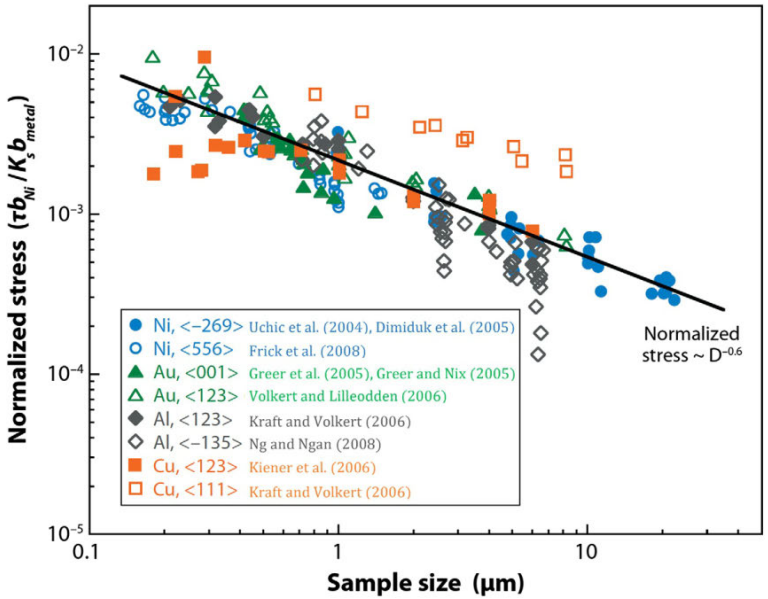

FIG. 1.39 Variation of normalized flow or yield shear stress $\tau b_{Ni}/K_s b_{metal}$ as a function of pillar diameter for different FCC metals. The original experimental data has been reported by Uchic et al. (2004), Dimiduk et al. (2005), Frick et al. (2008), Greer et al. (2005), Greer and Nix (2005), Volkert and Lilleodden (2006), Kraft and Volkert (2006), Ng and Ngan (2008), and Kiener et al. (2006). *(After Uchic, M.D., Shade, P.A., Dimiduk, D.M., 2009. Plasticity of micrometer-scale single crystals in compression. Annu. Rev. Mater. Res. 39, 361–386.)*

Au samples have been favorable since the oxide layers may alter the observed results during pillar compression experiments.

It was observed that the relation between the sample yield or flow stress σ
and the pillar diameter d can be captured using a power law as follows:

$$\sigma = Ad^{-n}$$

where A is a constant, and n is the power-law exponent, which is reported to be 0.61–0.97.

The figure illustrates the results of pillar compression experiments for several FCC metals. Assuming that τ_0 is negligible and considering the Burgers vector of Ni as the reference
one, a reasonable fit can be obtained for n = 0.6.

G.Z. Voyiadjis and M. Yaghoobi. (2018)

rectangular walls

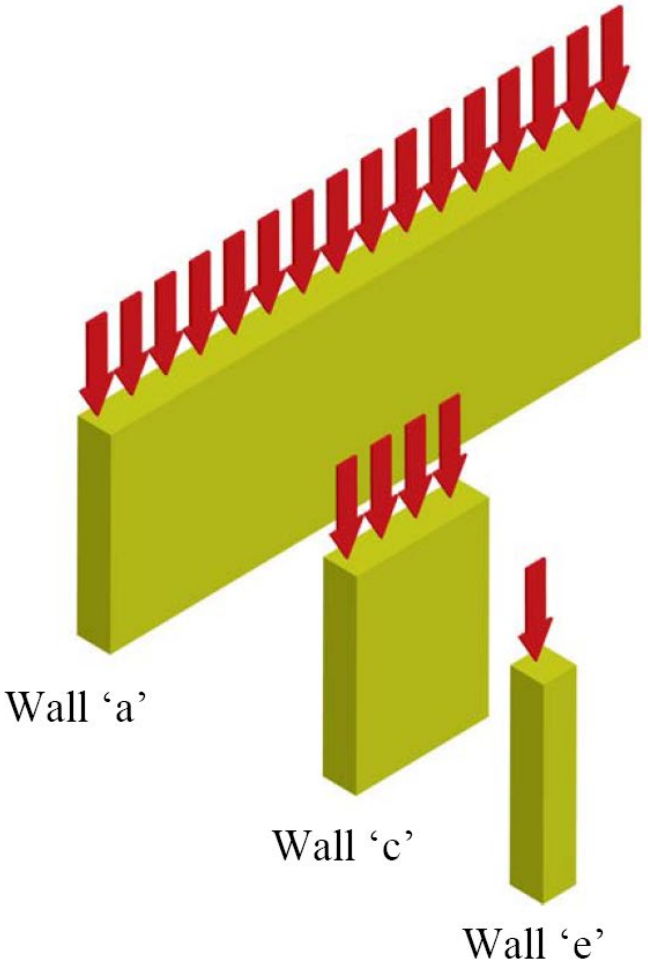

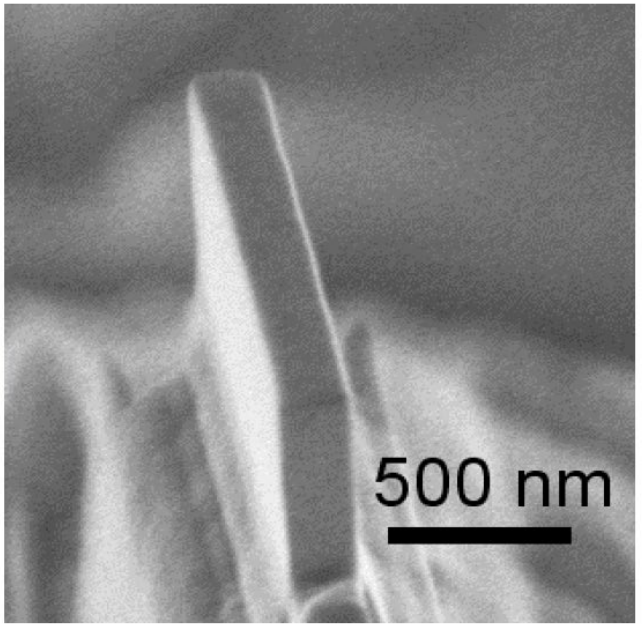

tungsten <001>

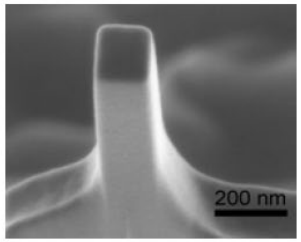

Jennett (2009) APL

rectangular walls versus circular pillars

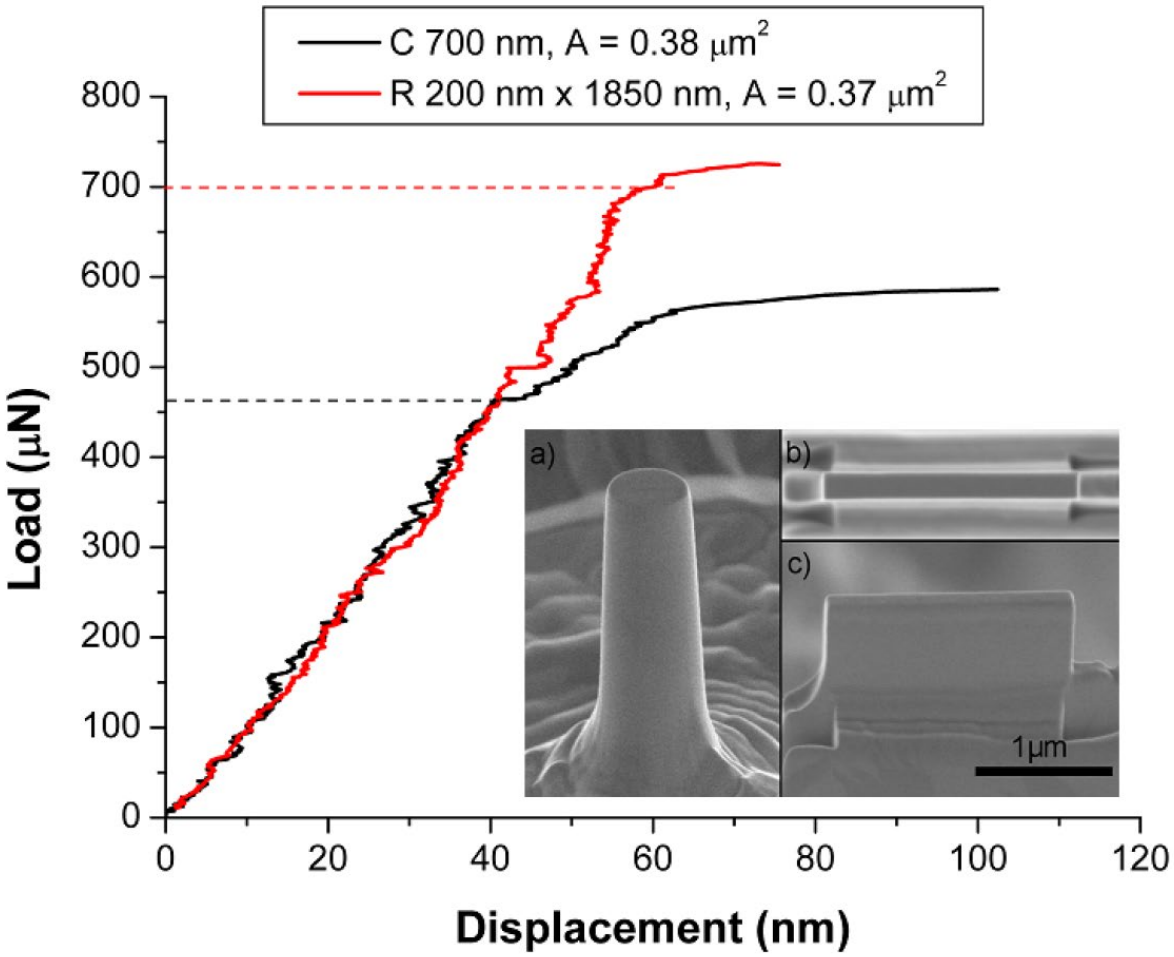

rectangular walls versus circular pillars

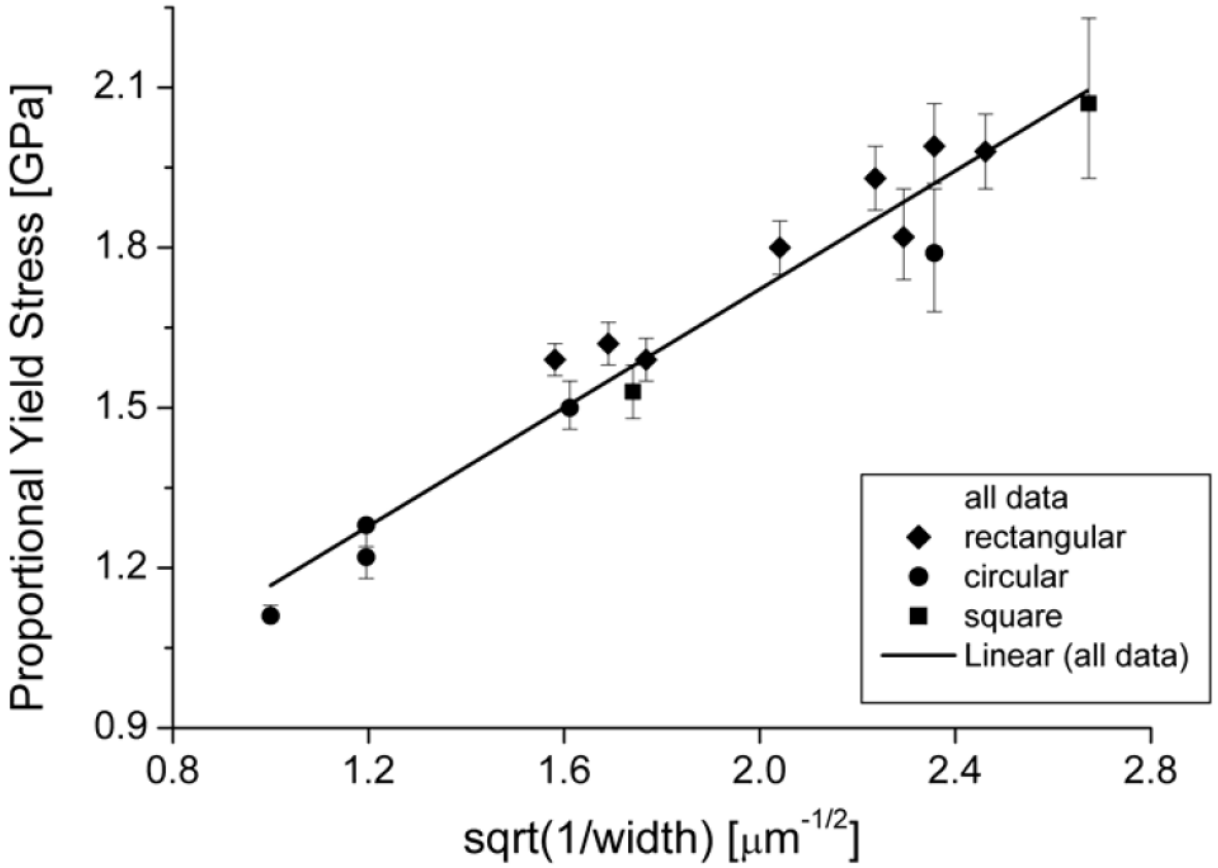

(Supporting info) Figure 2: The proportional yield point of all structures is proportional to the inverse square root of the smallest dimension. Square, rectangular and circular cross-section structures behave equivalently. Error bars represent 95% confidence intervals.

The "thinness effect"

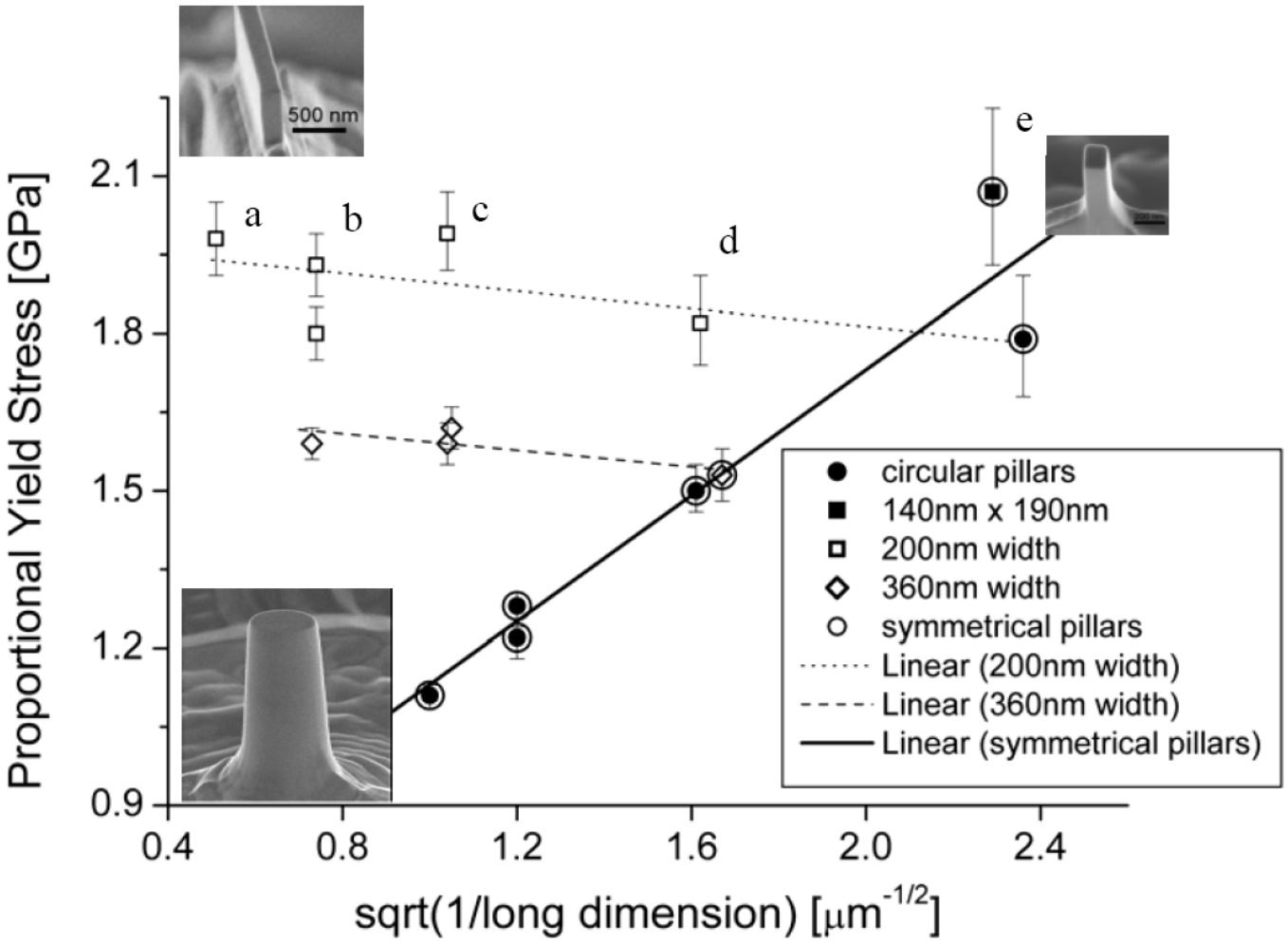

„From a practical engineering design perspective, this means that it is not necessary to shrink the entire size of the structure to obtain length-scale engineered strengthening; only the thinnest dimension needs to be reduced to obtain improved properties"

Jennett (2009) APL

Dislocation multiplication – Frank-Read source

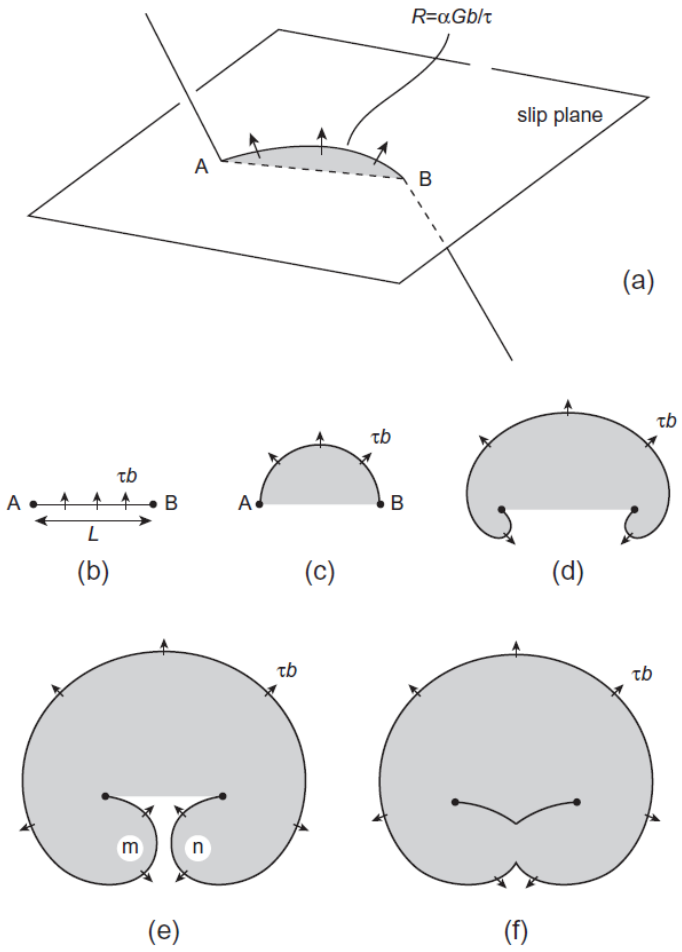

The dislocation segment is held at both ends by dislocation intersections, precipitates etc.

An applied resolved shear stress τ exerts a force τb per unit length of line and tends to make the dislocation bow

The radius of curvature R depends on the stress.

$$\tau_0 = \frac{\alpha G b}{R}$$

as τ increases, R decreases and the line bows out until the minimum value of R is reached at the position illustrated in Fig. c

Here, R equals L/2, where L is the length of AB, and the stress is

$$\tau_{max} = Gb/L$$

Hull and Bacon, Introduction to dislocations, 2010

Extrinsic size effect – source truncation

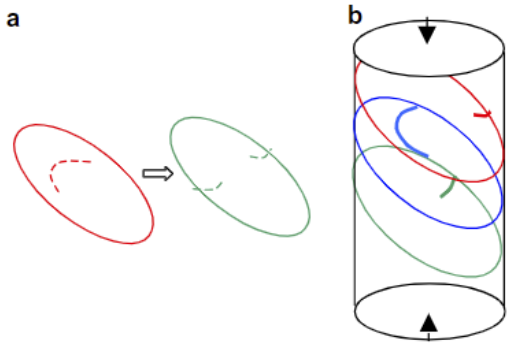

Figure 1. (a) A schematic sketch of how double-pinned Frank–Read sources quickly become single-ended sources in samples of finite dimensions. (b) Schematic sketch of single-ended sources in a finite cylindrical sample in critical configuration, which occur where the distance from the pin to the free surface is the shortest. The longest arm among the available sources (blue in this case) determines the critical resolved shear stress. Thus the statistics of pins within a sample of finite size determines the yield strength of the sample. (For interpretation of the references in colour in this figure caption, the reader is referred to the web version of this article.)

In the case of pillars with confined volumes, the double-ended dislocation sources are transformed into the single-ended ones due to the interaction of dislocations with the pillar free surfaces.

The length of the new dislocation source is a function of pillar size in a way that as the sample size decreases, the length of dislocation sources also decreases. Accordingly, a smaller sample has a higher strength.

G.Z. Voyiadjis and M. Yaghoobi. (2018)
T. A. Parthasarathy et al. / Scripta Materialia 56 (2007) 313–316

Extrinsic size effect – source truncation

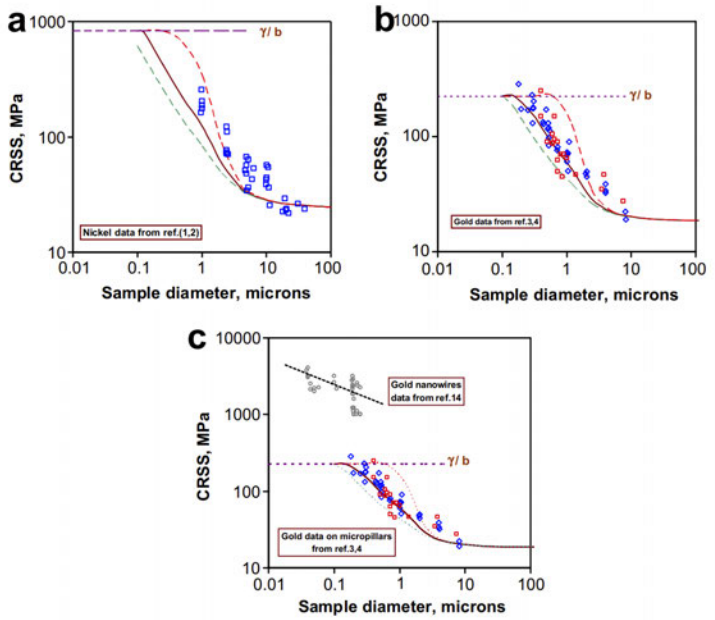

Figure 3. The model predictions for (a) nickel and (b) gold are shown in comparison with reported experimental data (from Refs. [1–4]). The dotted lines (green and red in the web version) correspond to the lower and upper standard deviations from the mean as predicted by the model. The plot in (c) includes data for gold nanowires (from Ref. [18]) to show that these differ from gold micropillars, suggesting that the nanowires are likely dislocation free with smooth surfaces that do not favor easy nucleation as in whiskers [8]. (For interpretation of the references in colour in this figure caption, the reader is referred to the web version of this article.)

The statistical variation in the source length of dislocations imposed by finite dimensions of a cylindrical sample is sufficient to rationalize much of the effect of sample size on the measured flow stress of micropillars.

Correction factor

$$\Delta\tau_{pillar} = \frac{\alpha G b}{\bar{\lambda}_{\max}}$$

Pillar diameter

T. A. Parthasarathy et al. / Scripta Materialia 56 (2007) 313–316

Micro compression tests

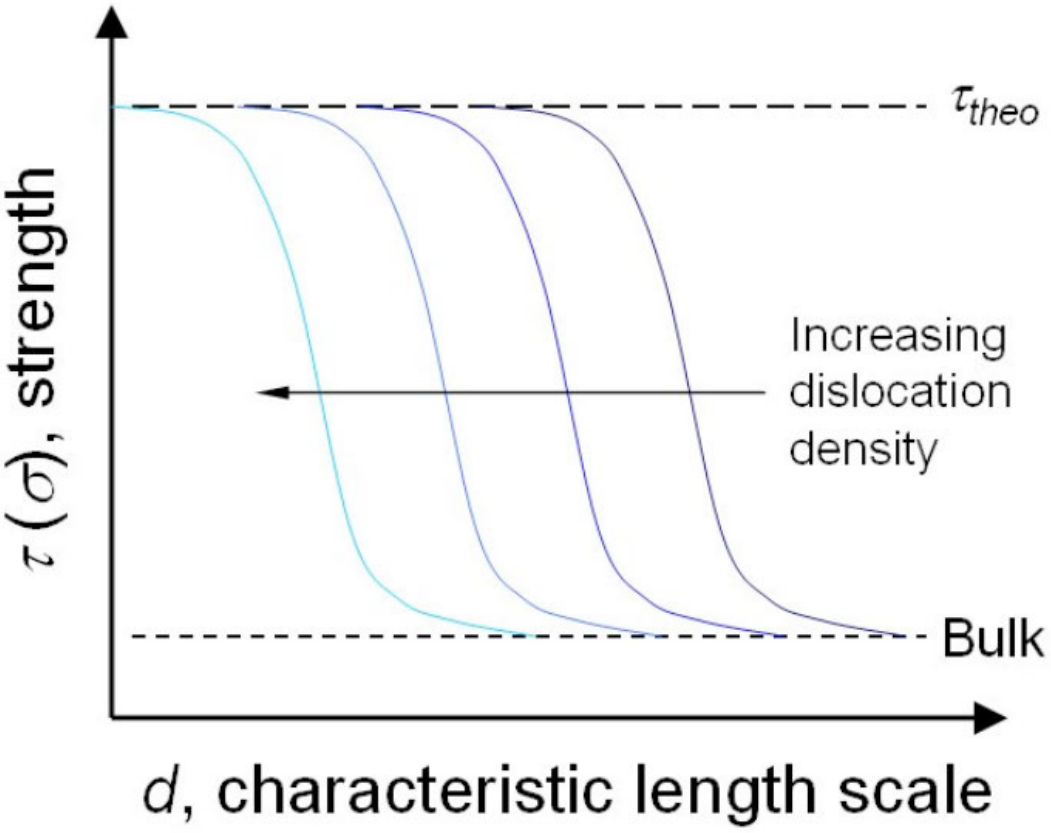

External size effects

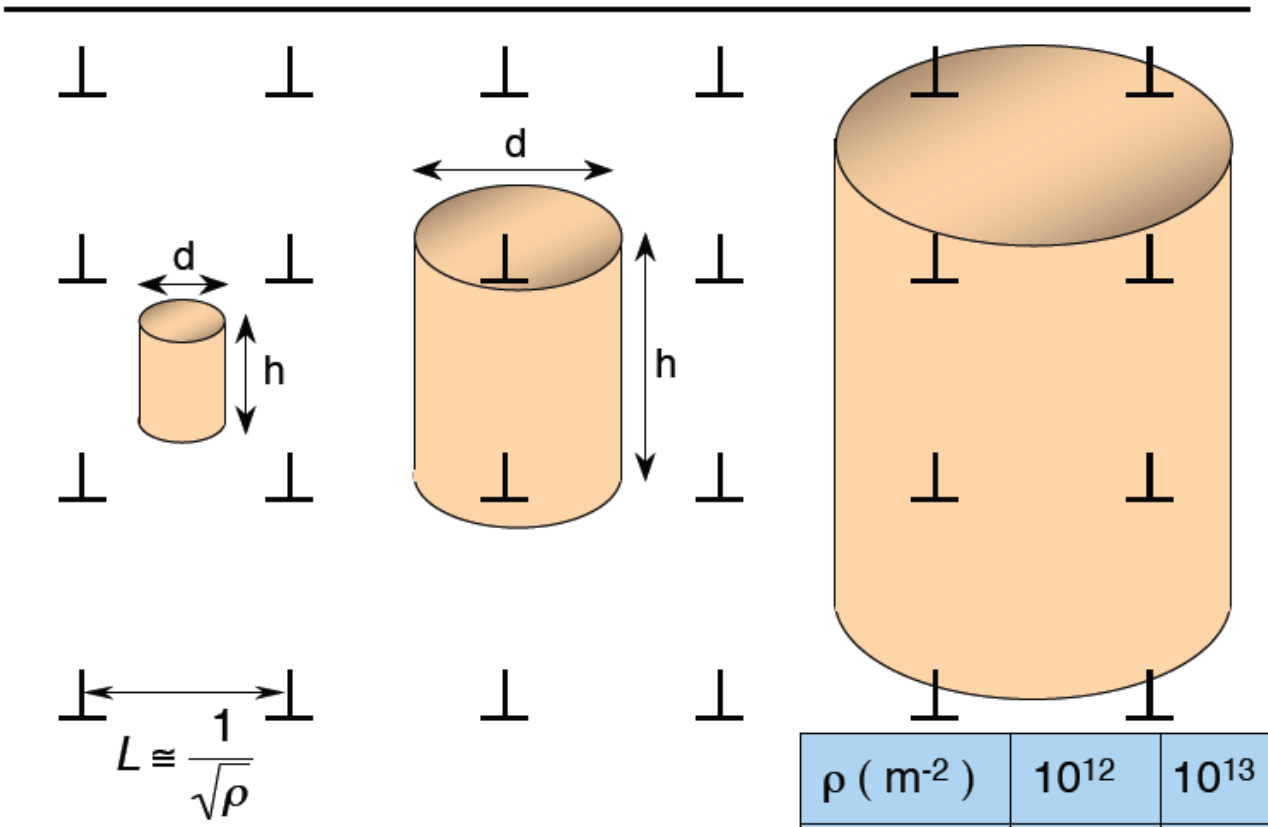

ρ (m^{-2})	10^{12}	10^{13}	10^{14}
L (μm)	1.0	0.3	0.1

Dislocation nucleation in micropillars

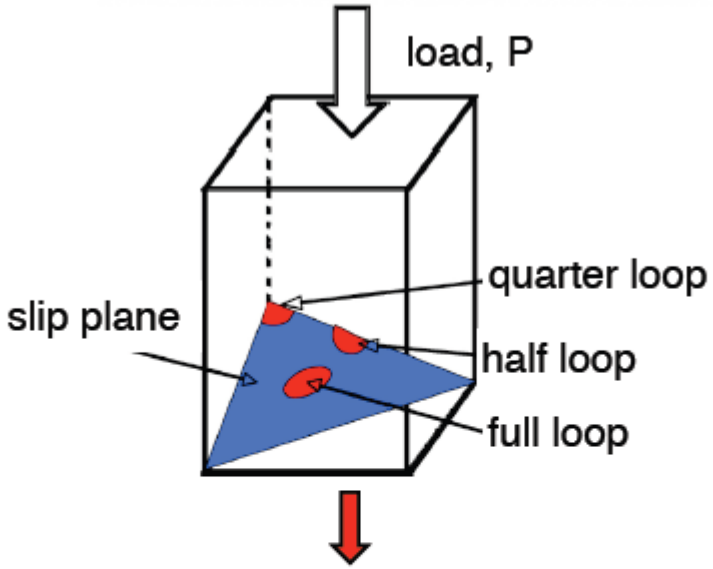

Heterogeneous

$$\tau_{crit} = \frac{Gb}{\pi e^2 r_o}\left(\frac{2-\nu}{1-\nu}\right) m \; ; \; m = \begin{bmatrix} 1 & \textit{(full loop)} \\ \sim 0.5 & \textit{(half loop)} \\ \sim 0.3 & \textit{(quarter loop)} \end{bmatrix}$$

Extrinsic influences of FIB milling on pillar strength

Kiener et al, *Mater. Sci. Eng. A* **459**, 262 (2007)

TEM of polycrystalline Cu

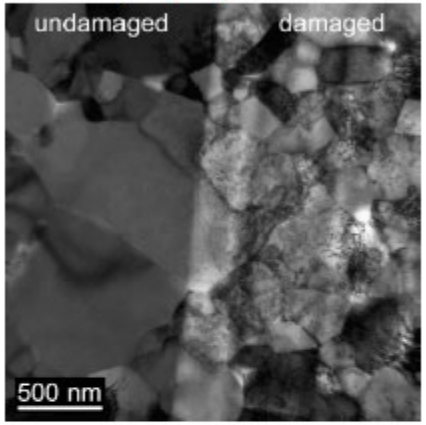

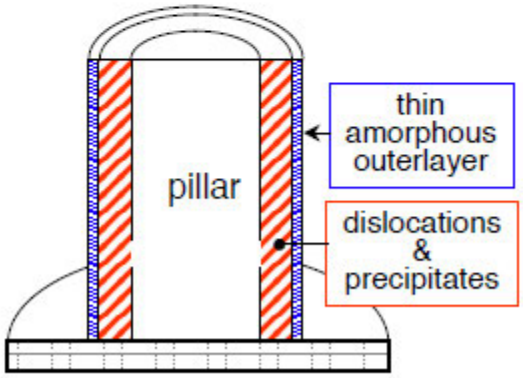

Important parameters

- beam incidence (normal/grazing)
- accelerating voltage (5-30 kV)
- current (10-2000 pA)

Strengthening mechanisms

- hard amorphous film formation
- dislocations
- precipitation

Conclusions

- FIB damage reduced at smaller accelerating voltages & grazing incidence
- even for grazing incidence, effects on strength may be significant for submicron pillars

20

Extrinsic size effect – source exhaustion

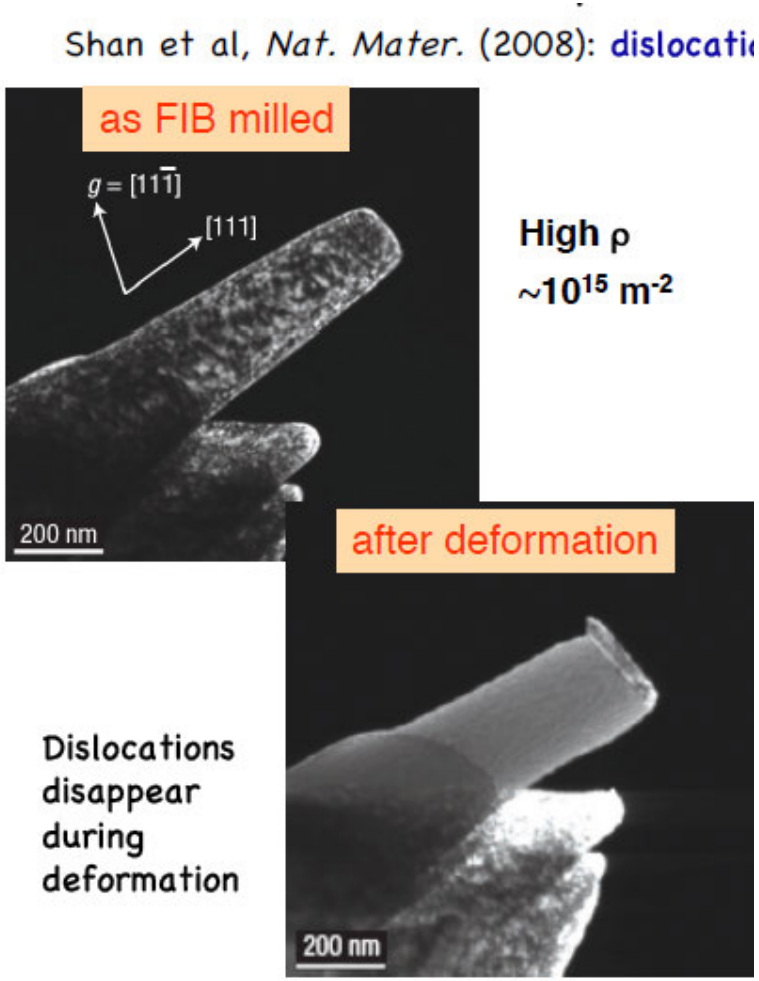

The second mechanism of hardening occurs when the available mobile dislocations are not adequate to sustain the applied plastic flow.

The loss of mobile dislocation density can occur due to the dislocation escape from the free surfaces, dislocation source shutdown, and mechanical annealing.

Consequently, the applied stress should be increased to activate stronger sources and sustain the required plastic flow, which is termed as exhaustion hardening

G.Z. Voyiadjis and M. Yaghoobi. (2018)
T. A. Parthasarathy et al. / Scripta Materialia 56 (2007) 313–316

In situ tension: single-crystal copper samples

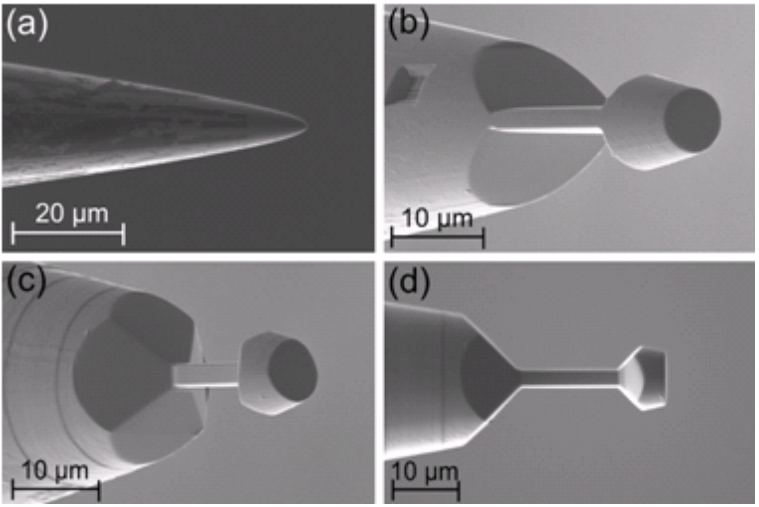

Fig. 1

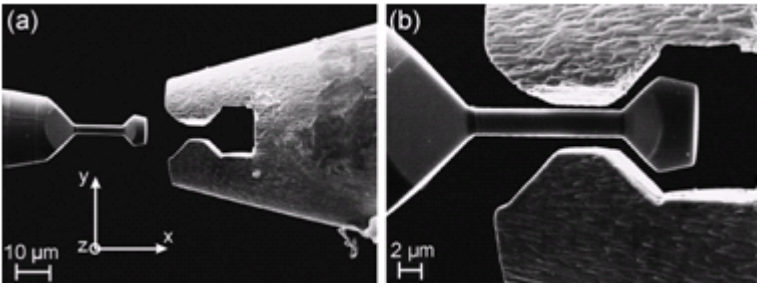

Fig. 2

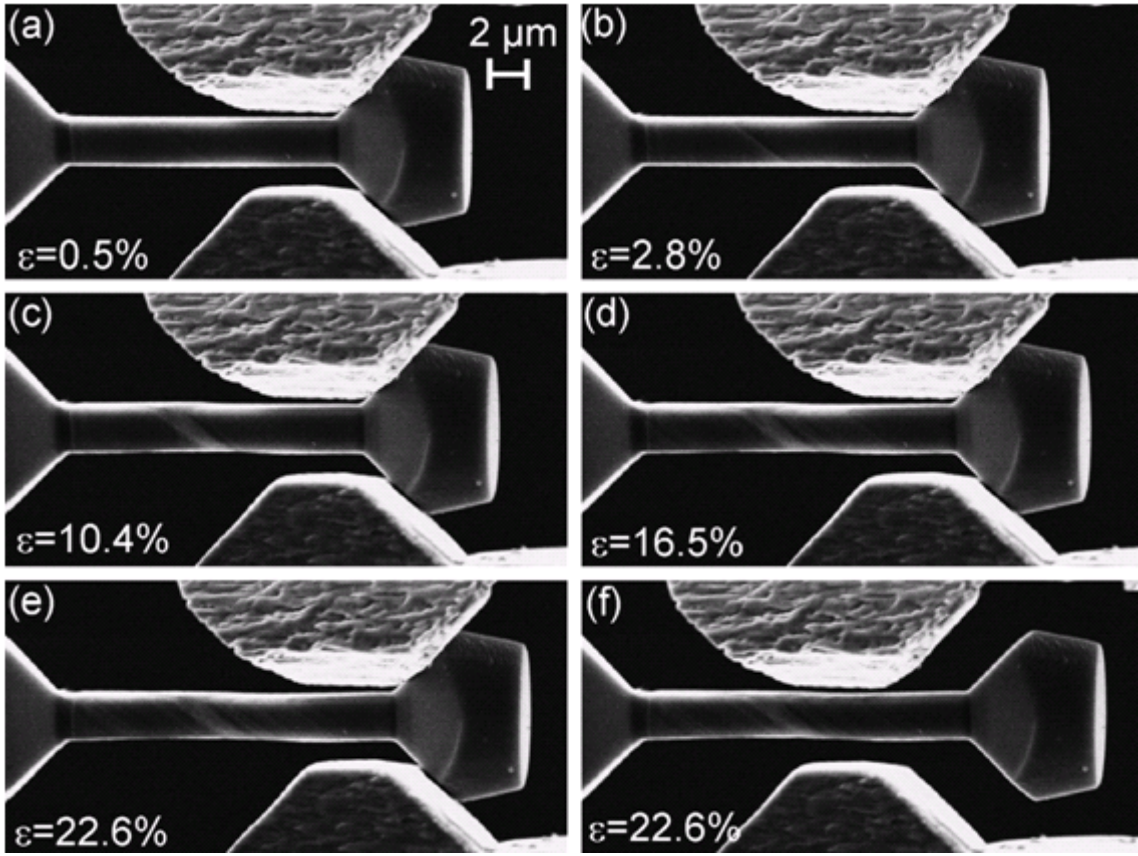

Fig. 3

Compression versus tension

Cu(100) oriented tensile and compression sample

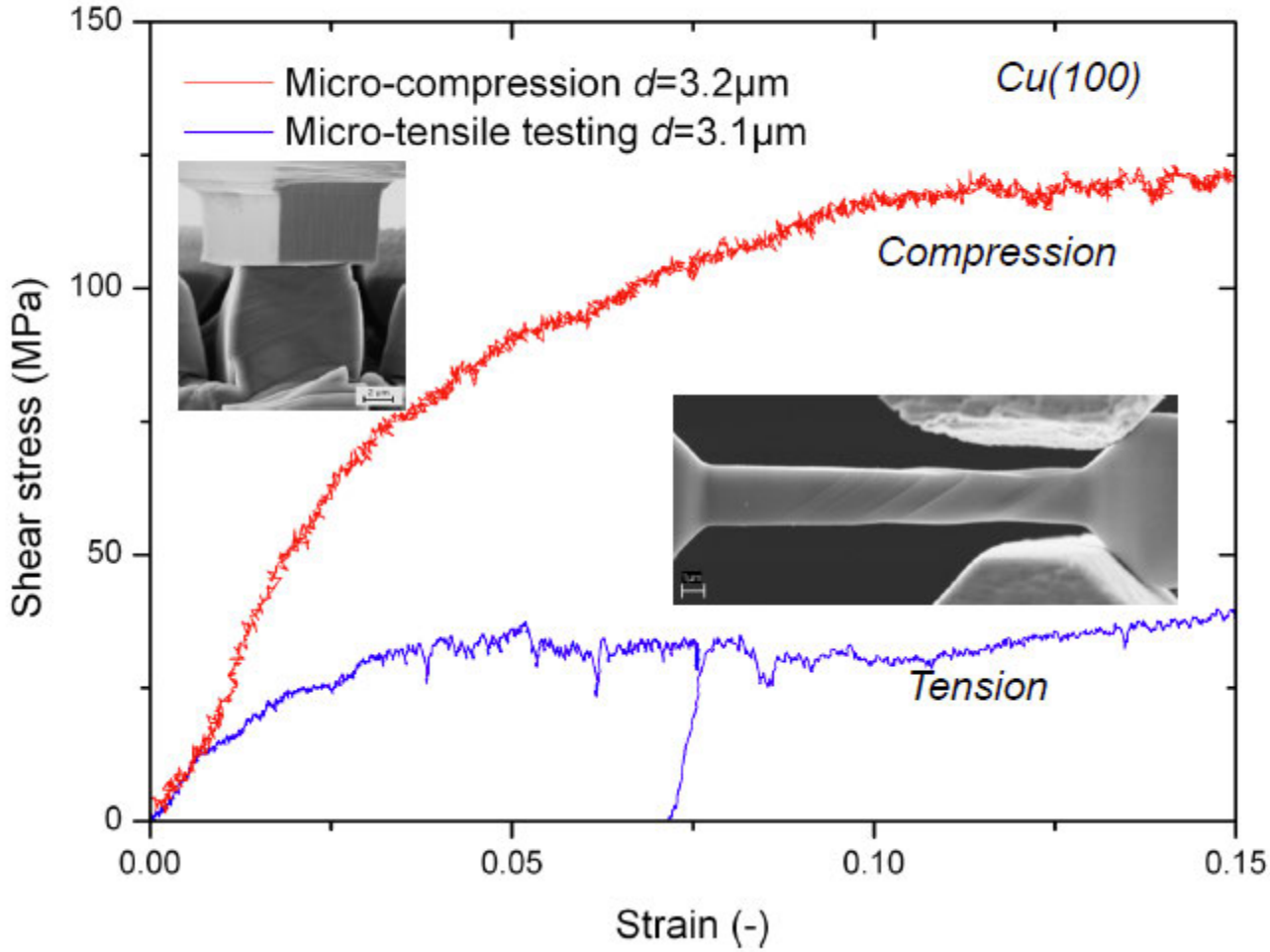

Strength from lateral constraint

Micro-compression of a Cu(100) sample with reduced lateral stiffness

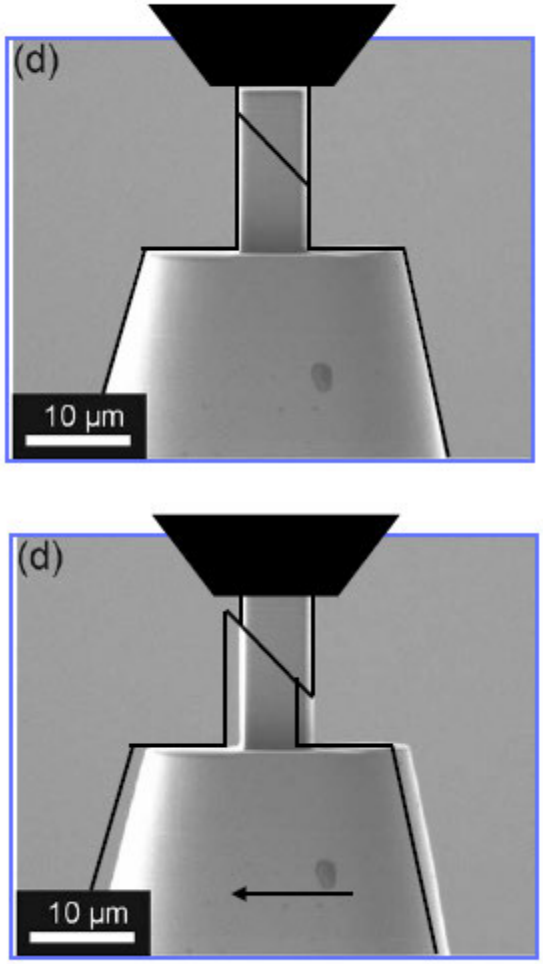

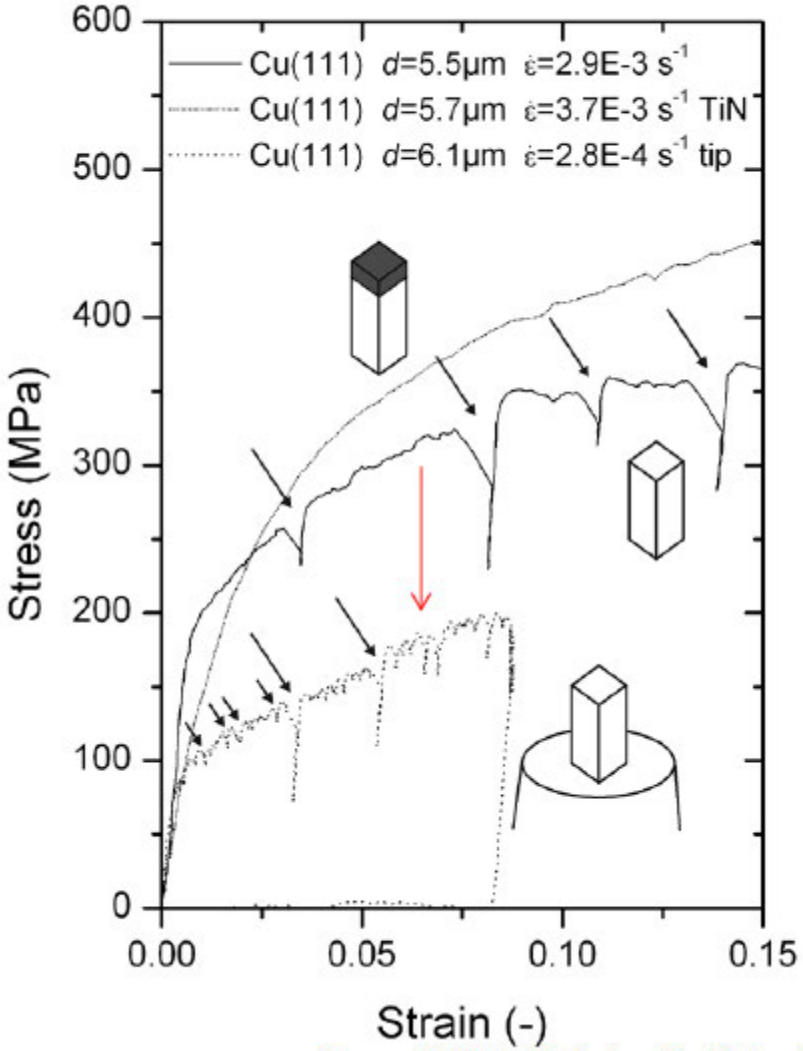

Kiener D, Motz C, Dehm G. Mater. Sci. Eng. A 2009;505:79.

Internal & external size effects

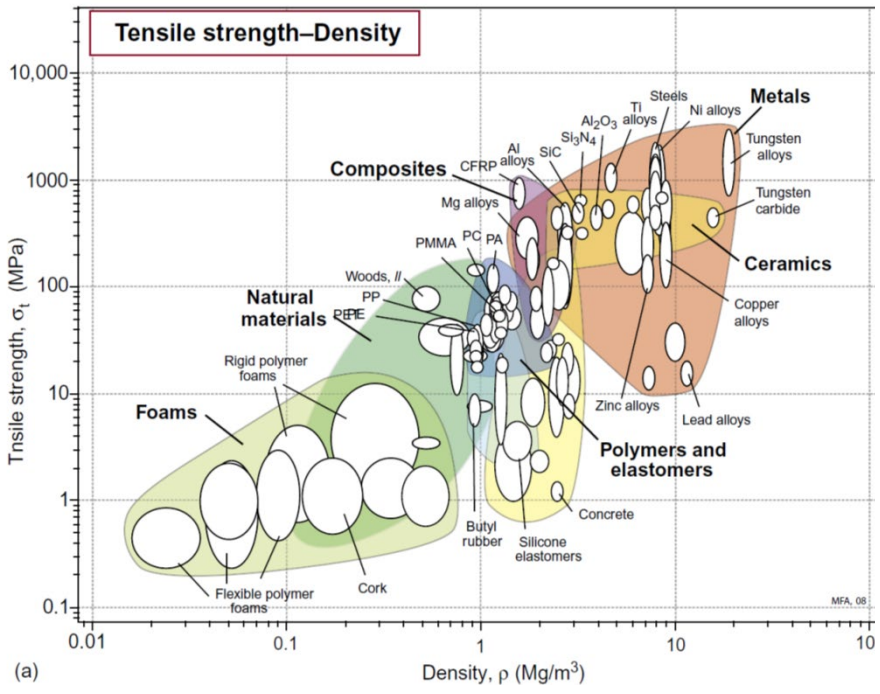

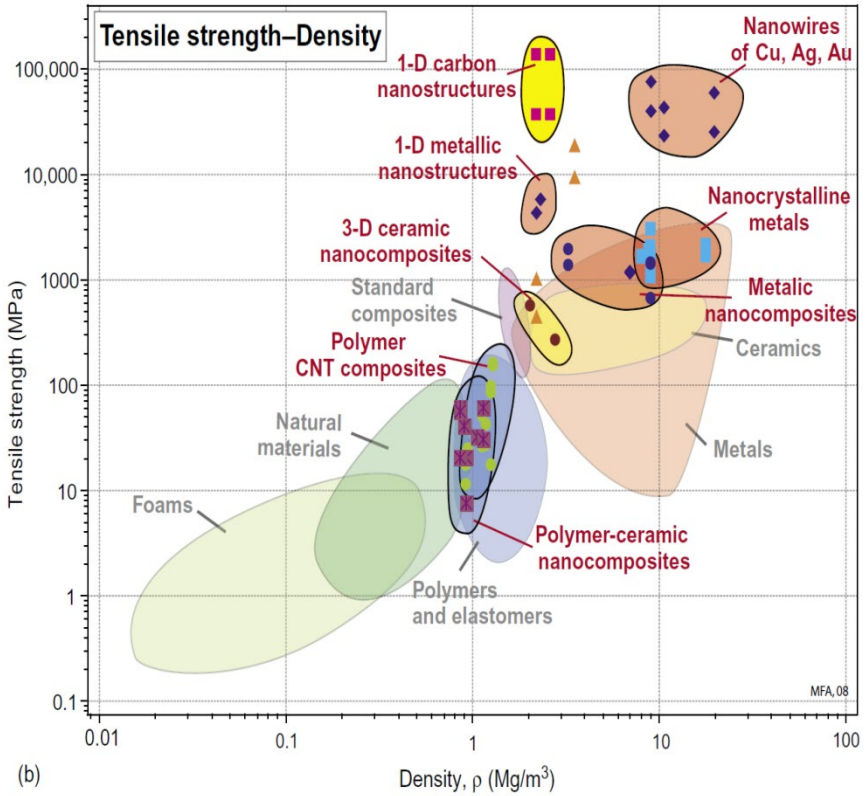

Size dependence of mechanical materials properties

physical size effects

Micro compression tests

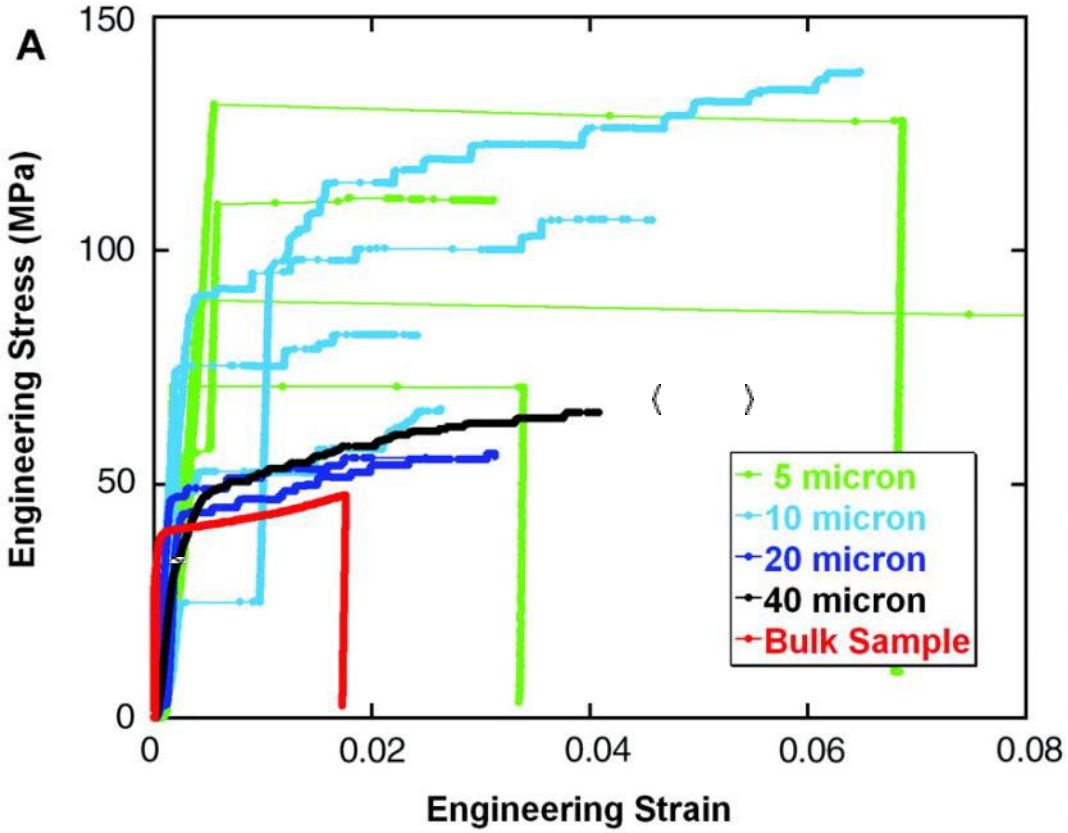

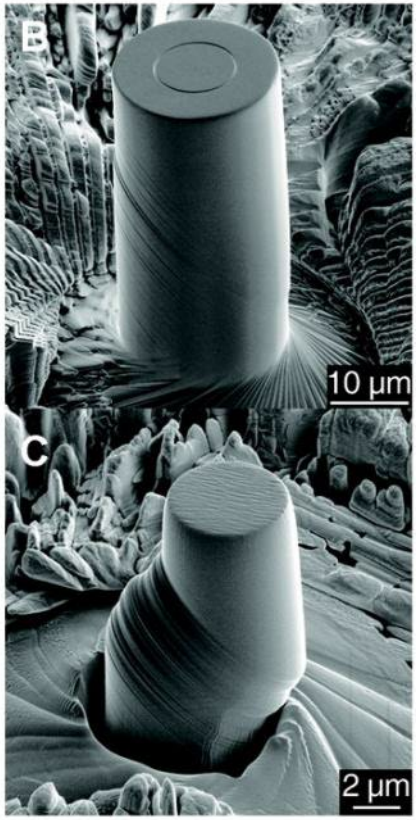

MD Uchic, DM Dimiduk, JN Florando, WD Nix (2004) Sample dimensions influence strength and crystal plasticity, SCIENCE 305, 986-989

In-situ TEM compression of nickel micropillars

Shan et al, *Nat. Mater.* (2008): dislocati

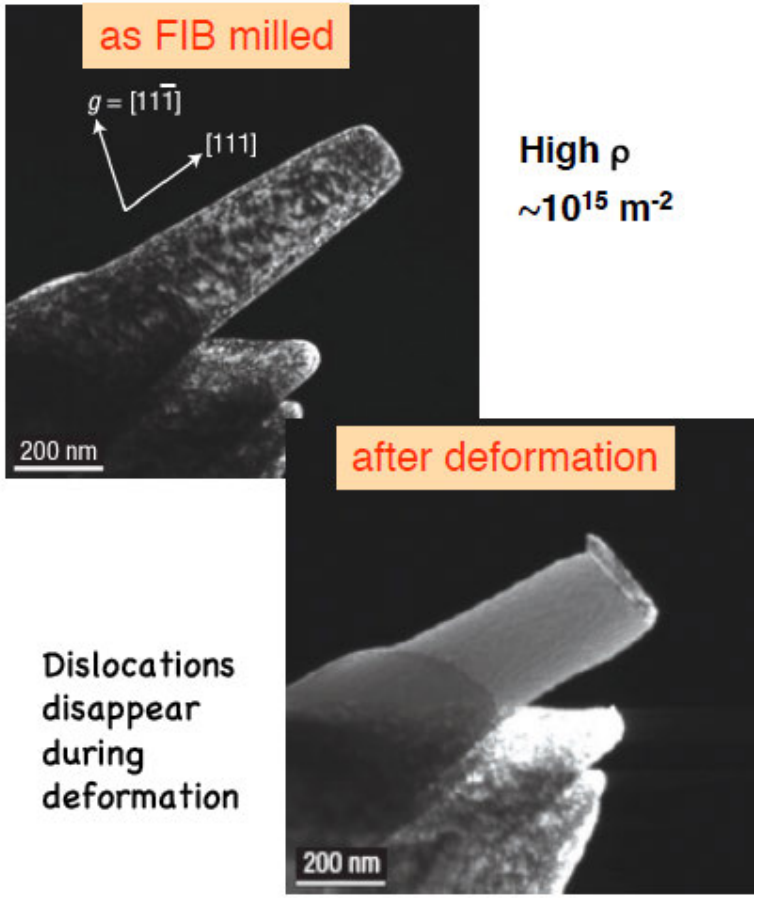

High ρ
~10^{15} m^{-2}

Dislocations disappear during deformation

Smaller is stronger

Smaller is stronger

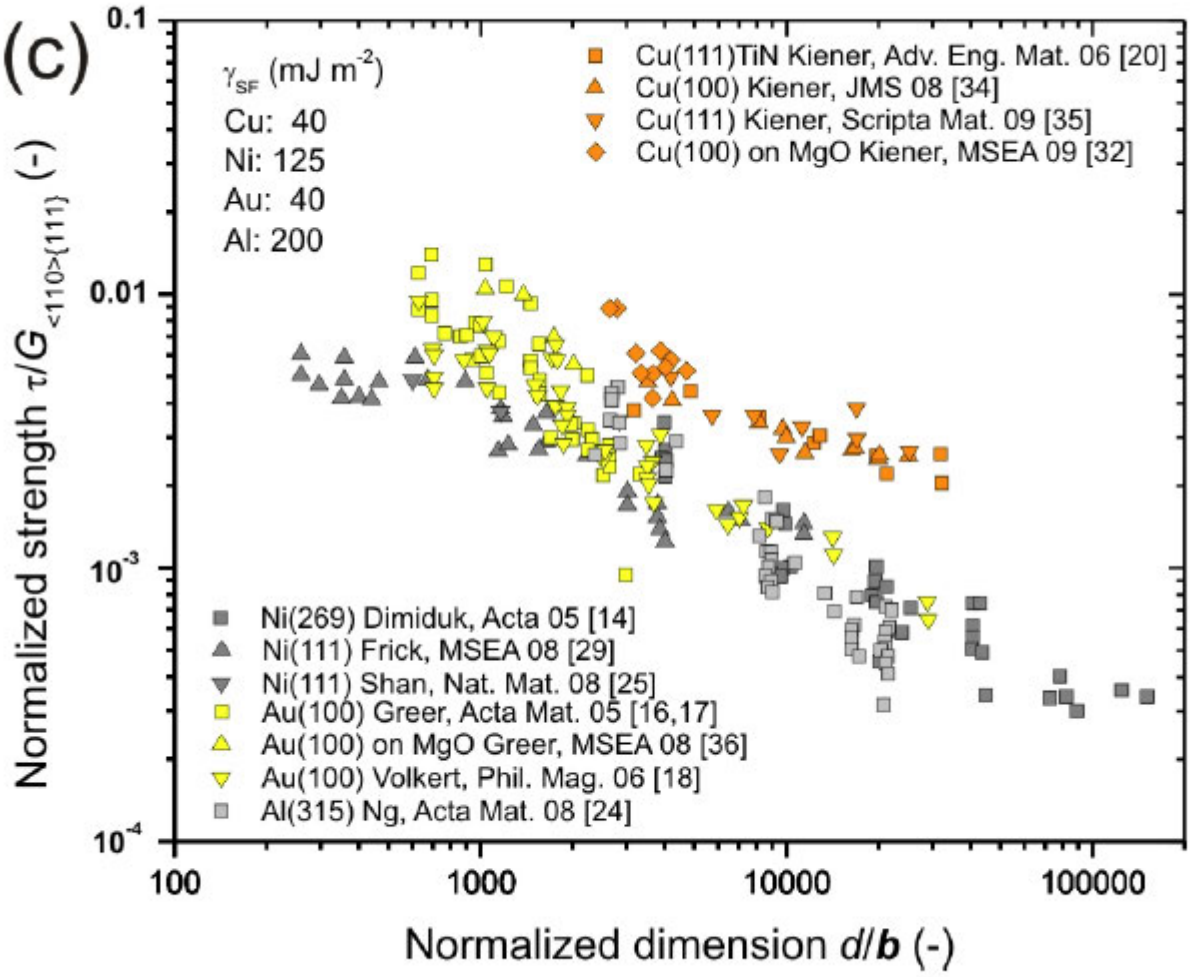

Kiener D, Motz C, Dehm G, Pippan R. Int. J. Mat. Res. 2009;100.

Micro compression tests

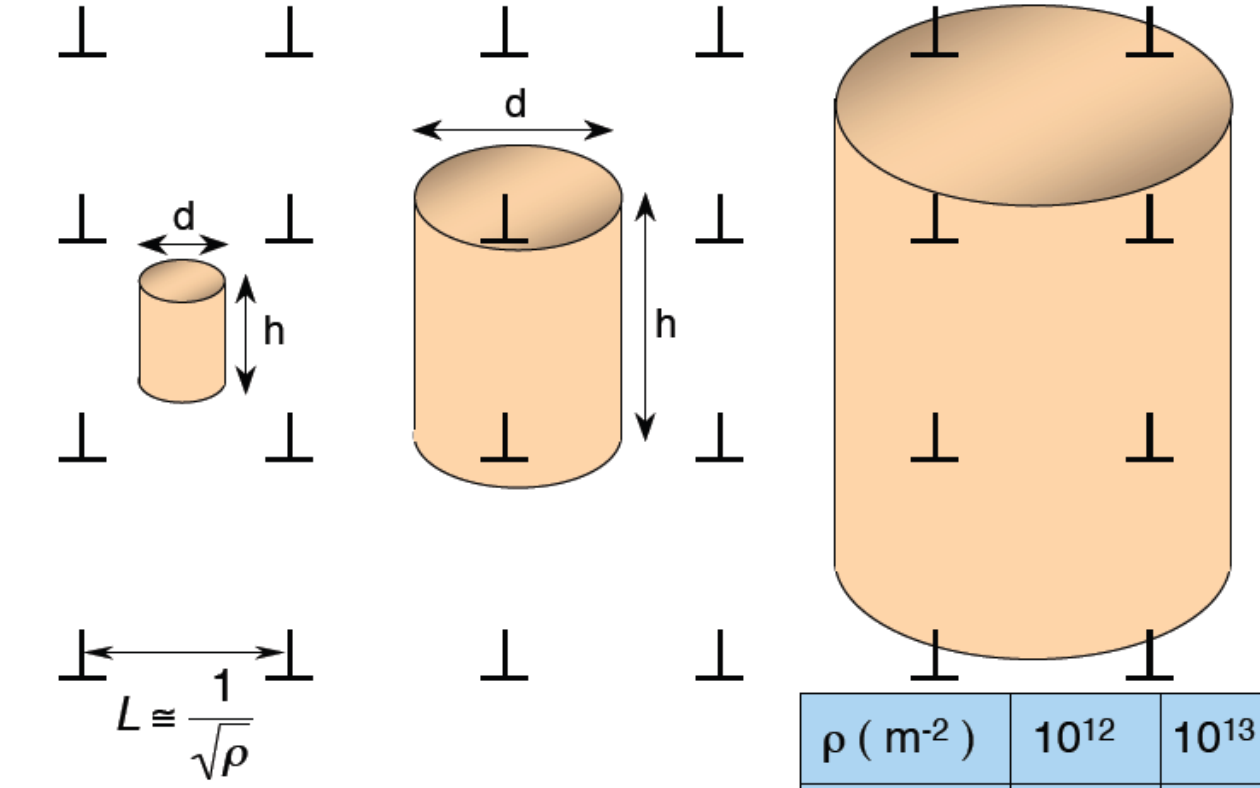

ρ (m^{-2})	10^{12}	10^{13}	10^{14}
L (μm)	1.0	0.3	0.1

The ideal strength

- The ideal strength is the stress required to plastically deform a "perfect" (defect-free) infinite crystal.

- $\tau_{ideal} >> \tau_{exp}$

$\tau_{ideal} \approx G/2\pi$
$\tau_{exp} \approx G/1000$

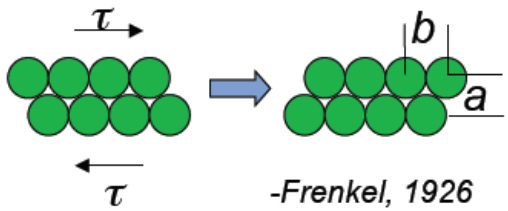

-Frenkel, 1926

•1934- Orowan, Taylor and Polyani independently discovered dislocations and showed that real plastic deformation could be described by their movement.

⇒Even a simple model of the force required to move a dislocation shows that shear is possible at much lower stresses than in a perfect crystal.

micro compression tests

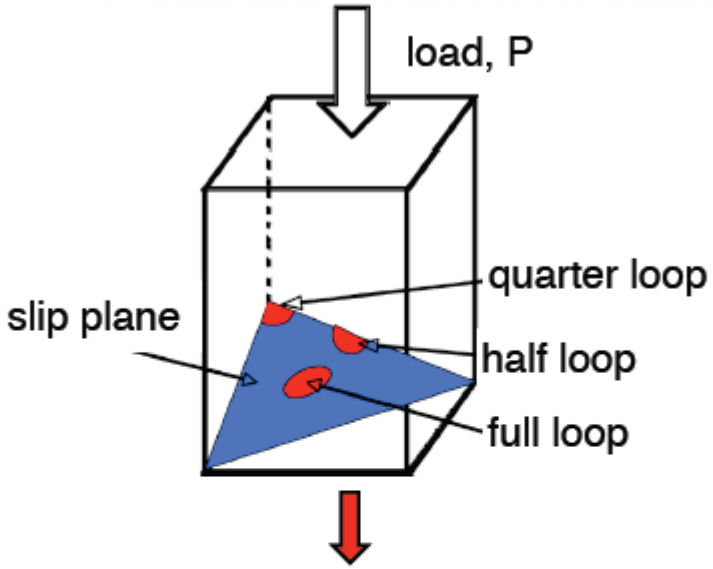

Heterogeneous

$$\tau_{crit} = \frac{Gb}{\pi e^2 r_o}\left(\frac{2-\nu}{1-\nu}\right) m \; ; \; m = \begin{bmatrix} 1 & \textit{(full loop)} \\ \sim 0.5 & \textit{(half loop)} \\ \sim 0.3 & \textit{(quarter loop)} \end{bmatrix}$$

Micro compression tests

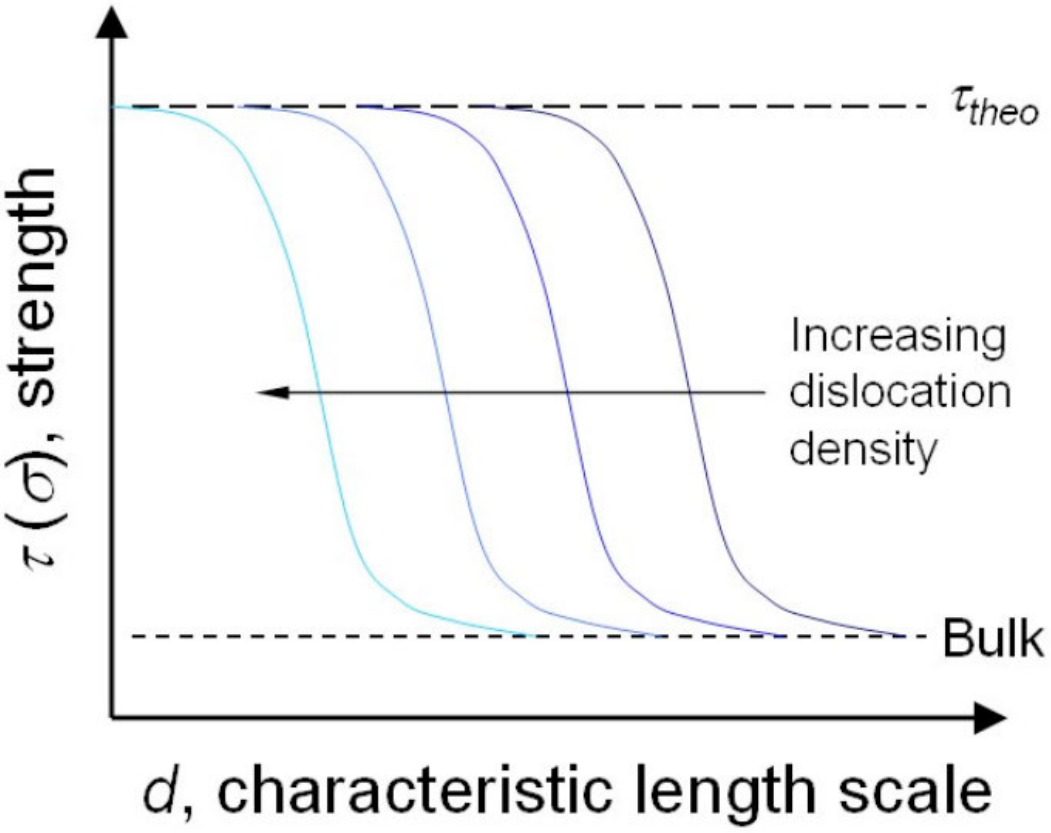

fracture and plasticity of GaAs and Si micropillars

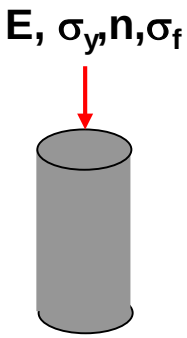

room temperature plasticity of brittle materials

two main types of experiments to prevent brittle fracture:

macroscopic uniaxial loading with confining pressure
e.g. J. Rabier (2000) Phys. Stat. Sol. (b), 22, 63

or

macro-, micro- and nanoindentation experiments with "built-in" hydrostatic pressure components
e.g. E. Le Bourhis and G. Patriarche, Prog. Crystal Growth and Charact. 47, 1

What happens if we scale down the uniaxial compression experiment to the micro- and nanoscale?

fracture of silicon and GaAs micropillars

Silicon micropillars (001)

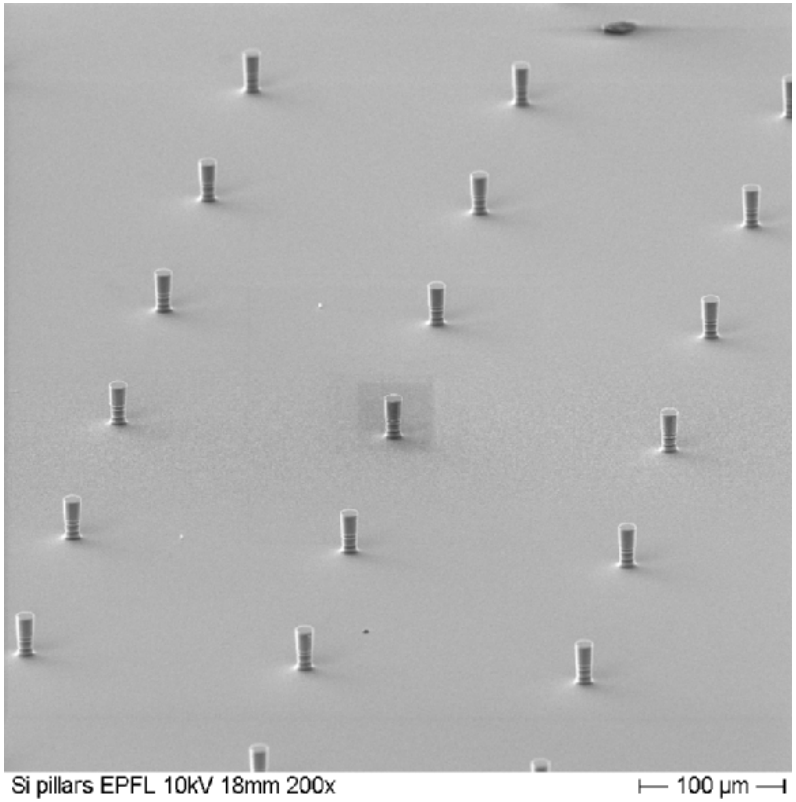

Electron beam lithography & deep reactive ion etching, collaboration with P. Hoffmann, EPFL, Lausanne

GaAs micropillars, <001> orientation

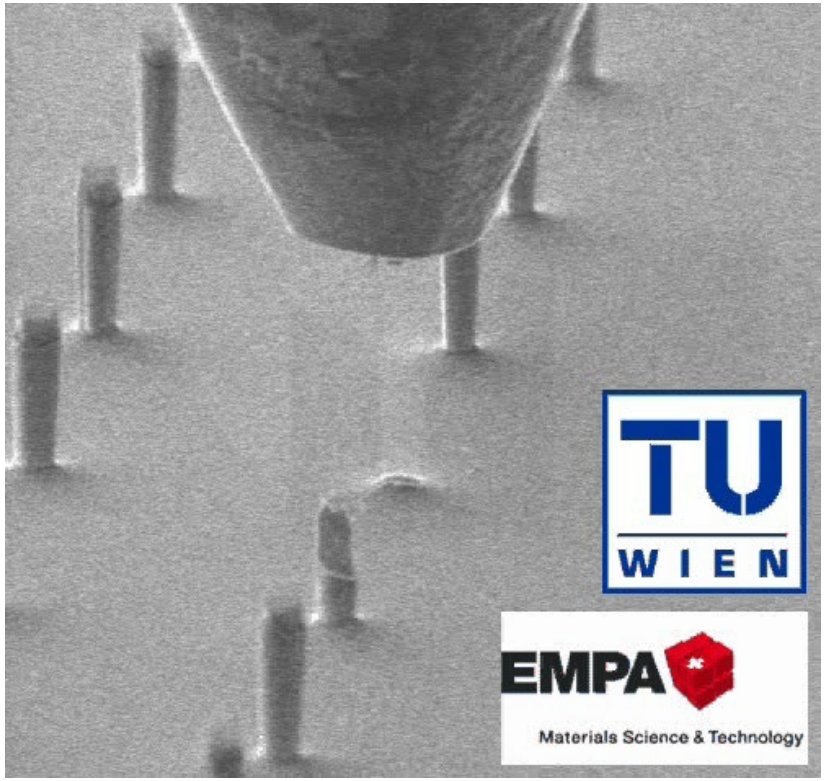

UV-lithographie wet chemical etching, collaboration with A. Lugstein, TU Wien

fracture of silicon micropillars

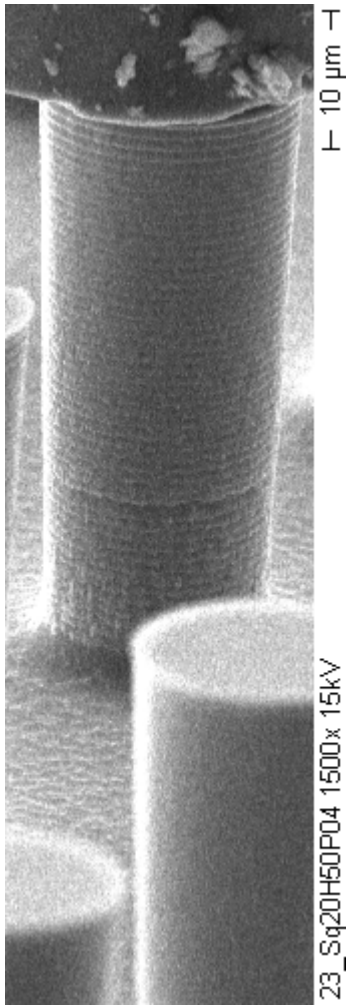

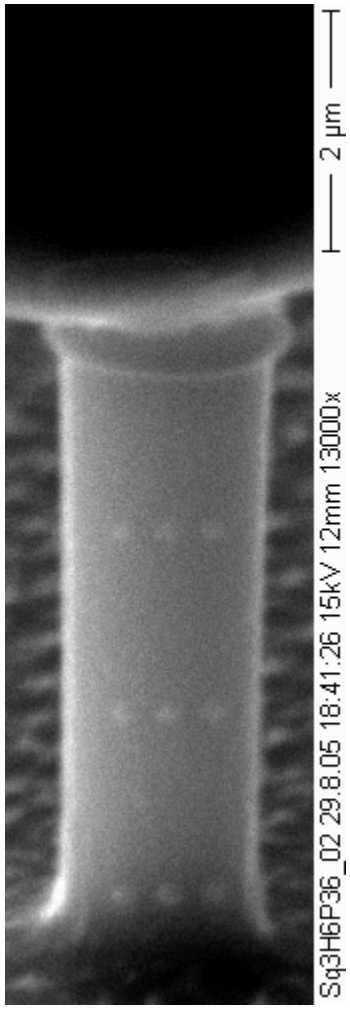

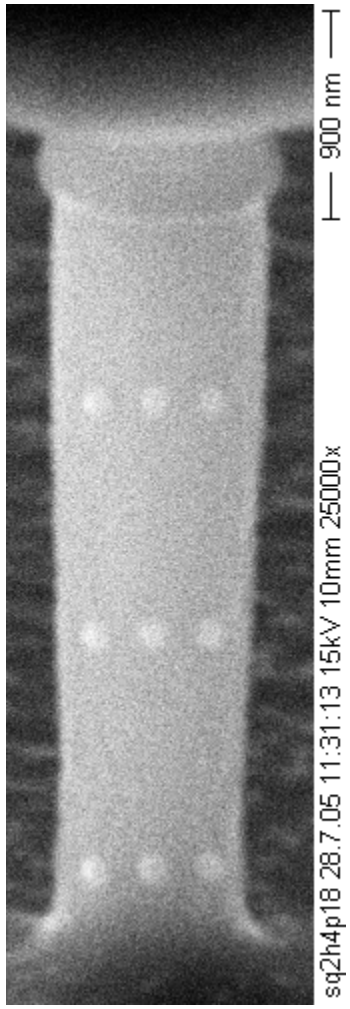

Moser B. et al (2007) J. Mater Res.

Si (001)

the pain with the strain (-measurement)

$$\varepsilon = \frac{x}{L_0}$$

$$\varepsilon = \frac{x - C \cdot P}{L_0}$$

$$\varepsilon = \frac{x - C \cdot P}{L_0} \cdot \left(1 - \frac{1}{1.43 \cdot \frac{h}{d} + 1} \right)$$

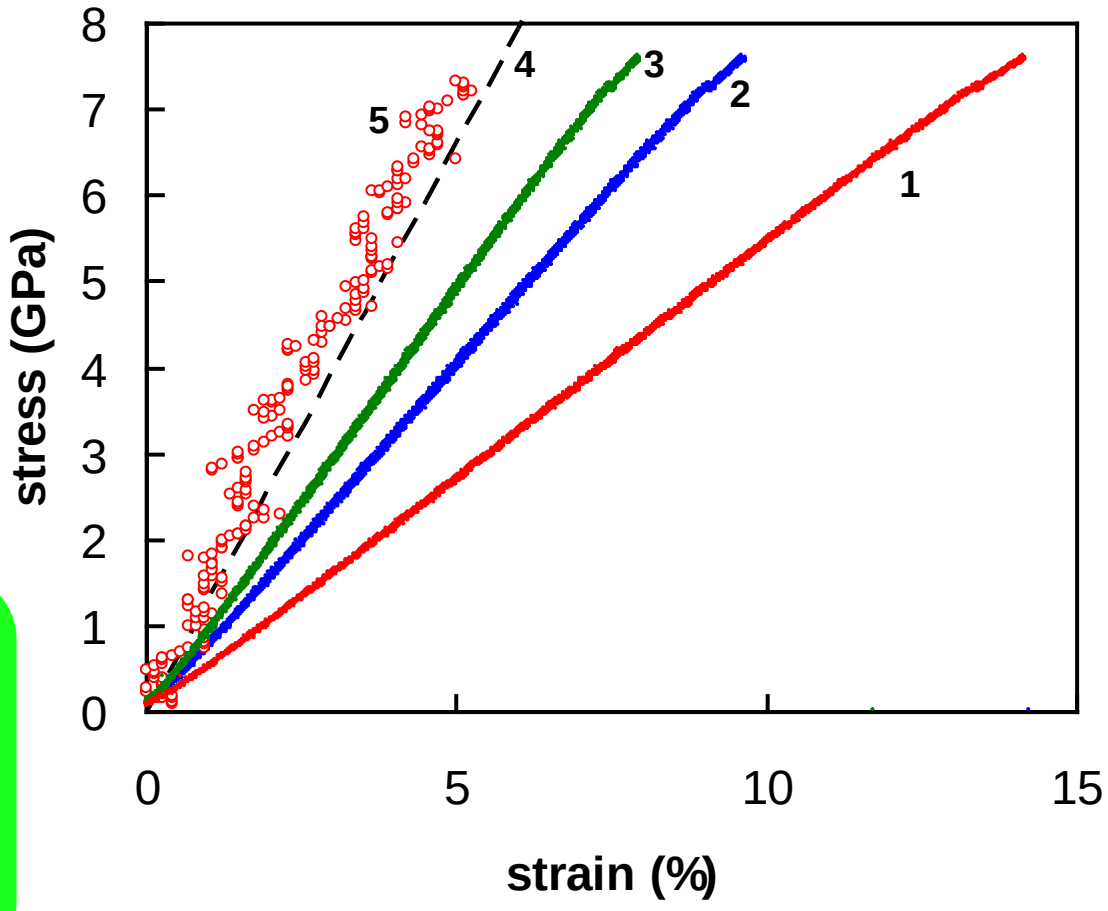

compare also Kiener (2009) Mater. Sc. Eng. A

fracture of silicon micropillars

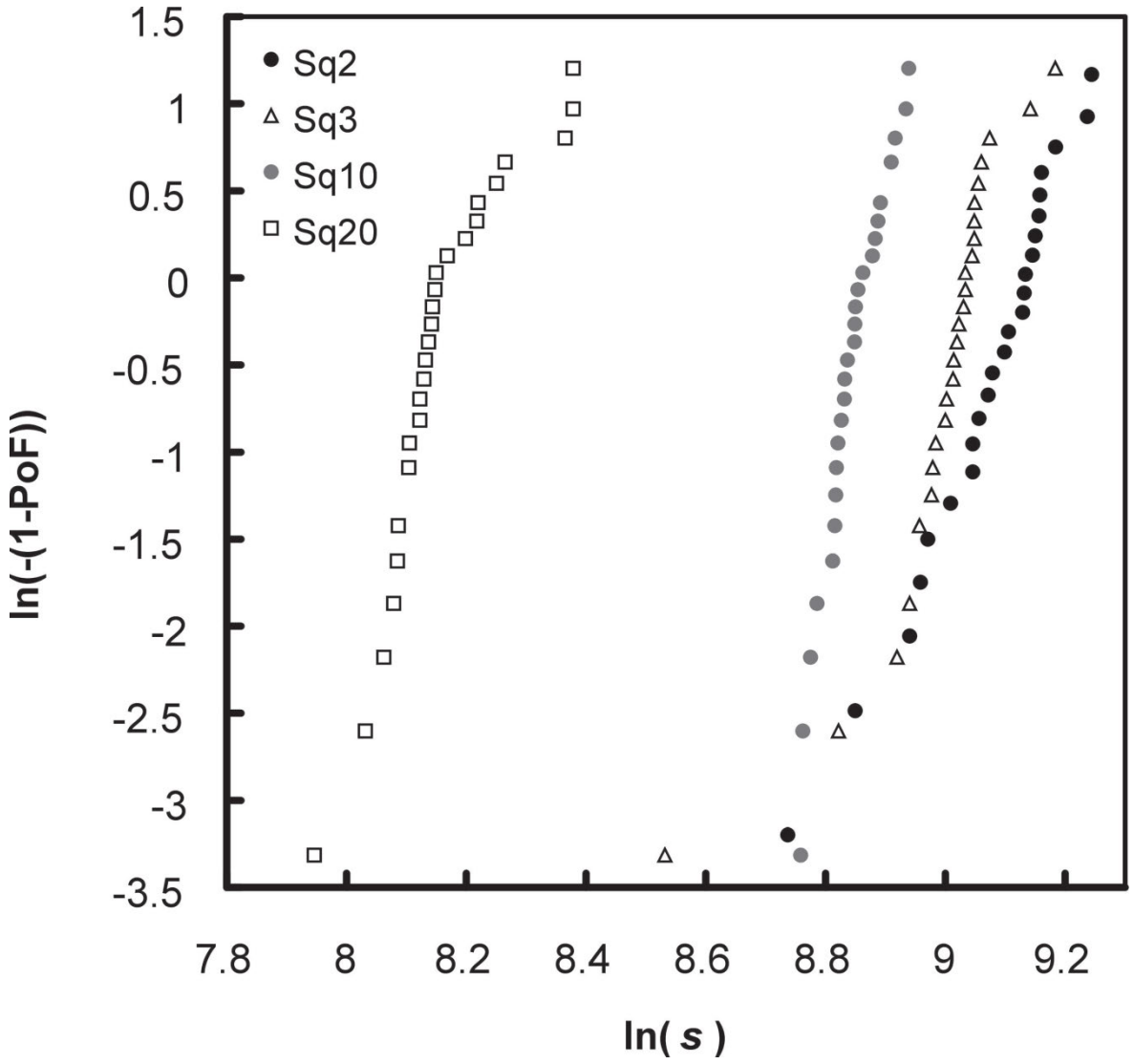

plasticity of silicon in uniaxial compression

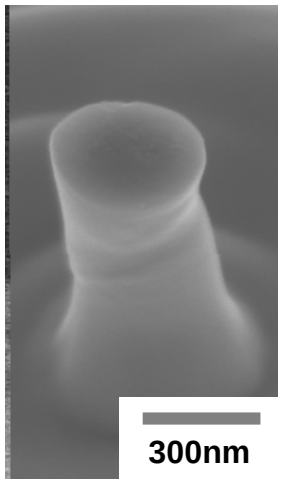

ductile – brittle transition

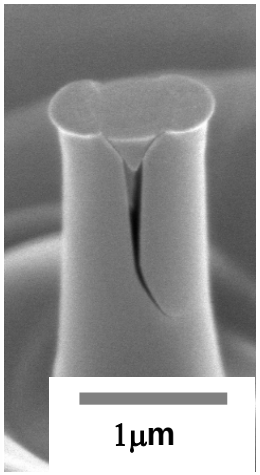

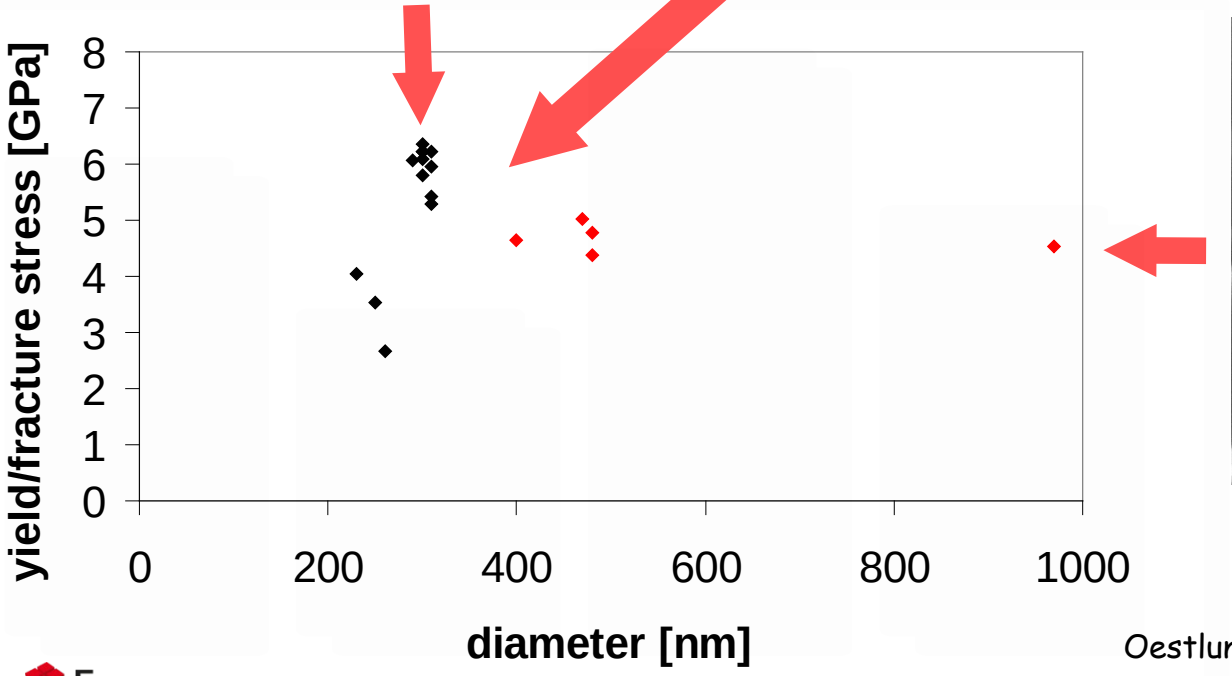

Oestlund (2009) Adv. Functional. Mater.,

plastic deformation of GaAs

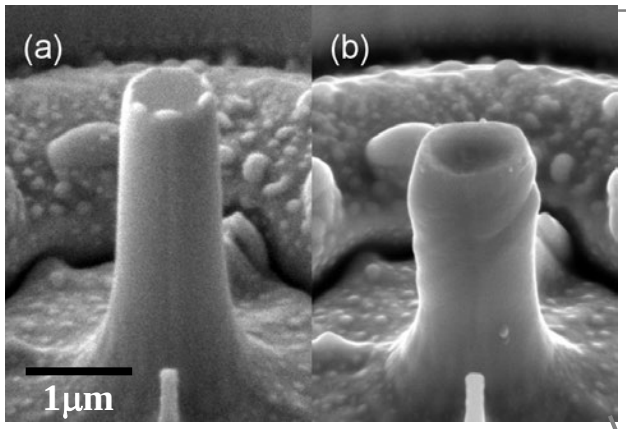

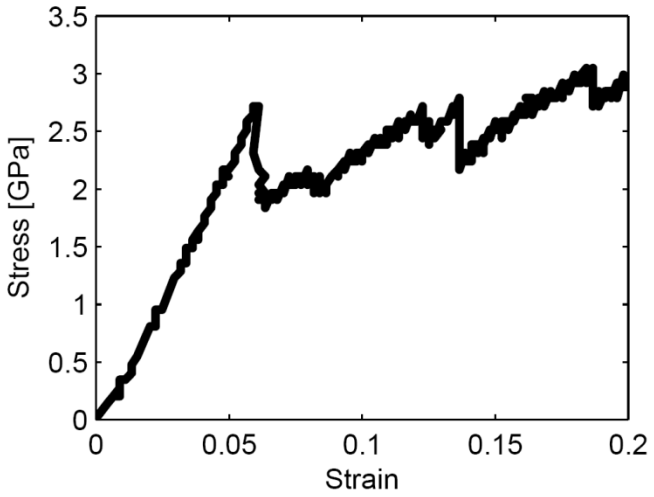

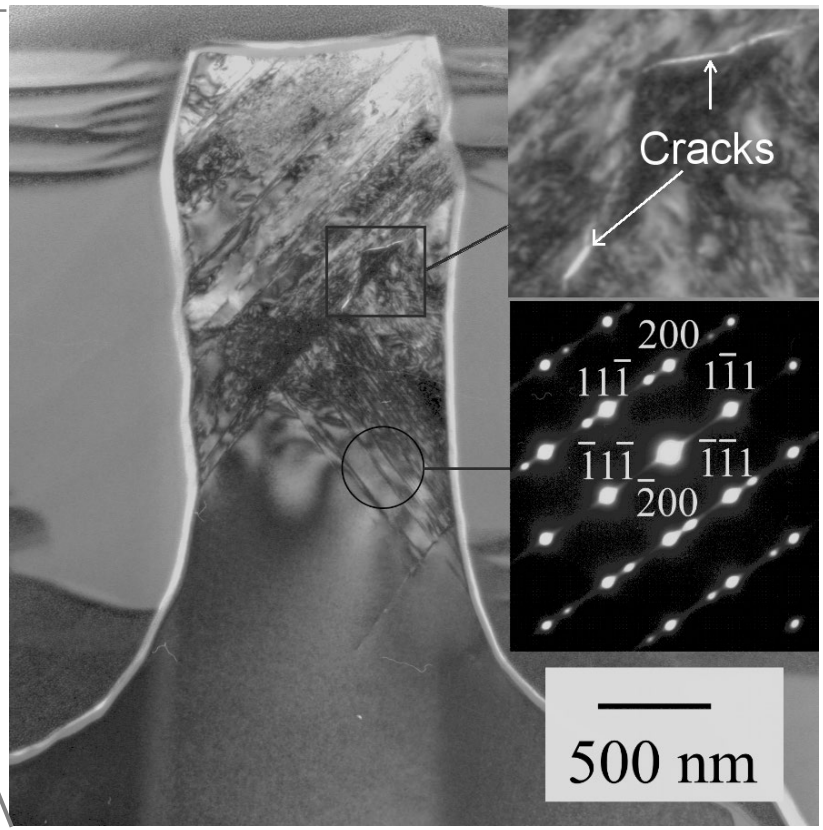

J. Michler (2007). Appl. Phys. Lett. 90, 043123

partial dislocations in GaAs

In Zinc-blende materials dislocations tend to dissociate into two Schockley partials

$$\frac{a}{2}[0\bar{1}1] \rightarrow \frac{a}{6}[\bar{1}\,\bar{1}2] + \frac{a}{6}[1\bar{2}1]$$

These are separated by a stacking fault

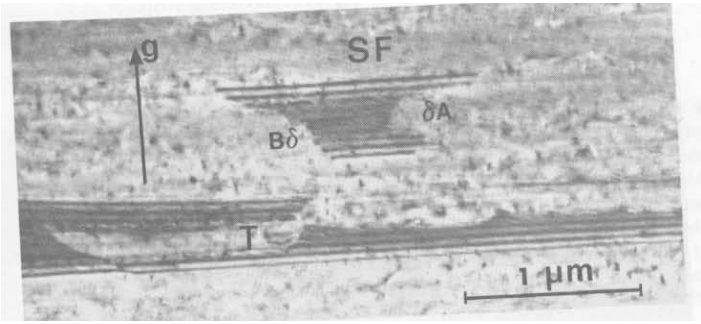

Lefebvre, Androussi, Vanderschaeve. Phil mag 56, 1985

Partials experience the following forces

- The repelling force through their strain fields
- The attracting force from the stacking fault
- Force from external loads
- A quasi-viscous drag force

Since the partials have different Burger's vectors, they generally experience different resolved shear stresses

For example, in uniaxial compression along <100> directions, their Schmid factors are 0.471 and 0.236 respectively

The mobility of the partial dislocation depends on:

- The character (30/90 degree)
- The core structure
- If it is leading or trailing

slip of partial dislocations in GaAs

Wessel and Alexander (1977) balanced the forces on the partials ending up with a formula for the dissociation distance:

$$d = \frac{d_0}{1 + \frac{b\tau}{2\gamma}\left[f - \frac{1-\alpha}{1+\alpha} \right]}$$

d_0 dissociation distance in the absense of external stress
b Burgers vector
τ Resolved shear stress on the full dislocation
γ Stacking fault energy
f A geometrical factor
α The ratio of the mobility of the trailing and leading partial

If the denominator tends to zero a very large splitting of the partials can be expected

For GaAs
b=4.0 Å
γ=46 mJ/m^2
α=1 (assumption)
f=-0.3

τ= 0.7GPa
σ_{001}=1.7 GPa

which needs to be compared to **σ_{yield}~2.9GPa**

theoretical shear strength of GaAs

theoretical shear strength of a material

$$\tau = \frac{b}{a_0}\frac{G}{2\pi}$$

(Hull & Bacon, "Introduction to dislocations")

taking the Schmid factor into account this gives roughly

σ_{001}=9.1 GPa for full dislocation
σ_{001}=4.5 GPa for partial dislocation

which needs to be compared to **σ_{yield}~2.9 GPa**

slip of partial dislocations

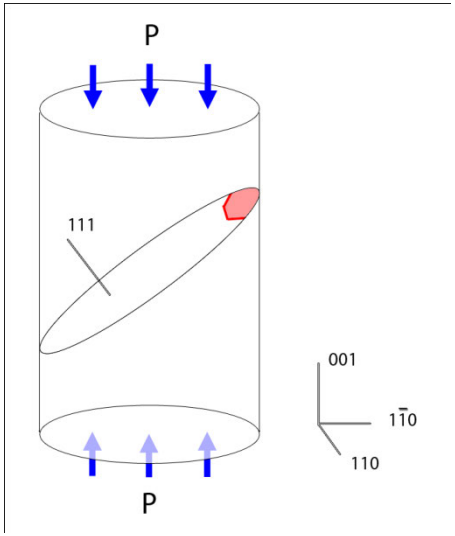

dislocation nucleation

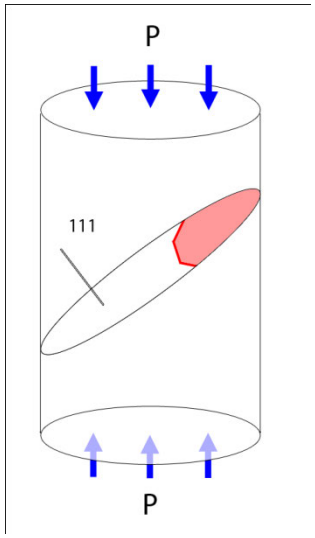

dislocation propagation & creating of SF

stress is high enough to nucleate a partial dislocation and pillar diameter smaller as eqilibrium distance of partial dislocations

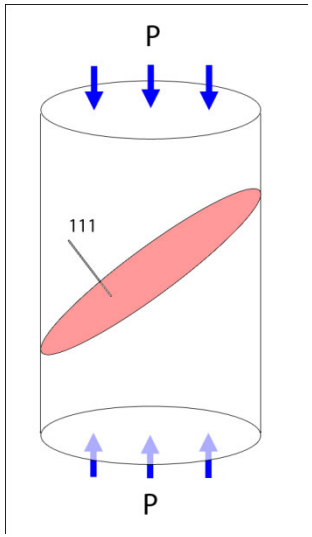

dislocation reaches the surface

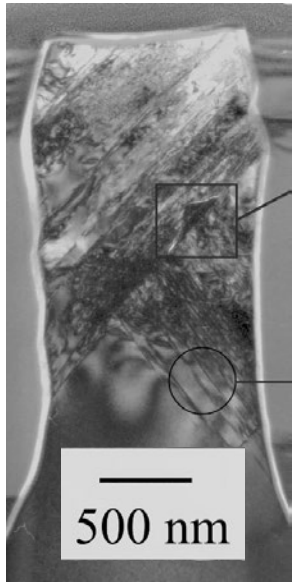

J. Michler, K. Wasmer, S. Meier, F. Oestlund, K..Leifer (2007). Appl. Phys. Lett. 90, 043123

S. Wang, P. Pirouz (2008) Acta Mat. 55, 5500

Plasticity of GaAs in uniaxial compression

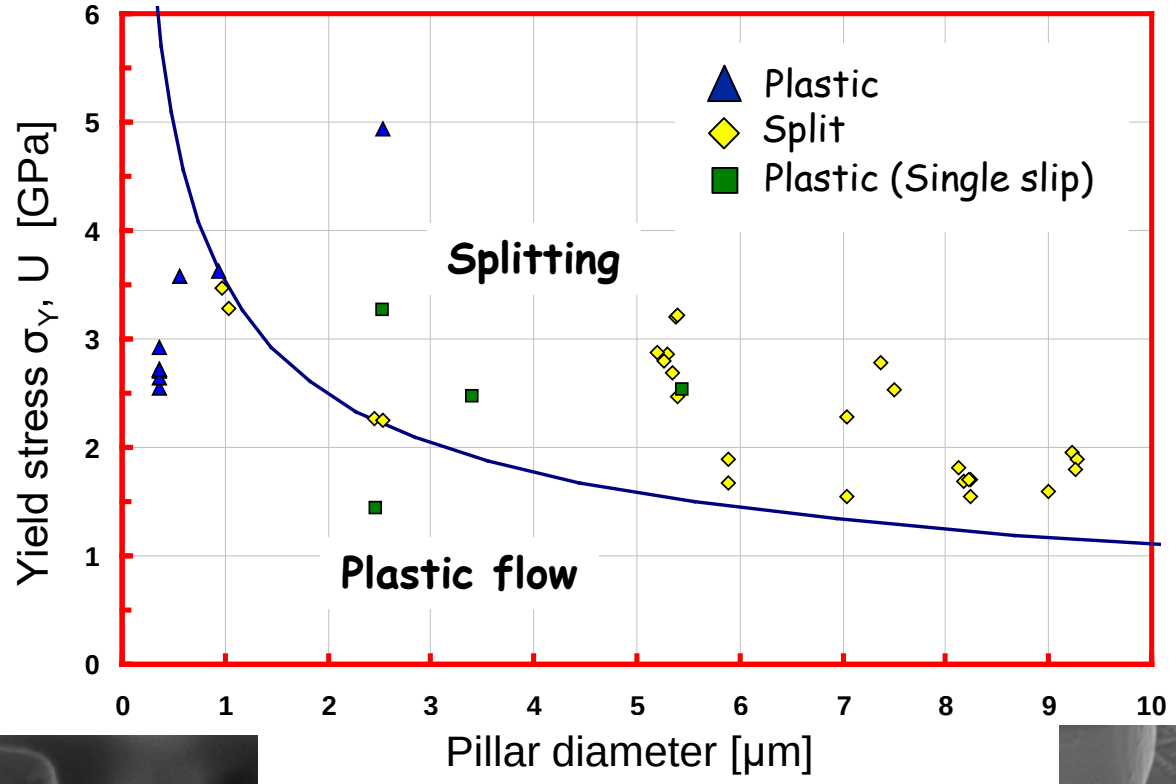

pillar orientation <001>
aspect ratio 1:3

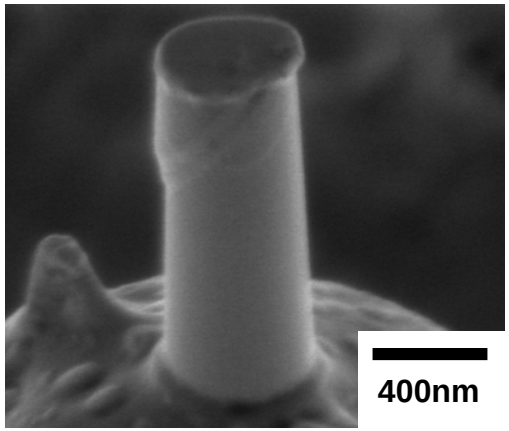

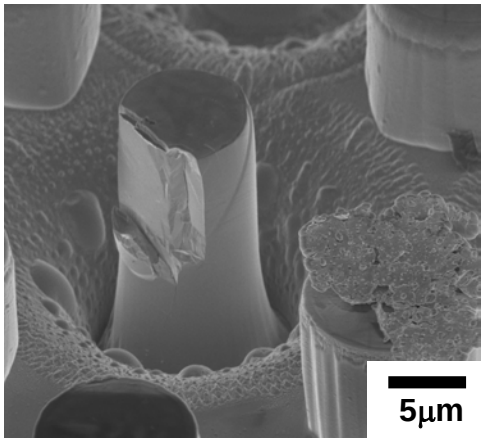

compression splitting

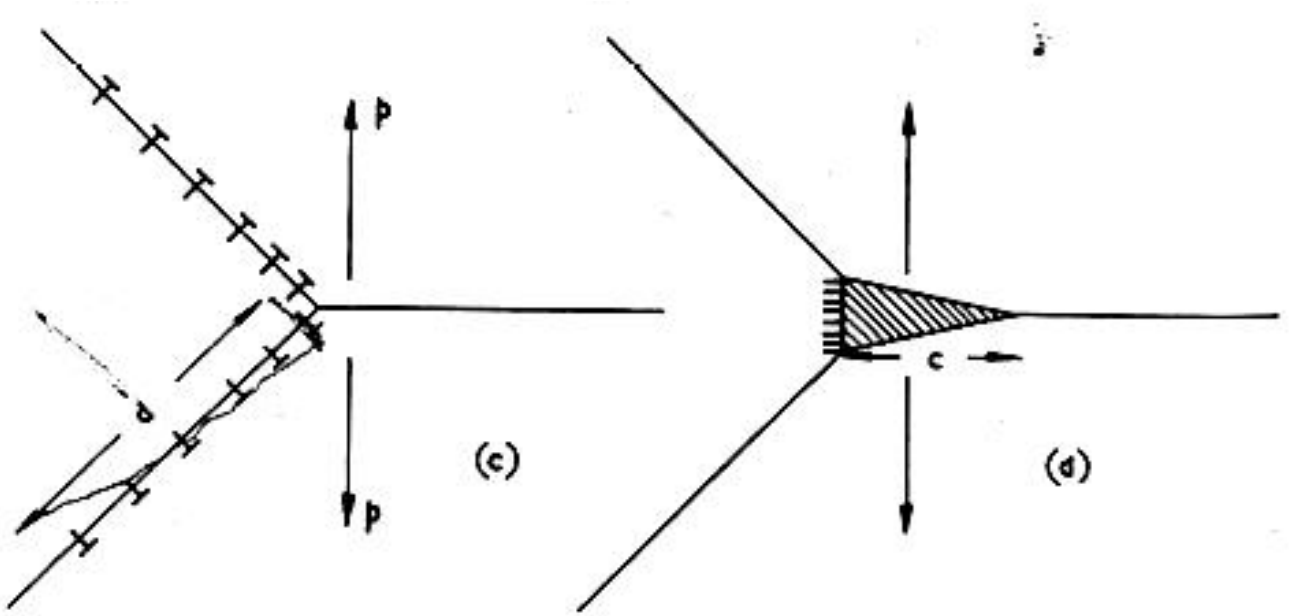

Cottrell, A.H., “Theory of brittle fracture in steel and similar metals”, *Trans. Metall. AIME* , **212** (1958), 192–203

compression splitting

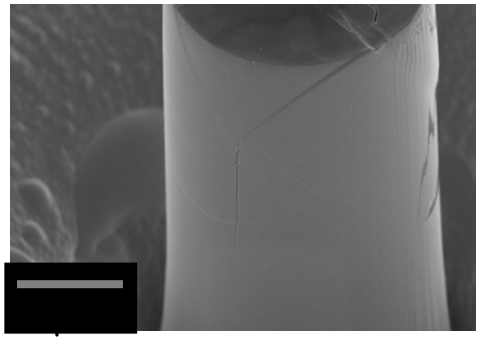

idea: cracking in larger pillars by the growth of a compression split nucleated at the intersection between the two glide bands in a pillar

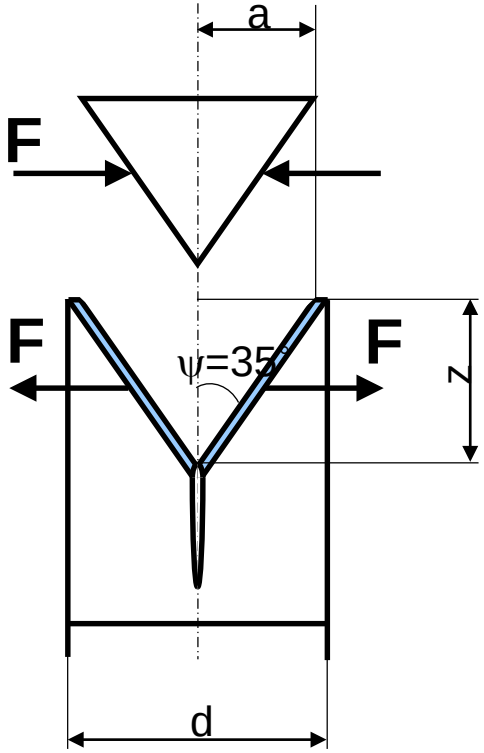

$$K_I = \beta \frac{F}{[\pi (l+z)]^{1/2}}$$

compression splitting

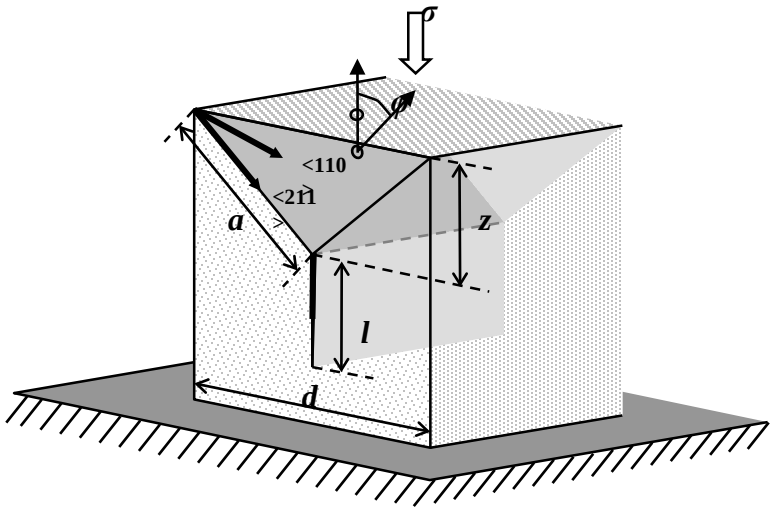

applied stress needed for splitting

$$\sigma_S = \frac{K_{Ic}}{0.158\,\beta\sqrt{d}}$$

critical diameter brittle – ductile transition with flow stress

$$d_{crit} = 40\left[\frac{K_{Ic}}{\beta\,\sigma_Y}\right]^2$$

~1μm

Oestlund et al (2010) Phil. Mag.

temperature effect - silicon <001>

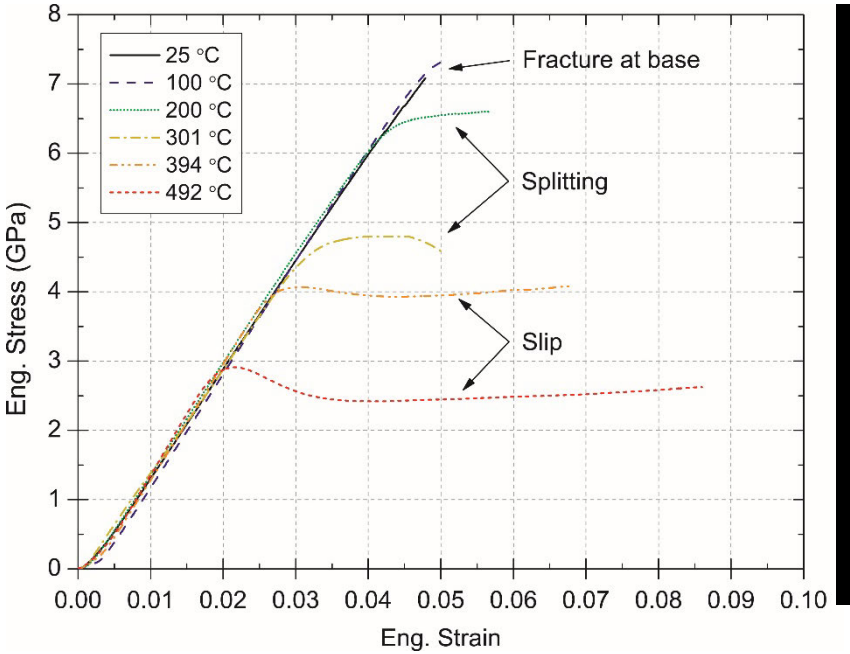

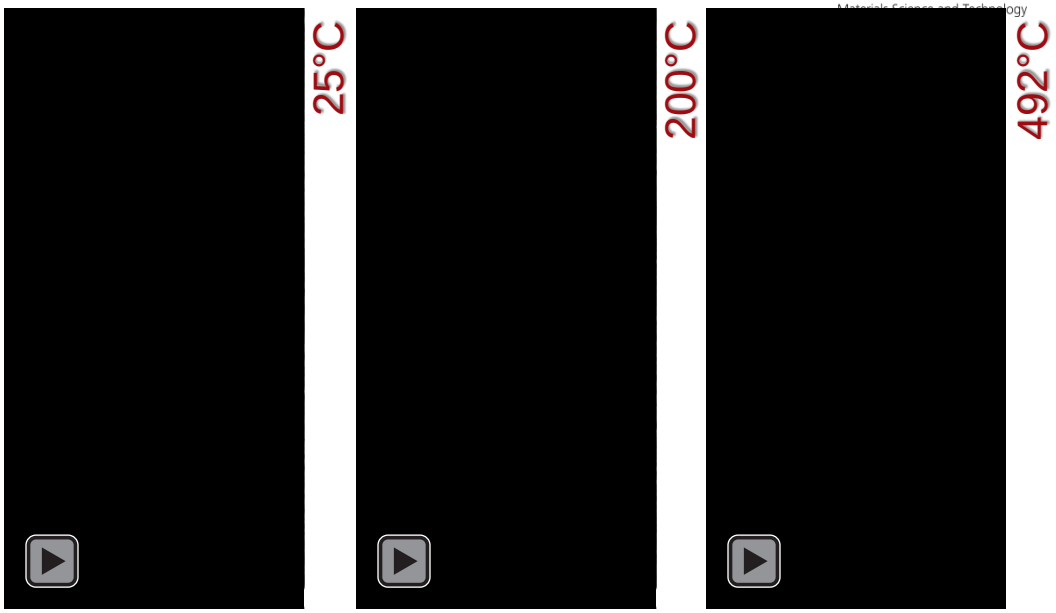

- Transitions between in deformation mechanisms between fracture, splitting, and plasticity directly observed.
- At a diameter of 6.7 µm, the brittle-ductile transition is seen at ~400°C – significantly lower than bulk silicon.
- Classic upper yield point consistent with dislocation nucleation observed during plastic deformation due to system's intrinsic displacement control.

*J.M. Wheeler & J. Michler, *Rev Sci Instrum* (2013)

size and temperature effect - silicon ‹001›

Empa
Materials Science and Technology

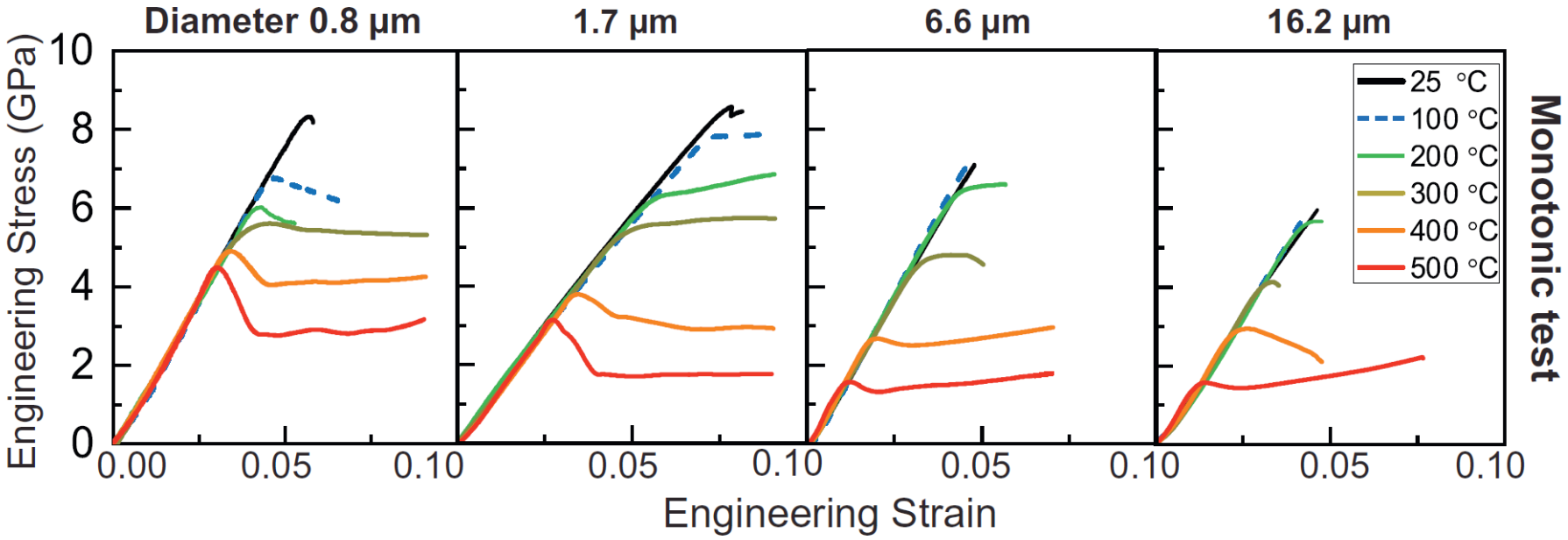

strain rate of $1 \times 10^{-3}\ s^{-1}$.

M. Chen et al. (2020) Materials and Design 189, 108506

strain rate effect - silicon <001> at 495°C

Empa
Materials Science and Technology

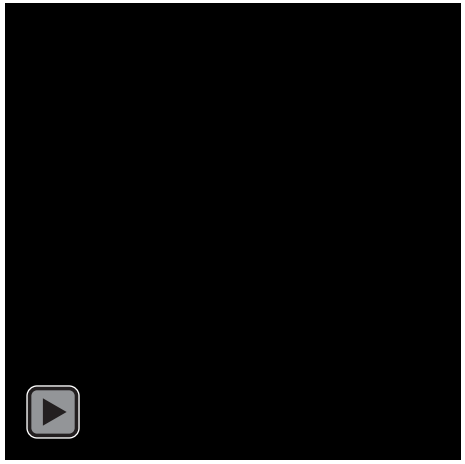

0.001/s

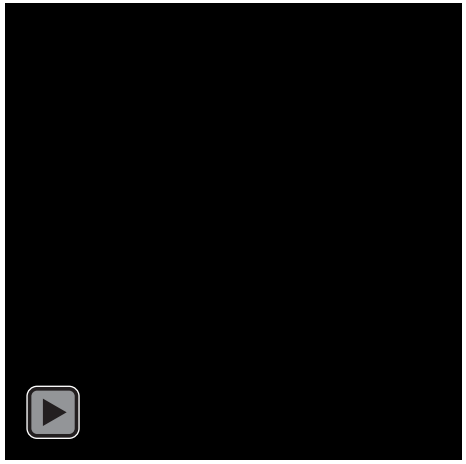

0.01/s

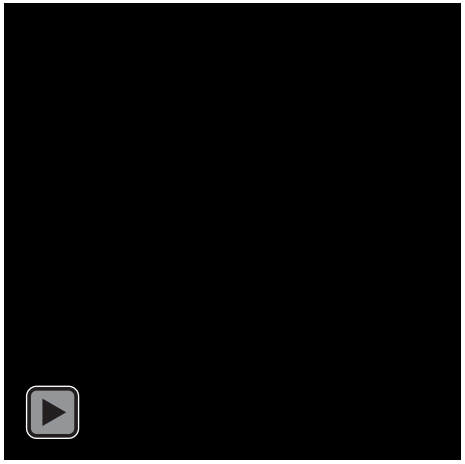

0.1/s

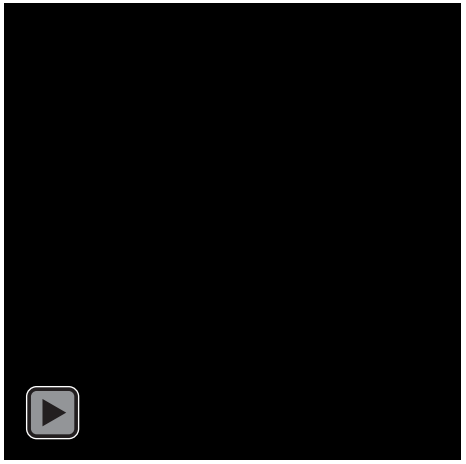

1/s

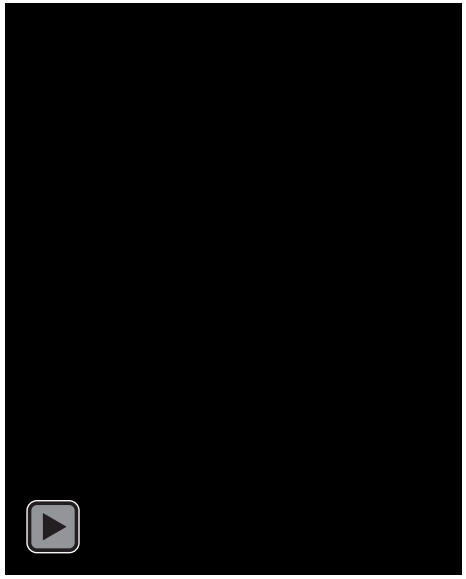

10/s

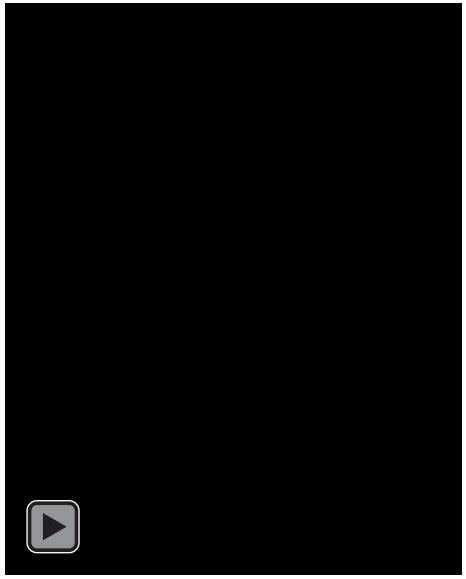

100/s

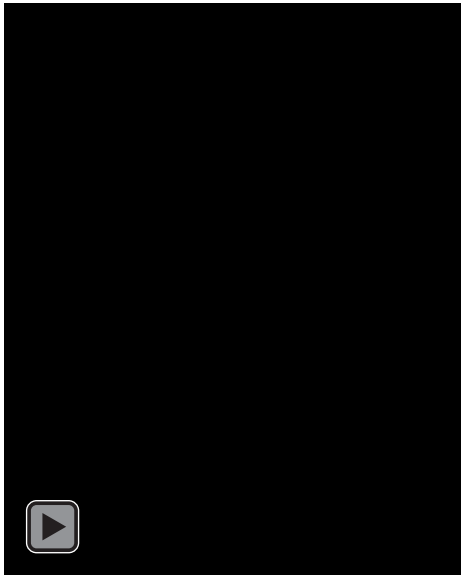

200/s

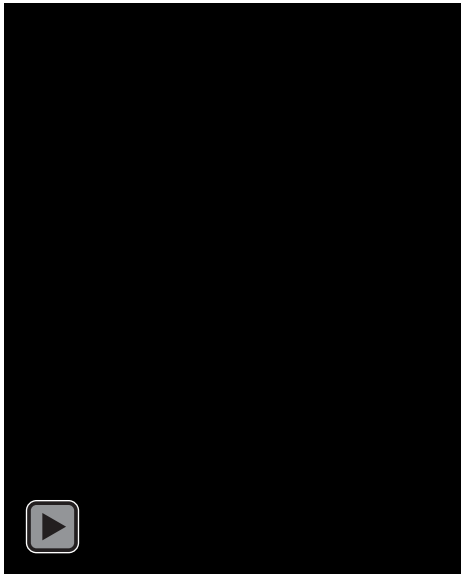

400/s

strain rate vs temperature - silicon <001>

Constant strain rate – 1e-3/s

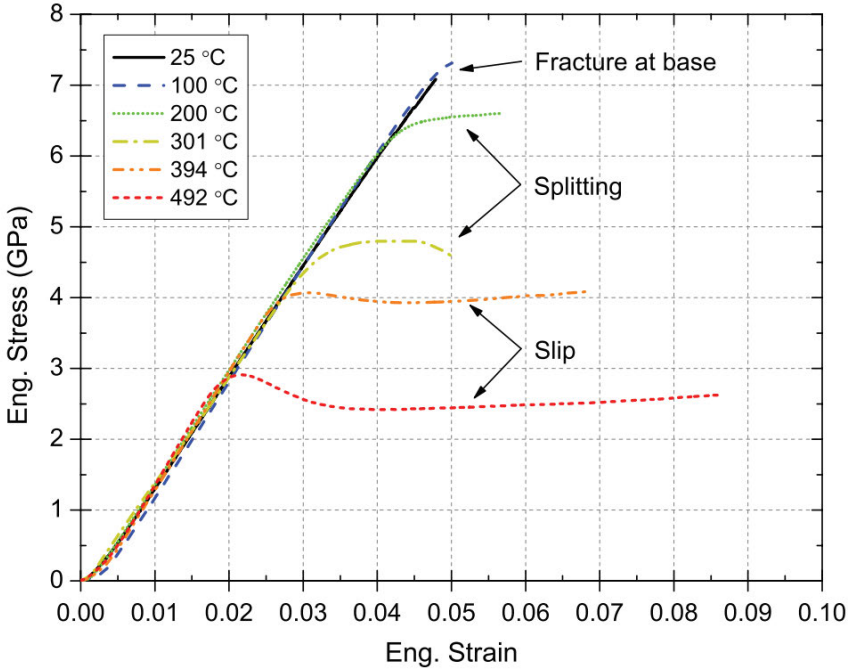

Wheeler et al., Rev. Sci. Ins. 2013.

Constant Temperature – 495°C

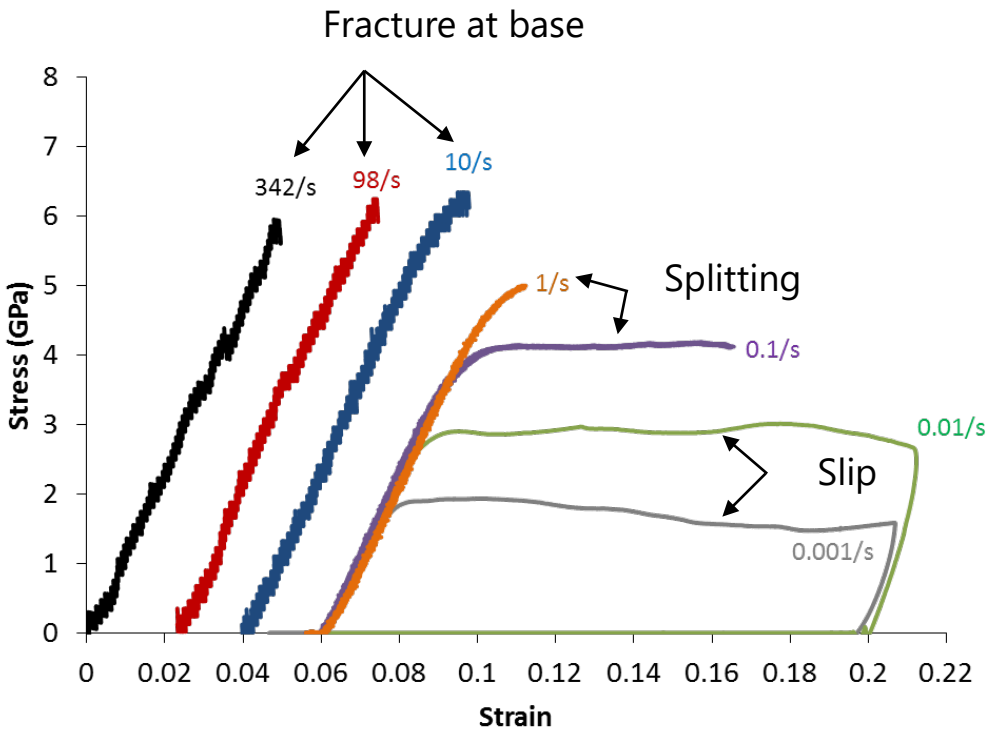

- 6.82um diameter

silicon two types of dislocations

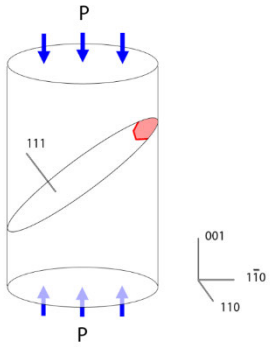

dislocation nucleation

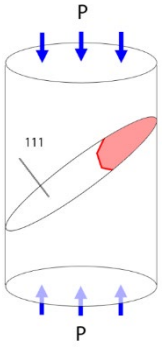

dislocation propagation & creating of SF if partial dislocation

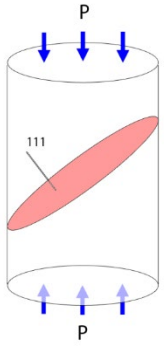

dislocation reaches the surface or interacts with other dislocations and multiplies

Perfect dislocations

Dissociated dislocations

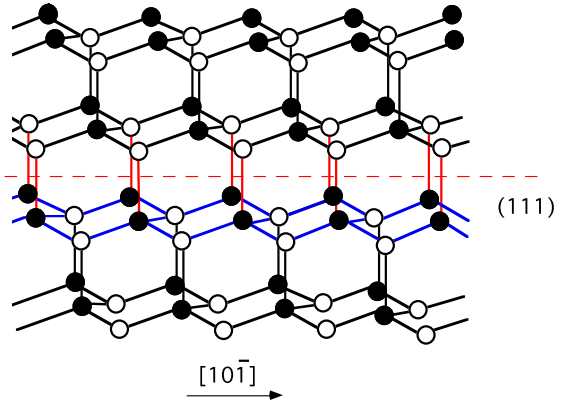

activation parameters of silicon

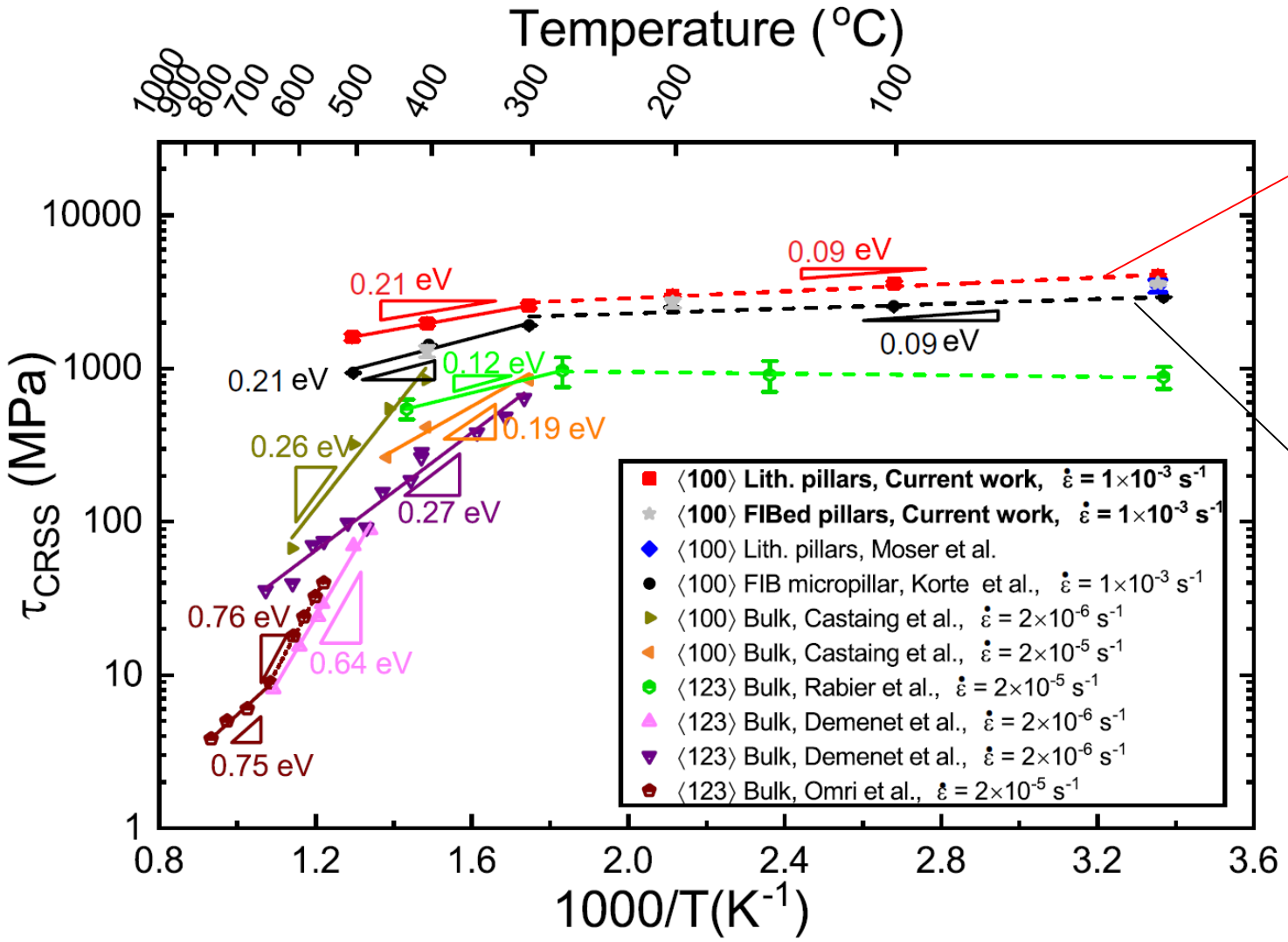

M. Chen et al. (2020) Materials and Design 189, 108506

change in deformation mechanism at 300°C

Empa
Materials Science and Technology

partial dislocations T>300°C

full dislocations T<300°C

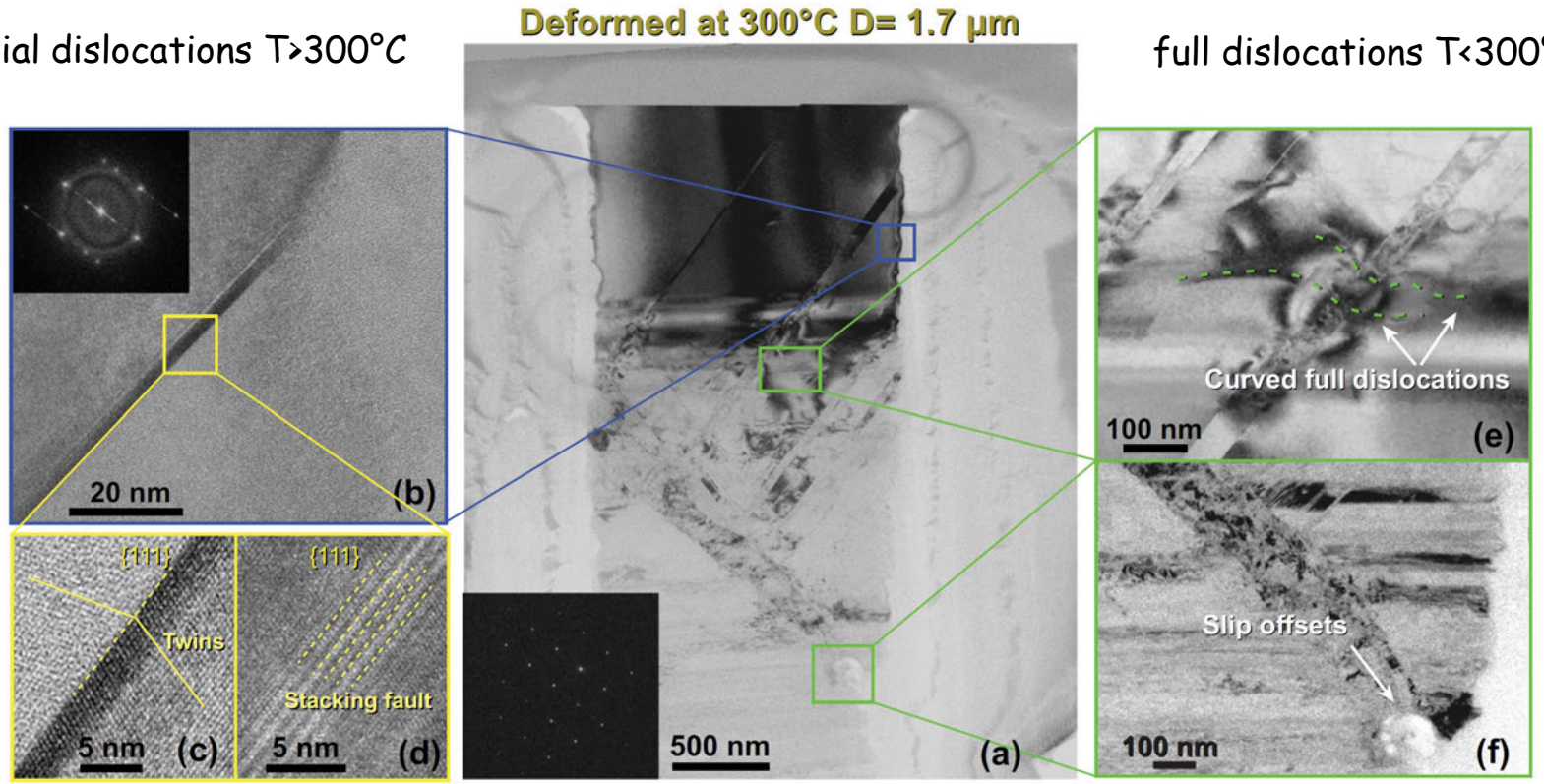

silicon <001>

M. Chen et al. (2020) Materials and Design 189, 108506

surface defects - theoretical strength & ductility?

Empa
Materials Science and Technology

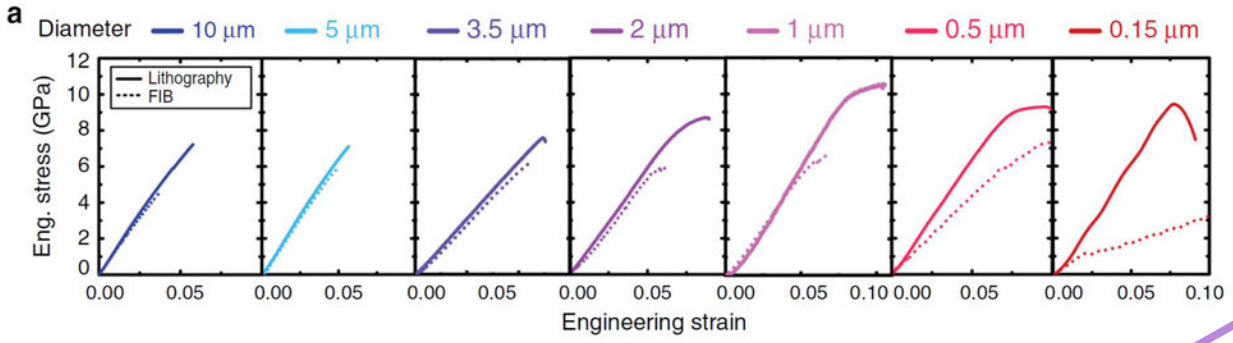

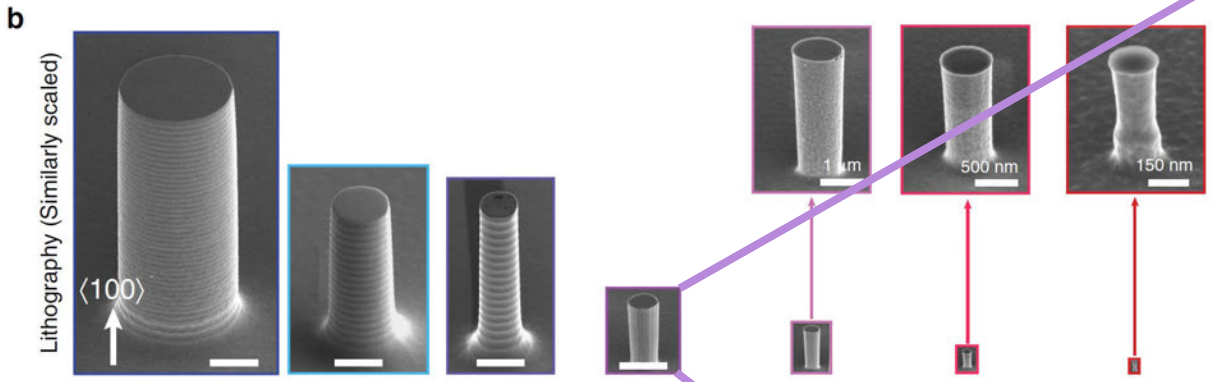

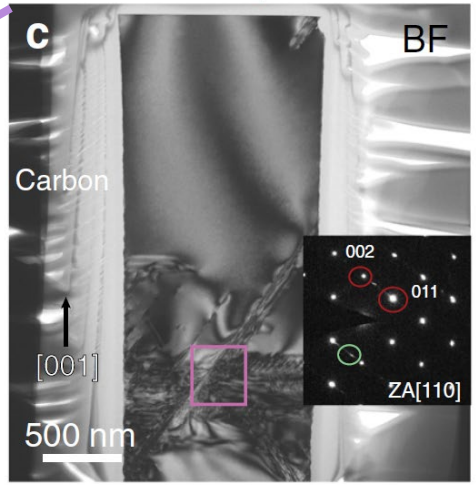

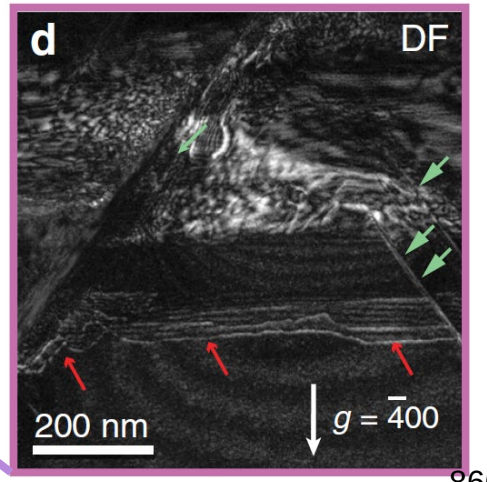

silicon <001>

M. Chen (2021) Nature Communications 11, 2681

Size effect in fracture behaviour

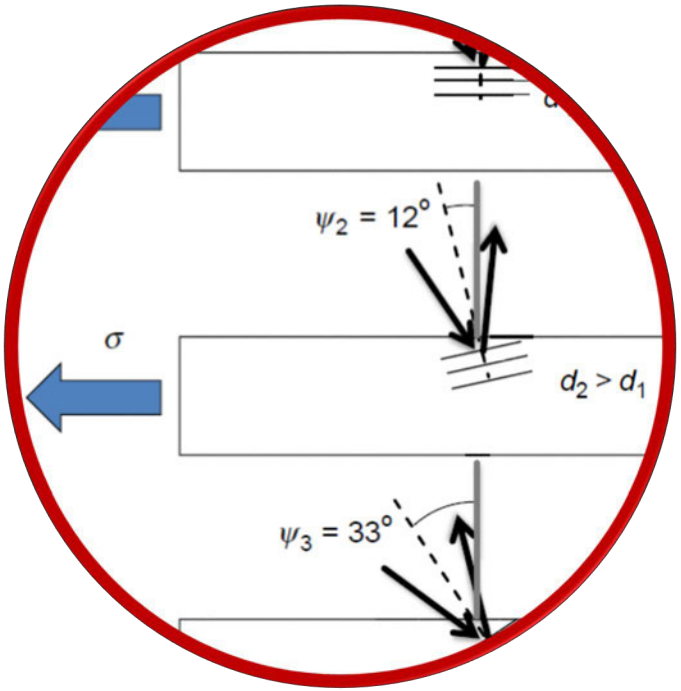

The brittle-ductile transition (BDT)

Empa
Materials Science and Technology

BCC W single crystals:

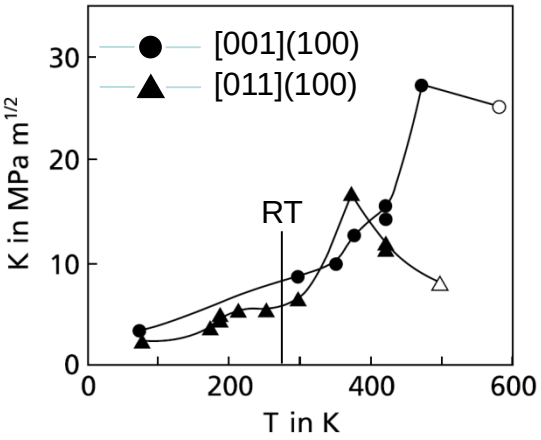

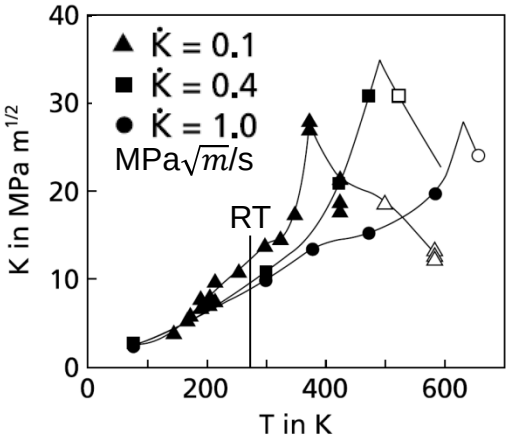

- Continuous increase of K_{Ic} with T
- BDT well above room temperature
- Fracture anisotropy: fracture plane and direction
- Loading rate dependency

Riedle et al., Phys. Rev. Lett., 1996
Gumbsch et al., Science, 1998

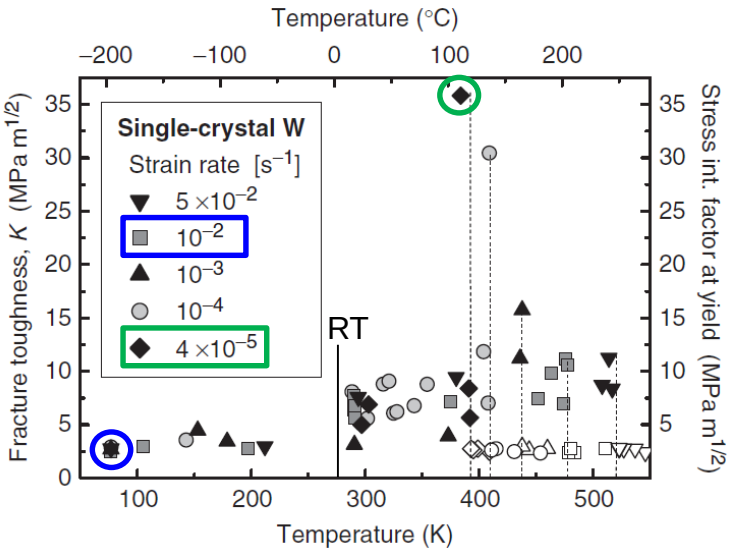

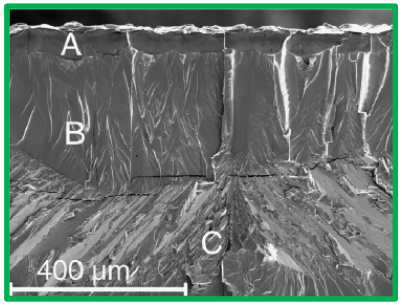

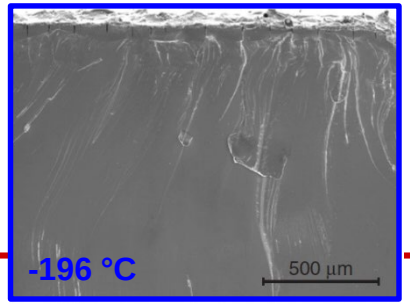

- Continuous increase of K_{Ic} with T
- BDT well above room temperature
- Loading rate dependency
- Low loading rate (moderate T): crack growth and final cleavage
- High loading rate (low T): brittle cleavage

Giannattasio and Roberts, Phil. Mag., 2007

[001](100) crack system

Size-dependent fracture behaviour

macro-scale

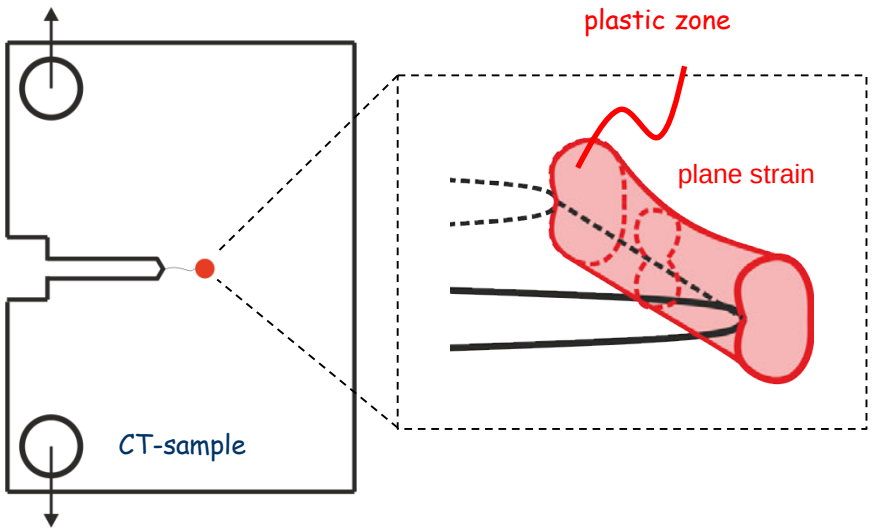

Estimation of the size of the plastic zone r_{pl} :

$$r_{pl,plane-strain} = \frac{1}{3\pi}\left(\frac{K_{Ic}}{\sigma_y}\right)^2$$

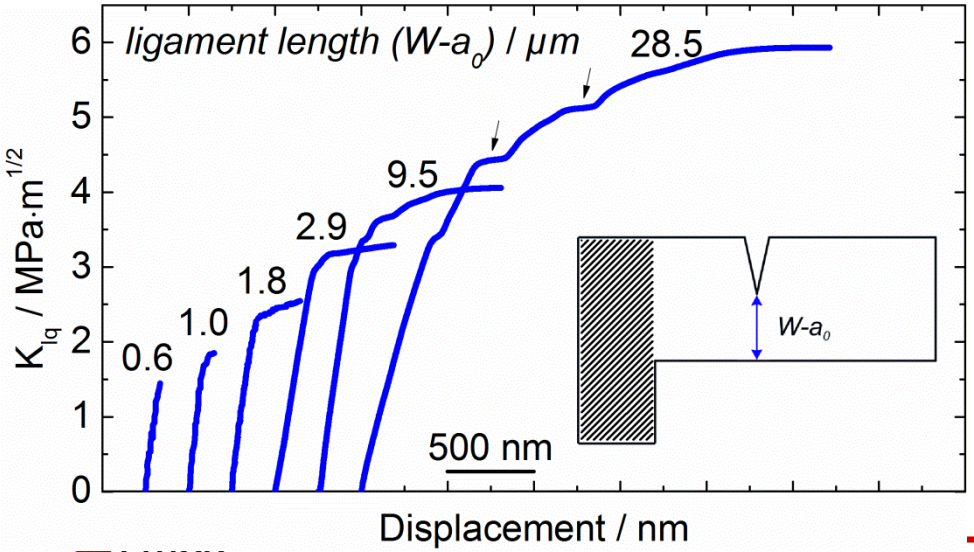

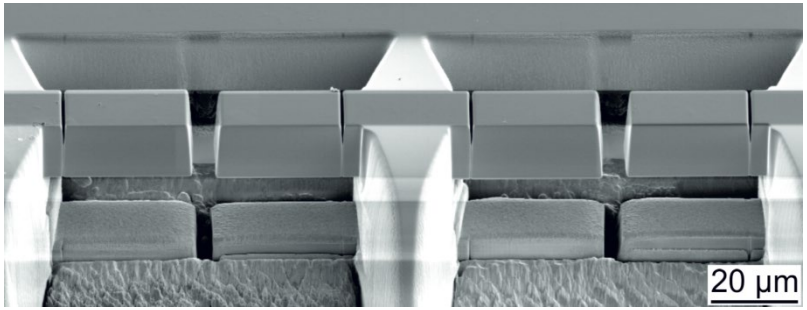

cantilevers in W , <100>{100} crack system

Ast et al., Acta Mater. 138, 2017

Fracture testing from -90°C to 250°C

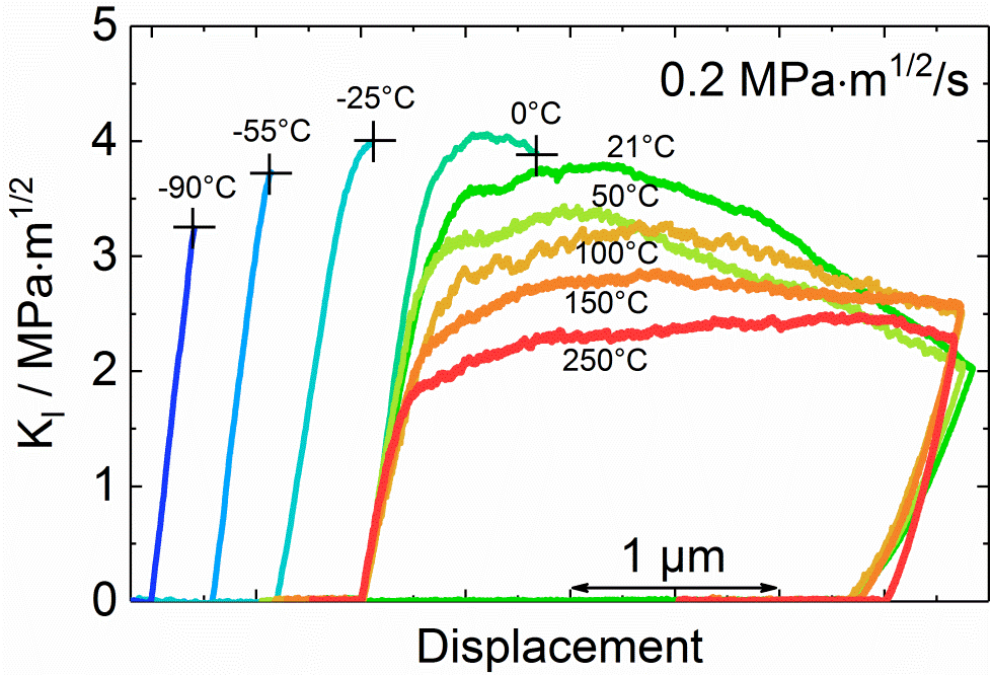

$$K_I = \frac{F\,L}{B\,W^{3/2}} f(a/W)$$

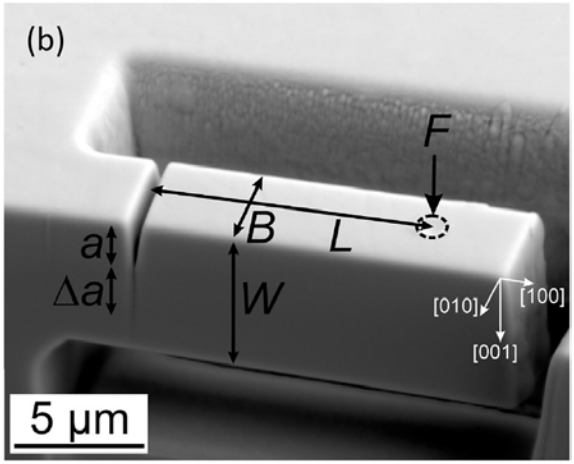

- -90°C: purely brittle, cleavage fracture along {100} planes
- -55°C / -25°C: limited crack tip plasticity prior to cleavage
- 0°C: crack tip plasticity and finite stable crack growth prior to cleavage
- 21°C: crack tip plasticity and stable crack growth
- 150°C: stress intensity factor decreases, stable crack growth
- >250°C: enhanced crack tip plasticity, finite crack growth in final stage

Brittle-ductile transition (BDT)

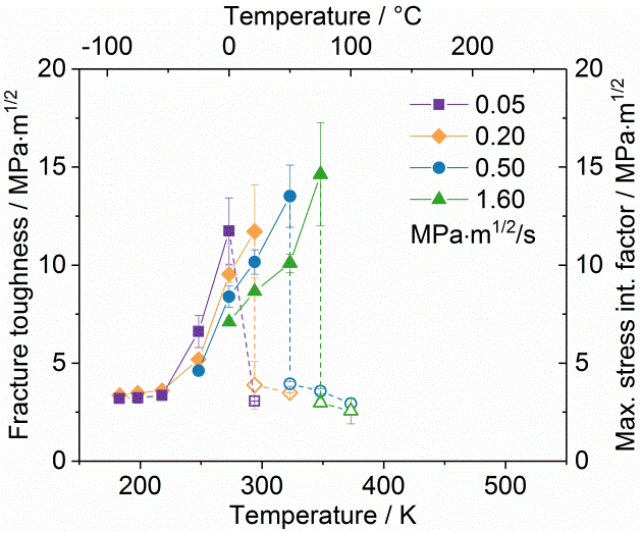

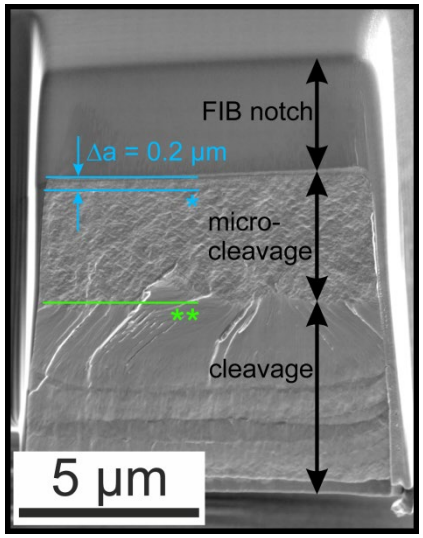

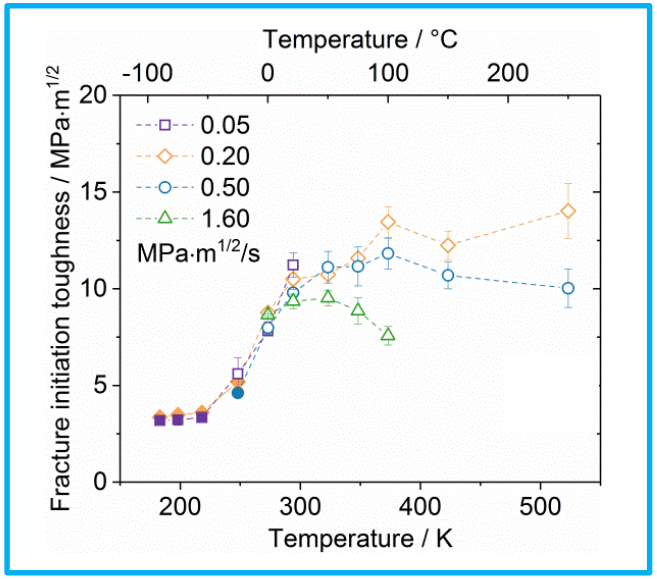

Cleavage Fracture toughness

- J-Integral determined at onset of cleavage
- Below -50 °C: no loading rate dependency
- Lower loading rate → sharper transition
- BDT is shifted to higher temperatures with higher loading rates

Fracture initiation toughness

- J-Integral determined at Δa = 0.2 μm
- Below room temperature → no loading rate dependency
- Above room temperature → loading rate dependency

Comparison: micro- vs. macro-scale

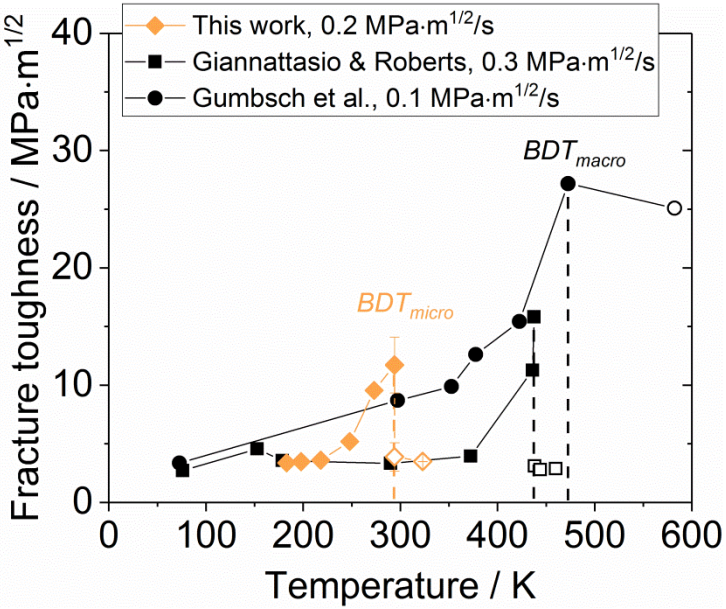

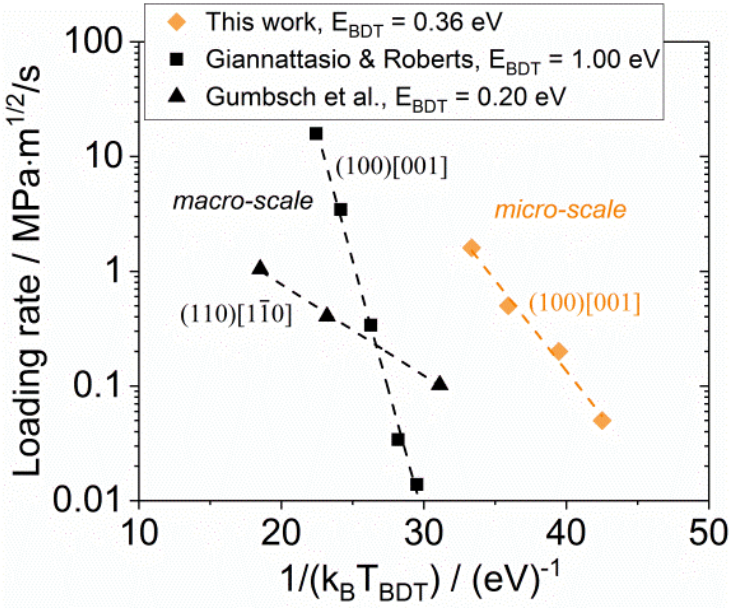

- Arrhenius plot: $\dot{K} \propto \exp\left(-\frac{E_{BDT}}{k_B T_{BDT}}\right)$
- Different crack systems
- Difference between macro- and micro-scale: 1.00 eV vs. 0.36 eV
- Kink-pair formation in the screw dislocation is ***stress-assisted***

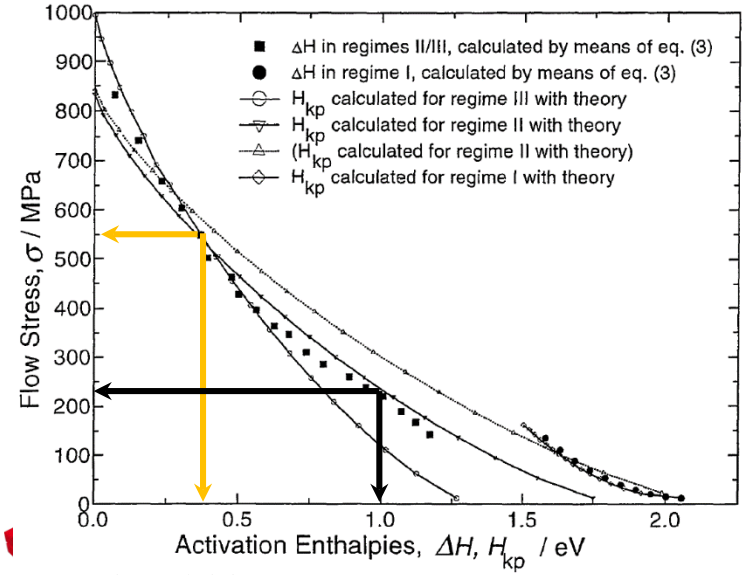

Brünner, Mater. Trans. JIM, 2000

Giannattasio and Roberts, Phil. Mag., 2007

Gumbsch et al., Science, 1998

HR-EBSD analysis

Empa
Materials Science and Technology

Cross-Correlation (CrossCourt4): GND density

SEM images: Cross-sections

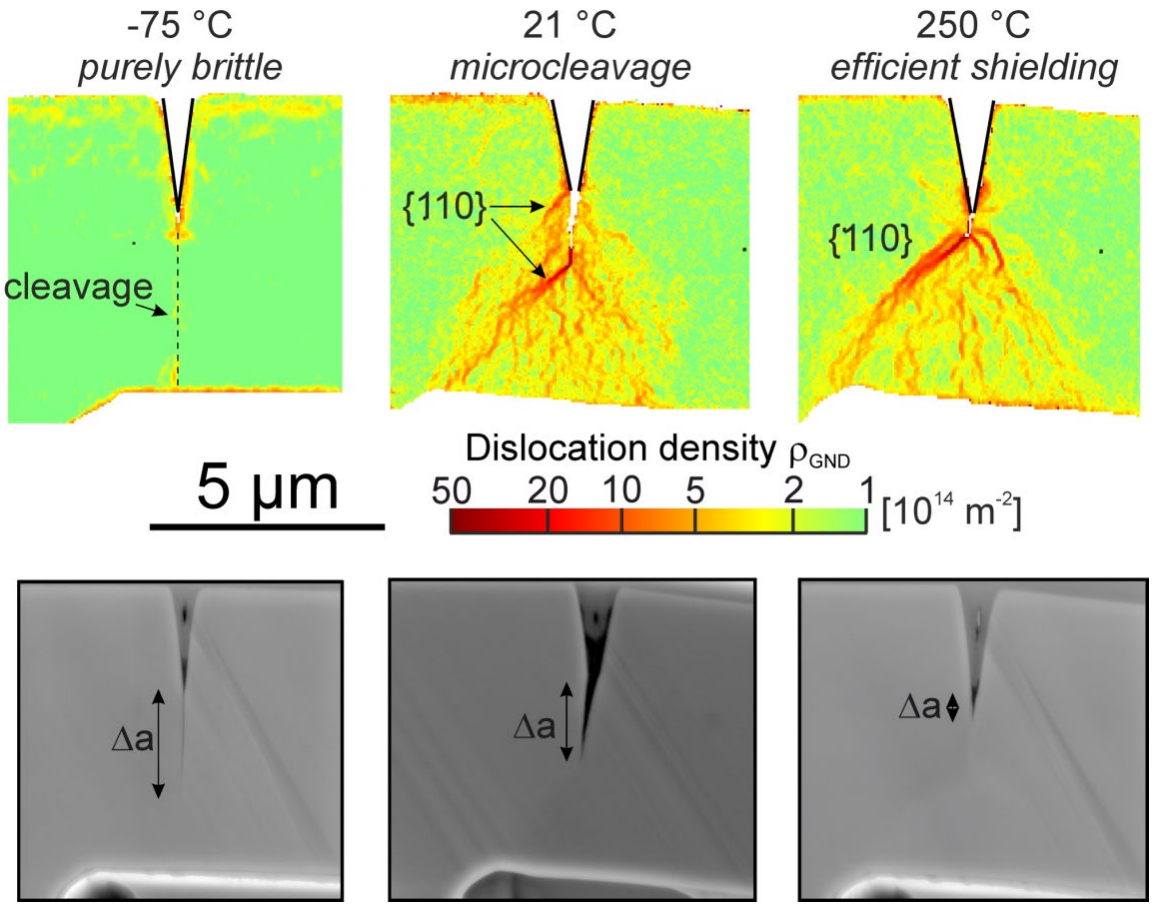

- Total density of geometrically necessary dislocations (GND)
- Brittle cleavage at low, dislocation-controlled microcleavage at intermediate and crack tip shielding at high temperatures

HR-EBSD analysis at BDT

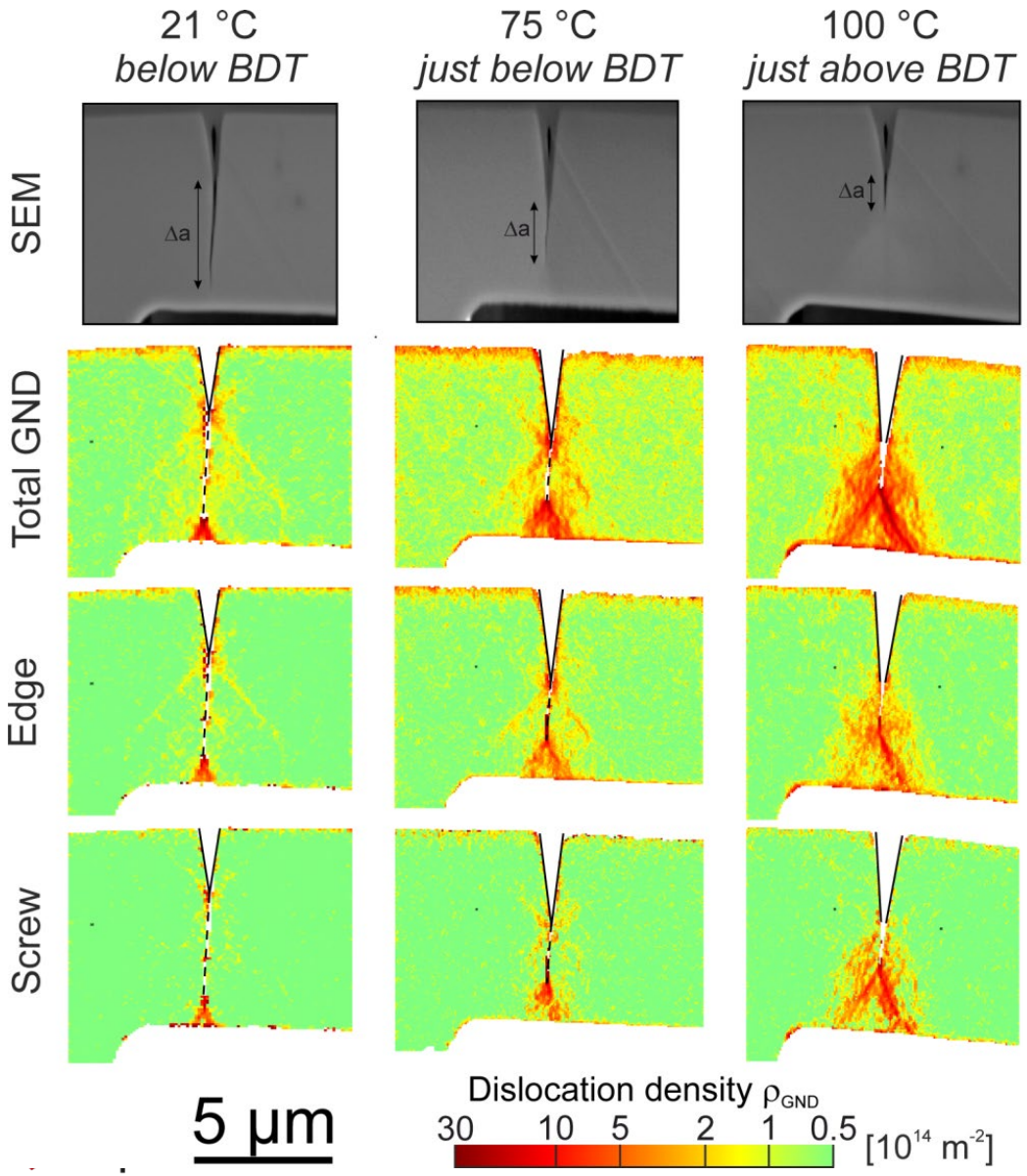

- → Reduction of crack growth with temperature
- → Increase of total GND density with temperature
- → Edge dislocations: increase in K_{Ic} mainly below BDT
- → Screw dislocation mobility: responsible for BDT transition

Summary of micro-scale fracture behaviour

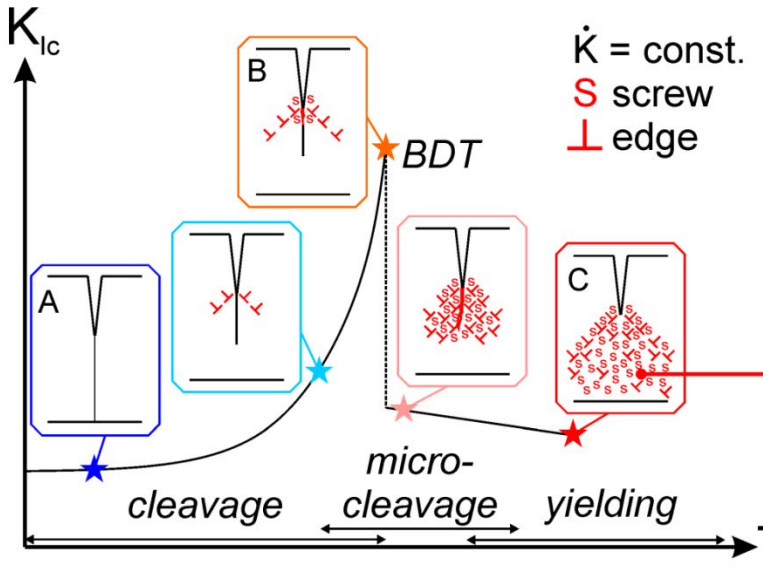

Bright-field STEM

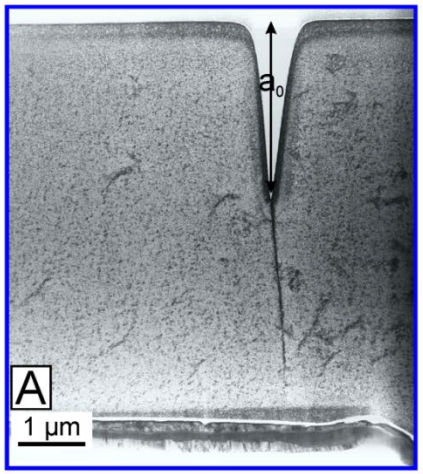

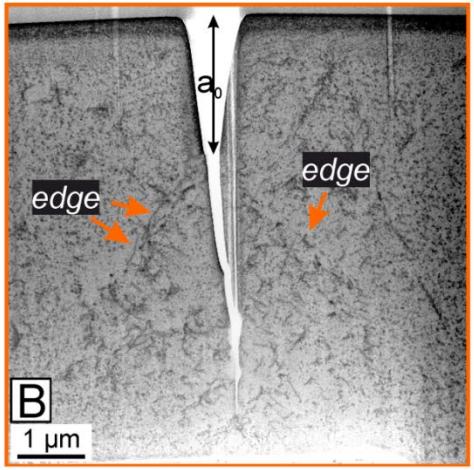

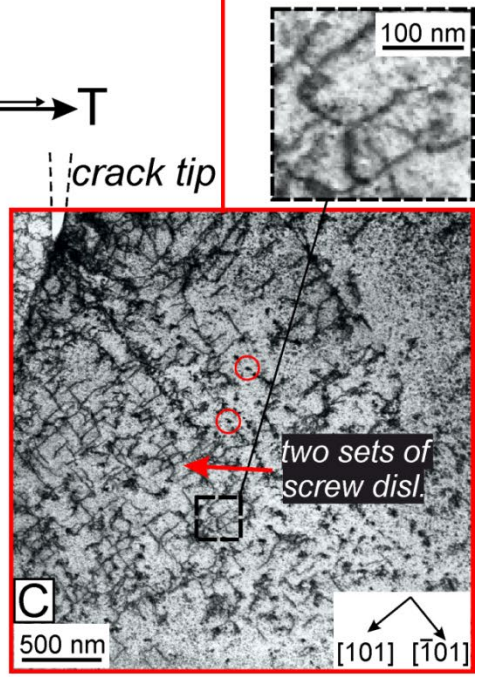

Conclusions

- Fracture behaviour of W single crystals depends on:
  - specimen size
  - temperature and
  - loading rate

- Comparison to macroscopic samples:
  - brittle-ductile transition at lower temperatures
  - lower activation energy → stress-assisted kink-pair formation (screw dislocations)

- HR-EBSD and STEM:
  - Transition: brittle → semi-brittle → plastic

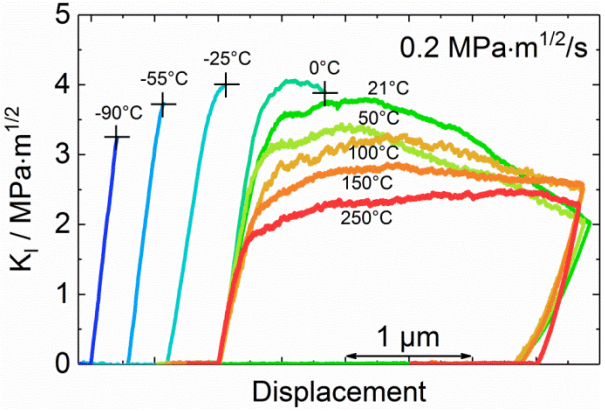

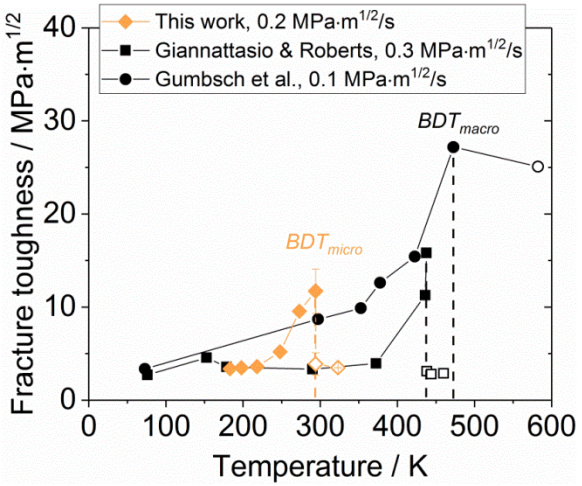

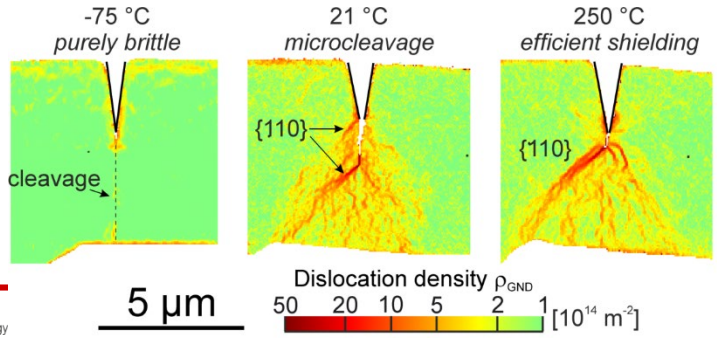

R-curve behaviour: J-Integral technique

[Ast et al., *J. Mater. Res.*, 2016]

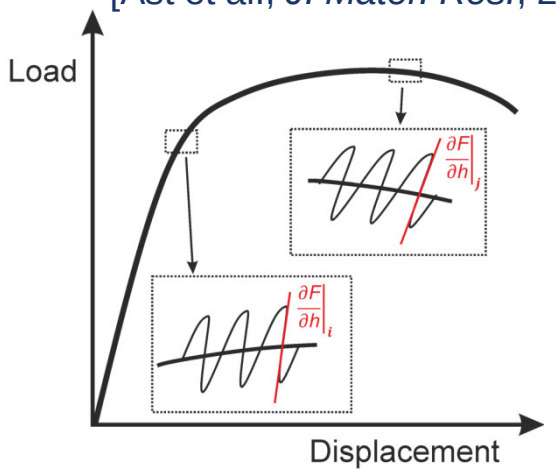

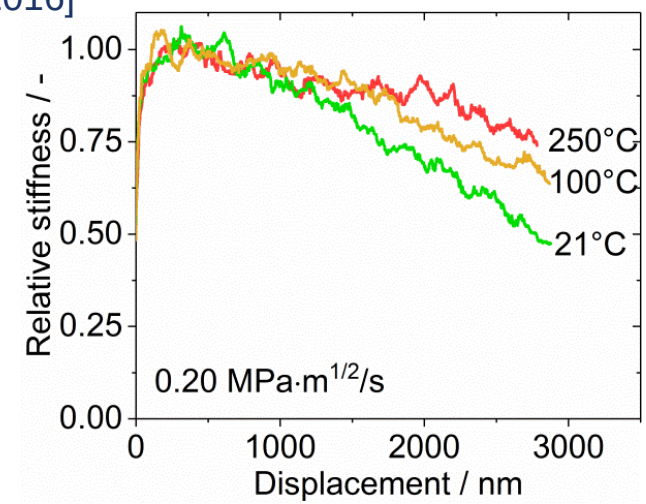

Continuous recording of specimen stiffness

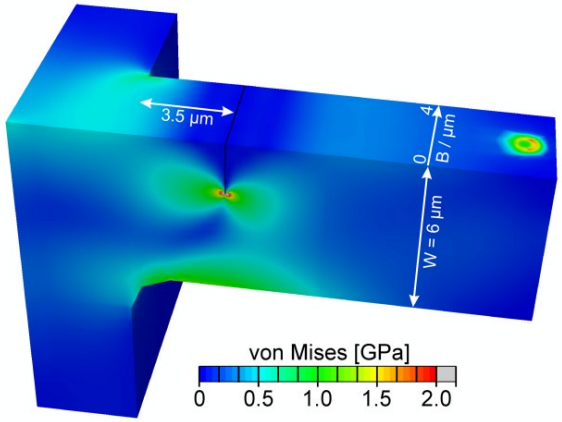

FE model to correlate stiffness with crack length

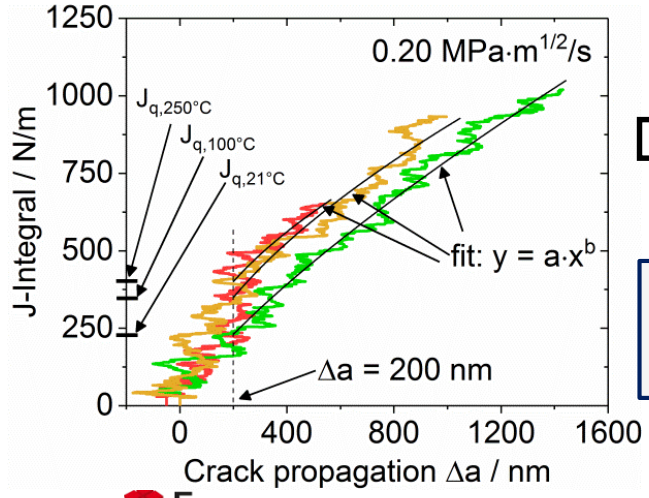

R-curves:

- Stable crack growth more significant at lower T
- Crack tip blunting more significant at higher T

$$J_{(i)} = \frac{\left(K_{Iq,(i)}\right)^2 (1-\nu^2)}{E} + \left[J_{pl,(i-1)} + \frac{\eta(A_{pl,(i)} - A_{pl,(i-1)})}{B(W - a_{(i-1)})}\right]\left[1 - \frac{a_{(i)} - a_{(i-1)}}{(W - a_{(i-1)})}\right]$$

ASTM standard E 1820

In-situ HR-EBSD: fracture behavior

Empa
Materials Science and Technology

Before testing

Elastic loading

After crack initiation

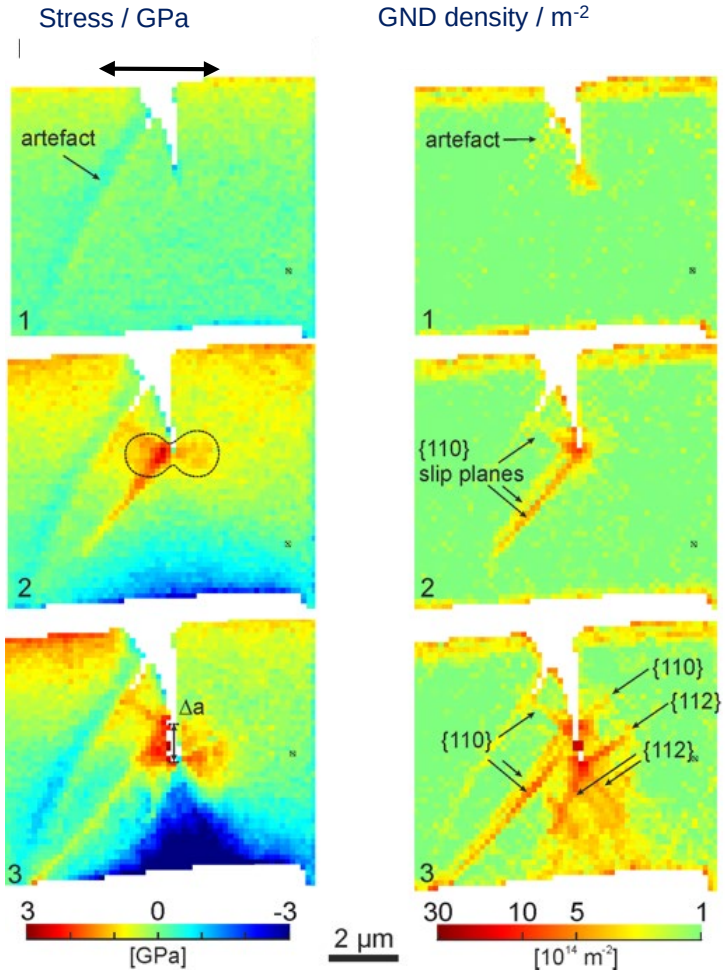

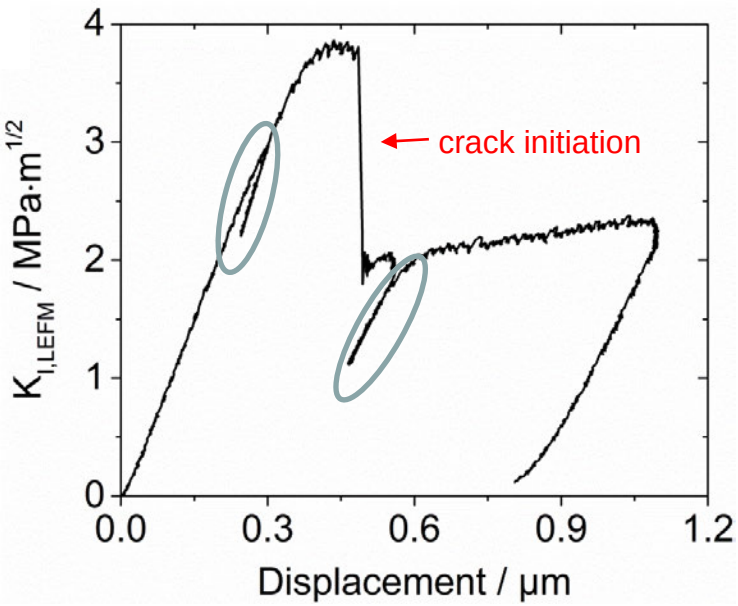

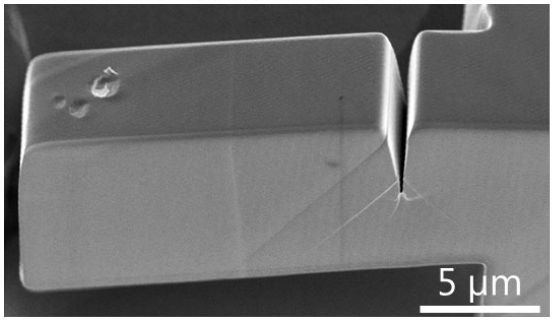

cantilever after testing

- Elastic regime: neutral axis separates tensile stresses at crack tip from compressive stresses at the lower free surface
- "Plastic zone" strongly depending on activated slip systems and not isotropic

Plasticity and fracture – loading mode dependence

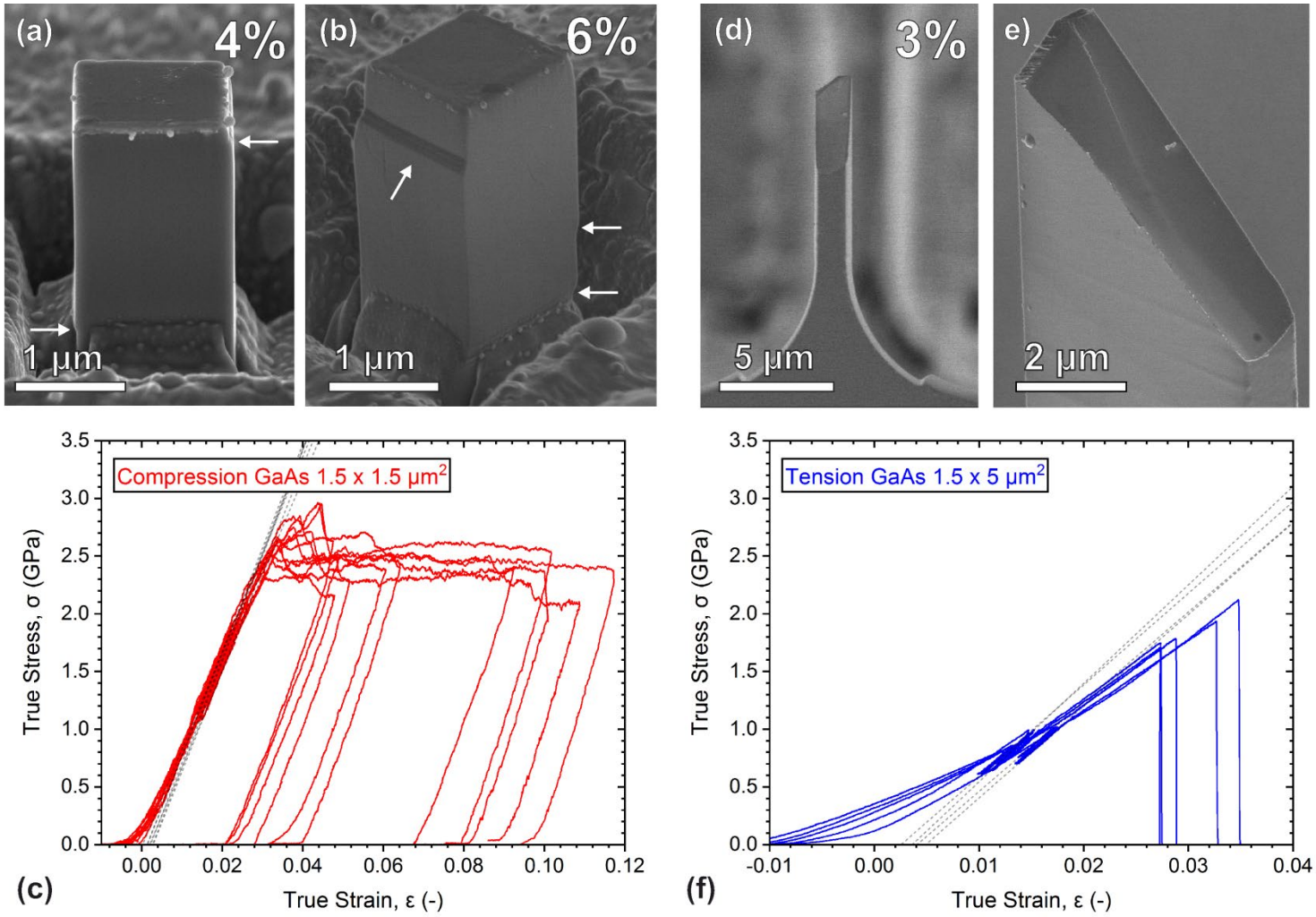

Plasticity and fracture – loading mode dependence

- Specimen sharing a common thinnest dimension of 1.70 ± 0.19 μm.
- GaAs tested along the [001] crystallographic orientation.
- Brittle-to-ductile transition under uniaxial compression (between 1.7 μm and 2.3 μm).
- Brittle failure in tension (no dislocations activity).
- Twin formation in compression.

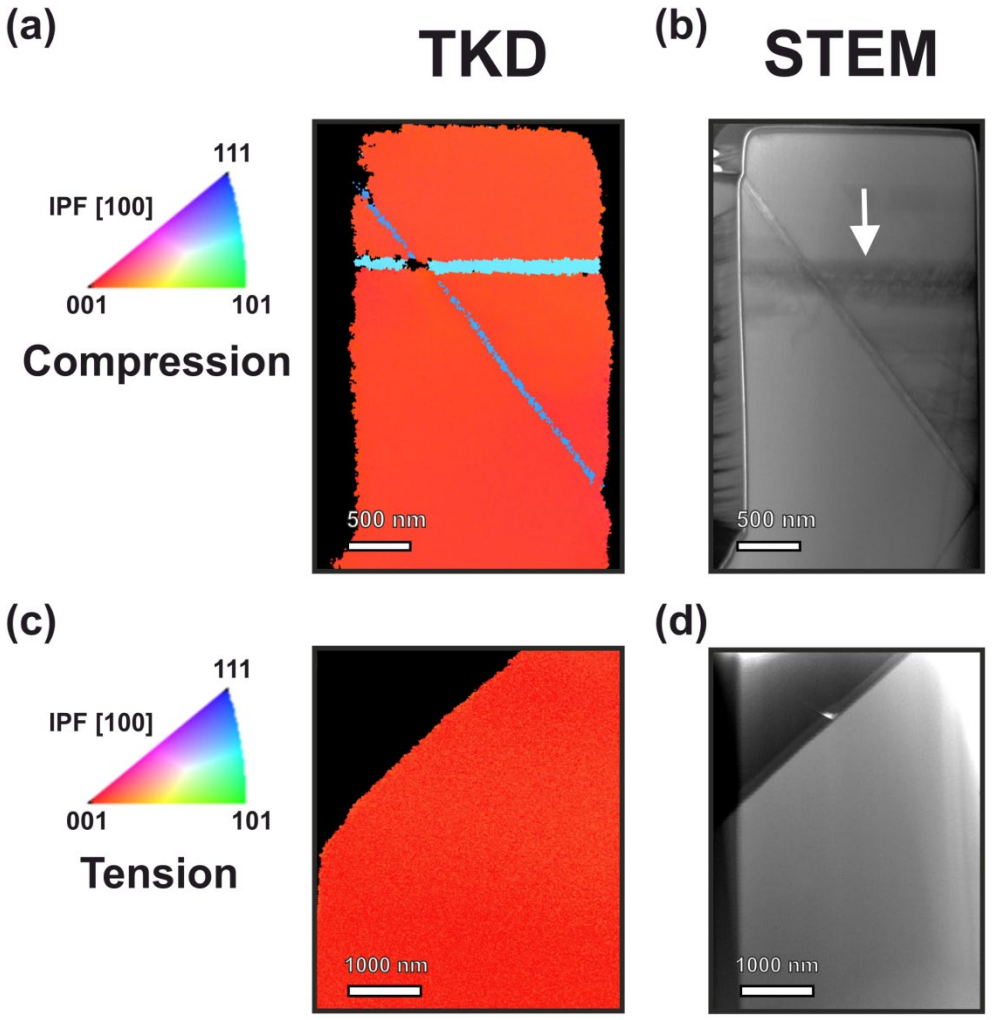

GaAs micropillar dimensions

- **Square** pillars 1.5x1.5 μm (N = 11)
  - **Side** = 1.72 ± 0.18 μm
  - **Height** = 3.49 ± 0.18 μm
  - **Geometry factor** = 2.05 ± 0.28

- **Rectangular** tensile samples 1.5x5 μm (N = 6)
  - **Width** = 1.67 ± 0.23 μm
  - **Thickness** = 5.34 ± 0.23 μm

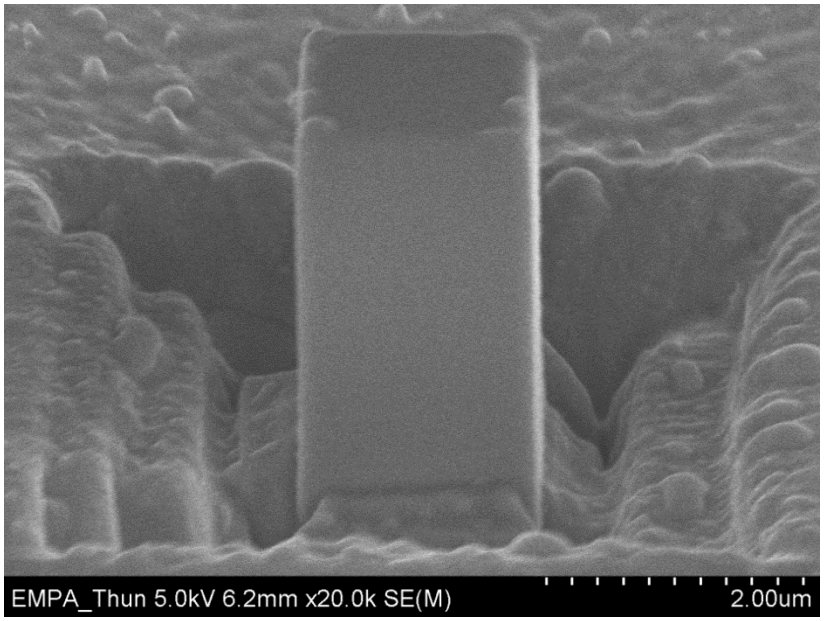

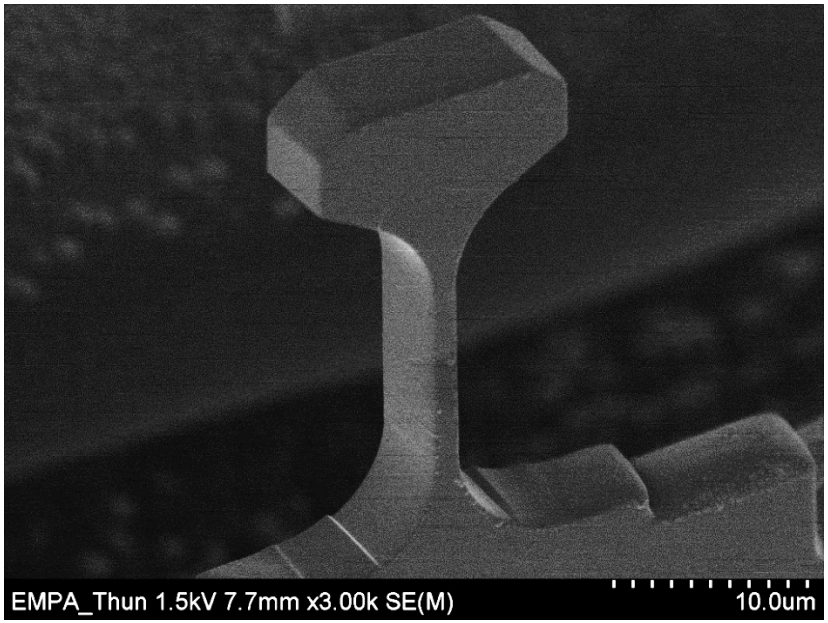

Thinness effect: thin structures exhibit the same enhanced yield strength regardless of total size volume or surface to volume ratio

N.M. Jennet et al. *Appl Phys Lett* 20098

Mechanical data

- Compression-tension strength asymmetry by a factor of 1.4.
- Same elastic modulus for the [001] crystallographic orientation.
- Plasticity in compression while brittle failure in tension.

Test	Strength, σ^{max} (GPa)	Elastic modulus, E (GPa)	Post-yield
Compression	2.61 ± 0.14 (N=11)	86.5 ± 3.1 (N=4)	Plasticity
Tension	1.86 ± 0.17 (N=6)	81.4 ± 4.6 (N=6)	Fragile
Factor	**1.4**	1.06	NA